# Nuclear Physics with Gamma Beams at ELI-NP

P. Constantin
ELI-NP/IFIN-HH, Bucharest

EUROPEAN UNION
GUVERNUL ROMÂNIEI
Structural Instruments 2014-2020
Competitiveness Operational Programme (COP)
eli nuclear physics
Extreme Light Infrastructure - Nuclear Physics (ELI-NP) - Phase II
Project Co-financed by the European Regional Development Fund
IFIN-HH

# Nuclear Physics at ELI-NP

- The ELI-NP Gamma Beam Facility

- Nuclear Physics with Gamma Beams at ELI-NP:
  1) Nuclear astrophysics
  2) Exotic neutron-rich nuclei
  3) Photofission
  4) Nuclear resonance fluorescence
  5) Photoneutron reactions

# The ELI (Extreme Light Infrastructure) Project

- **Project co-financed by the European Regional Development Fund**
- **Three facilities:**

  I. **ELI–Beamlines** (Prague, Czech Republic): development of ultra–short pulses of high–energy particles

  II. **ELI–ALPS** (Szeged, Hungary): attosecond laser science

  III. **ELI–NP** (Magurele, Romania): nuclear physics with high intensity lasers and brilliant gamma beams

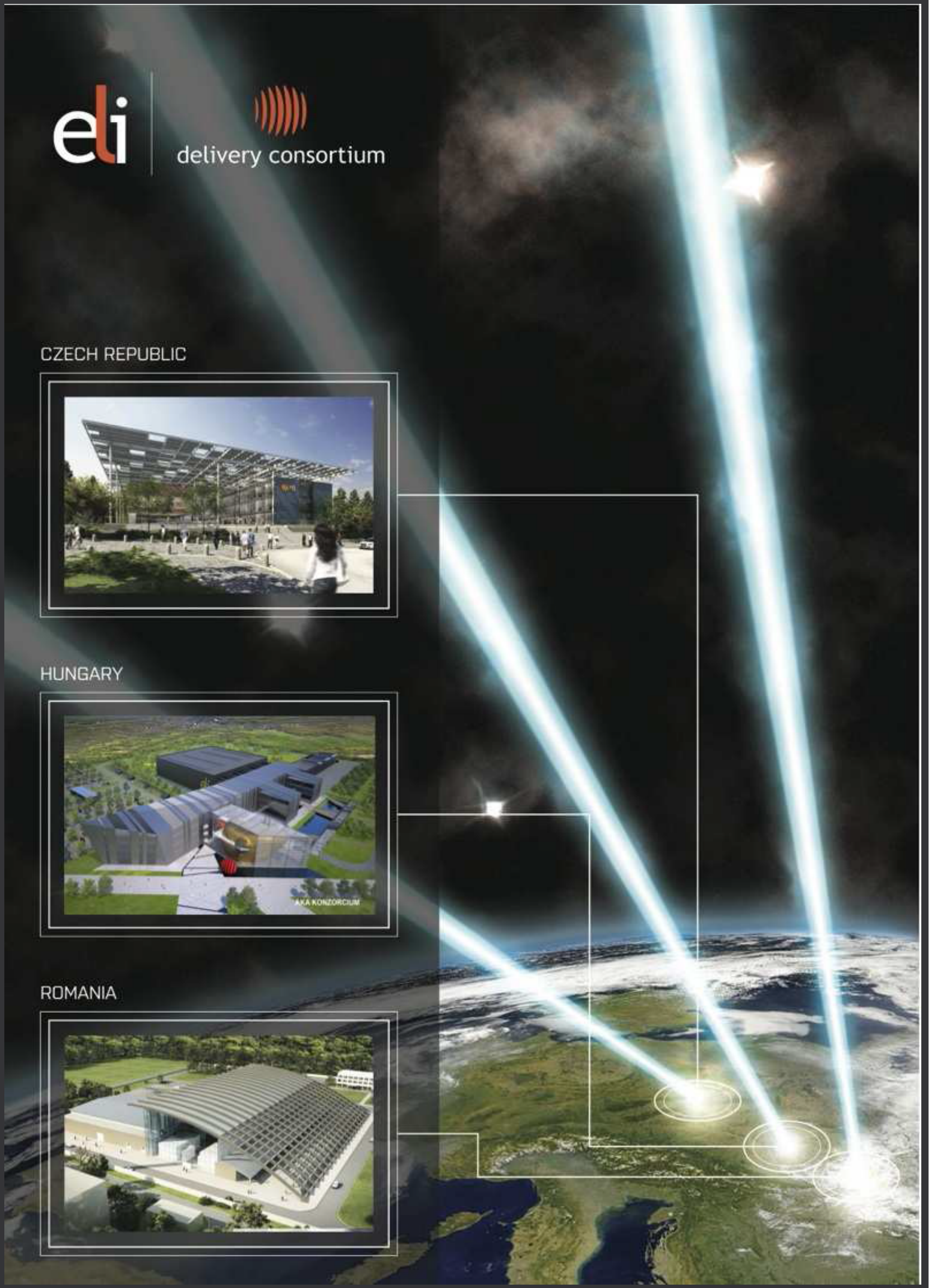

# The ELI (Extreme Light Infrastructure) Project

- **Project co-financed by the European Regional Development Fund**
- **Three facilities:**

  **I. ELI–Beamlines** (Prague, Czech Republic): development of ultra–short pulses of high–energy particles

  **II. ELI–ALPS** (Szeged, Hungary): attosecond laser science

  **III. ELI–NP** (Magurele, Romania): nuclear physics with high intensity lasers and brilliant gamma beams

- **ELI-NP:**
  - **laser driven** experiments: fission-fusion, nuclear reactions in plasma
  - **gamma driven** experiments: NRF, photofission, (γ,n), charged particles, exotic nuclei
  - **combined** experiments: high field QED

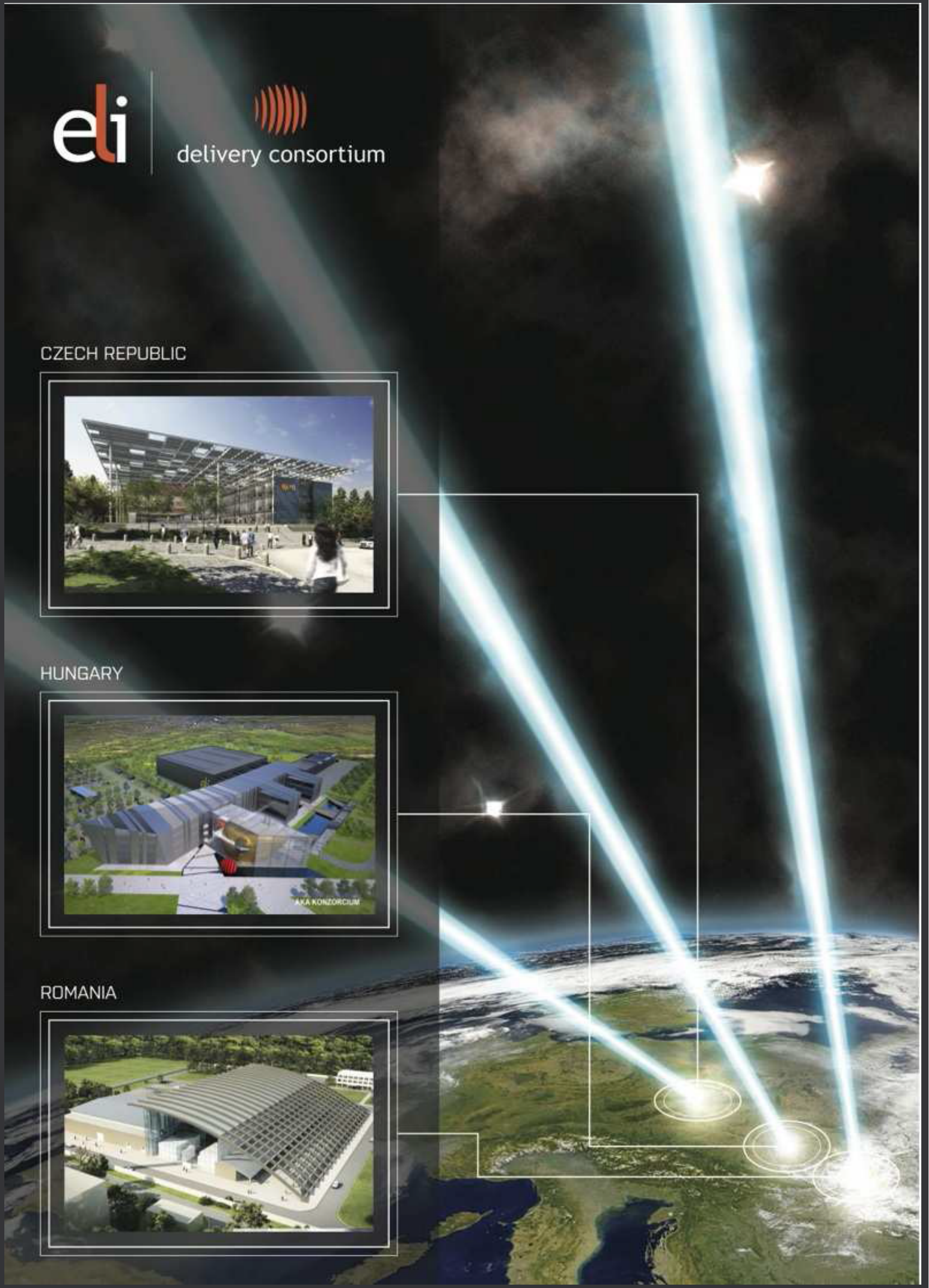

# ELI-NP Civil Construction

# ELI-NP Civil Construction

# Extreme Light Infrastructure – Nuclear Physics

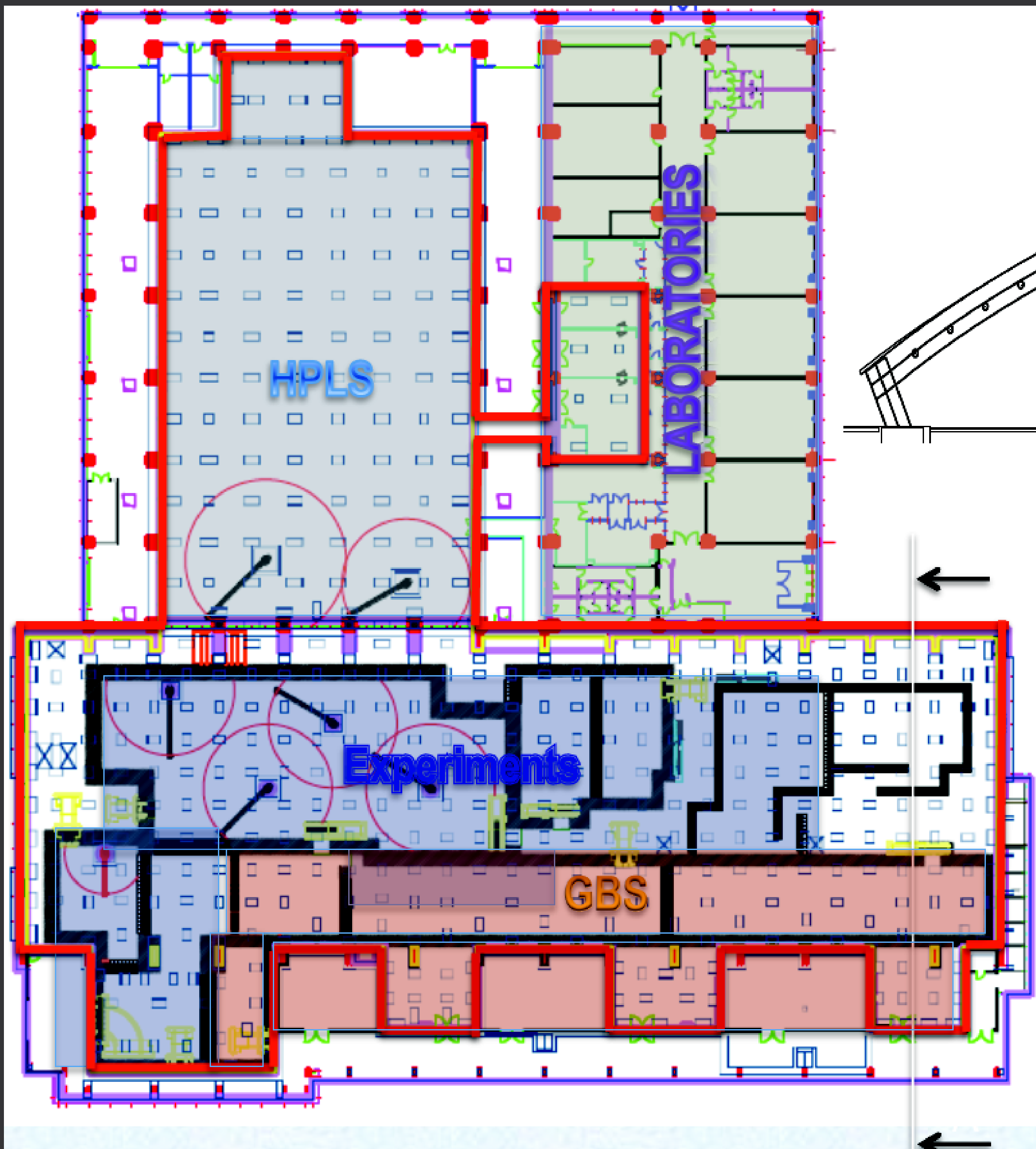

# Extreme Light Infrastructure – Nuclear Physics

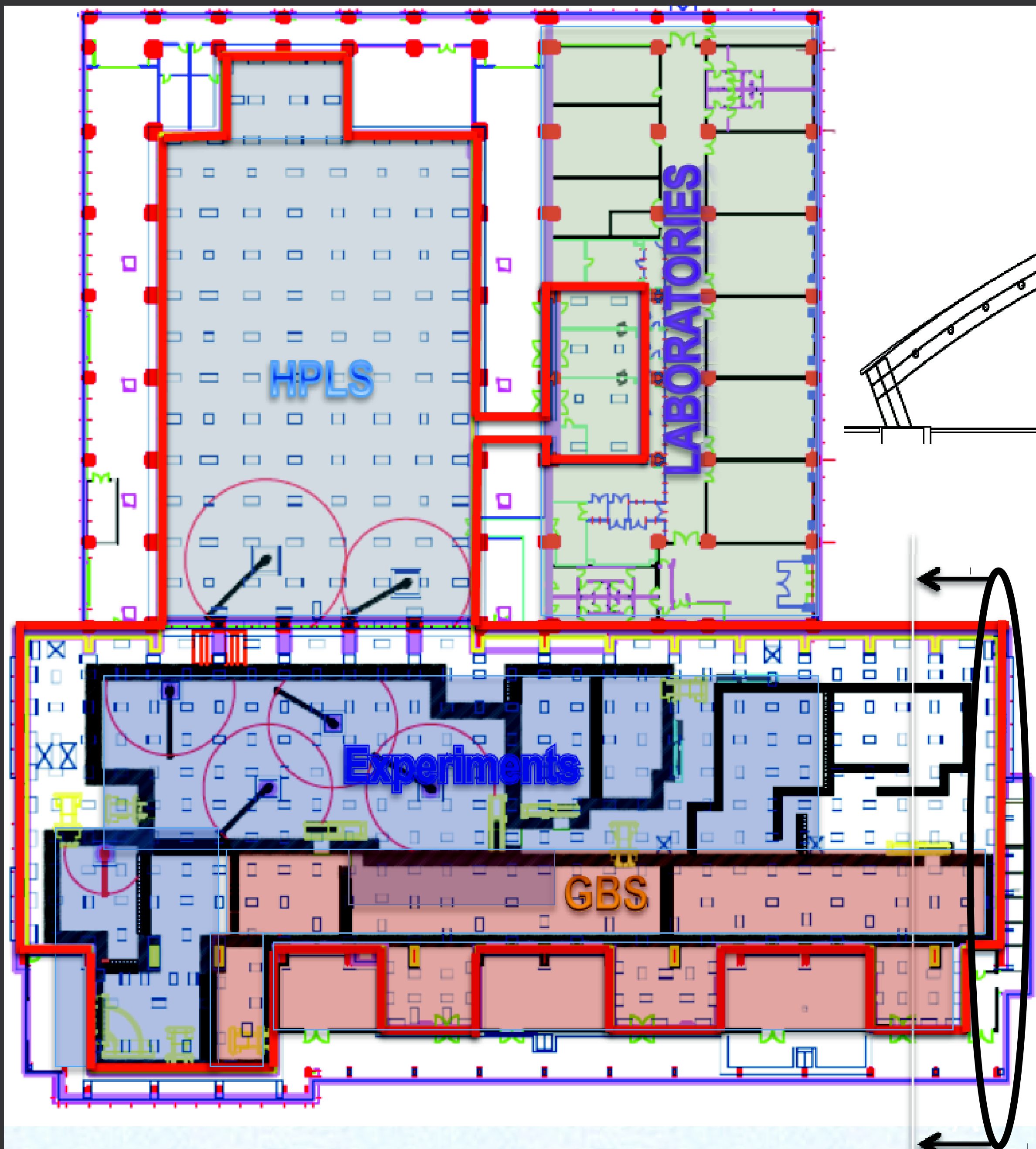


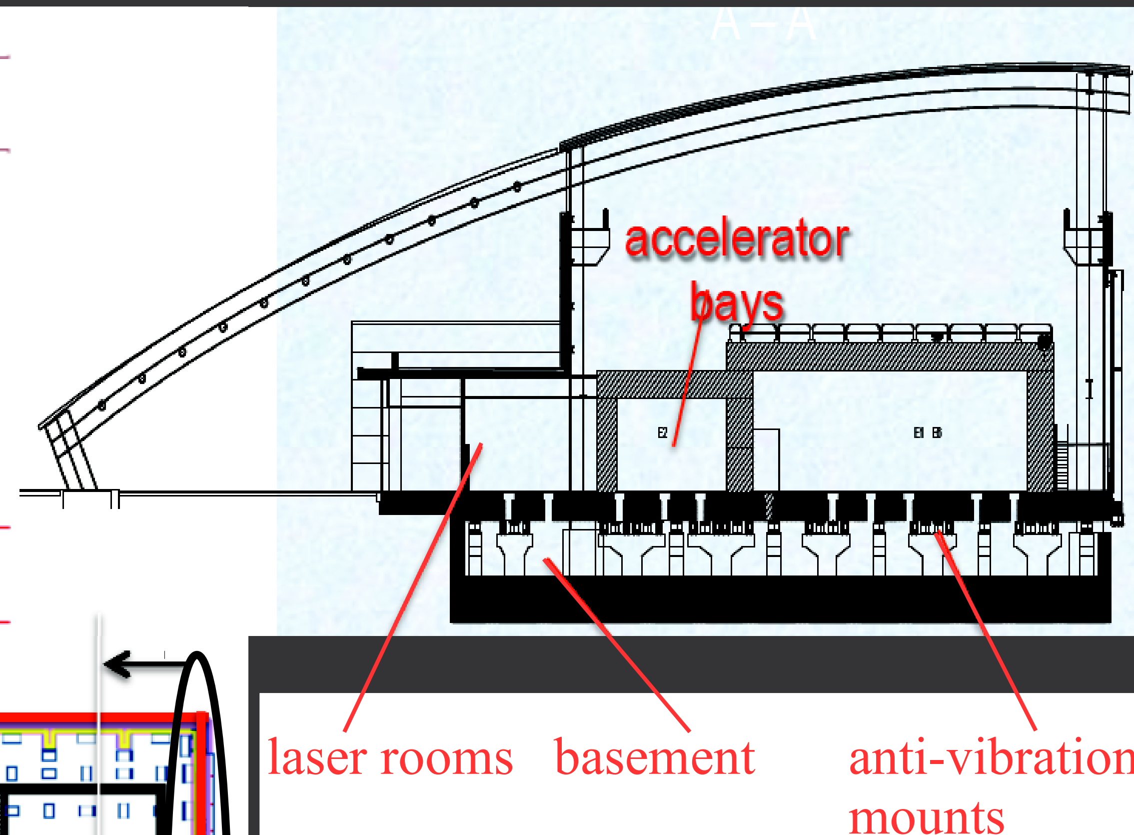

# Extreme Light Infrastructure – Nuclear Physics

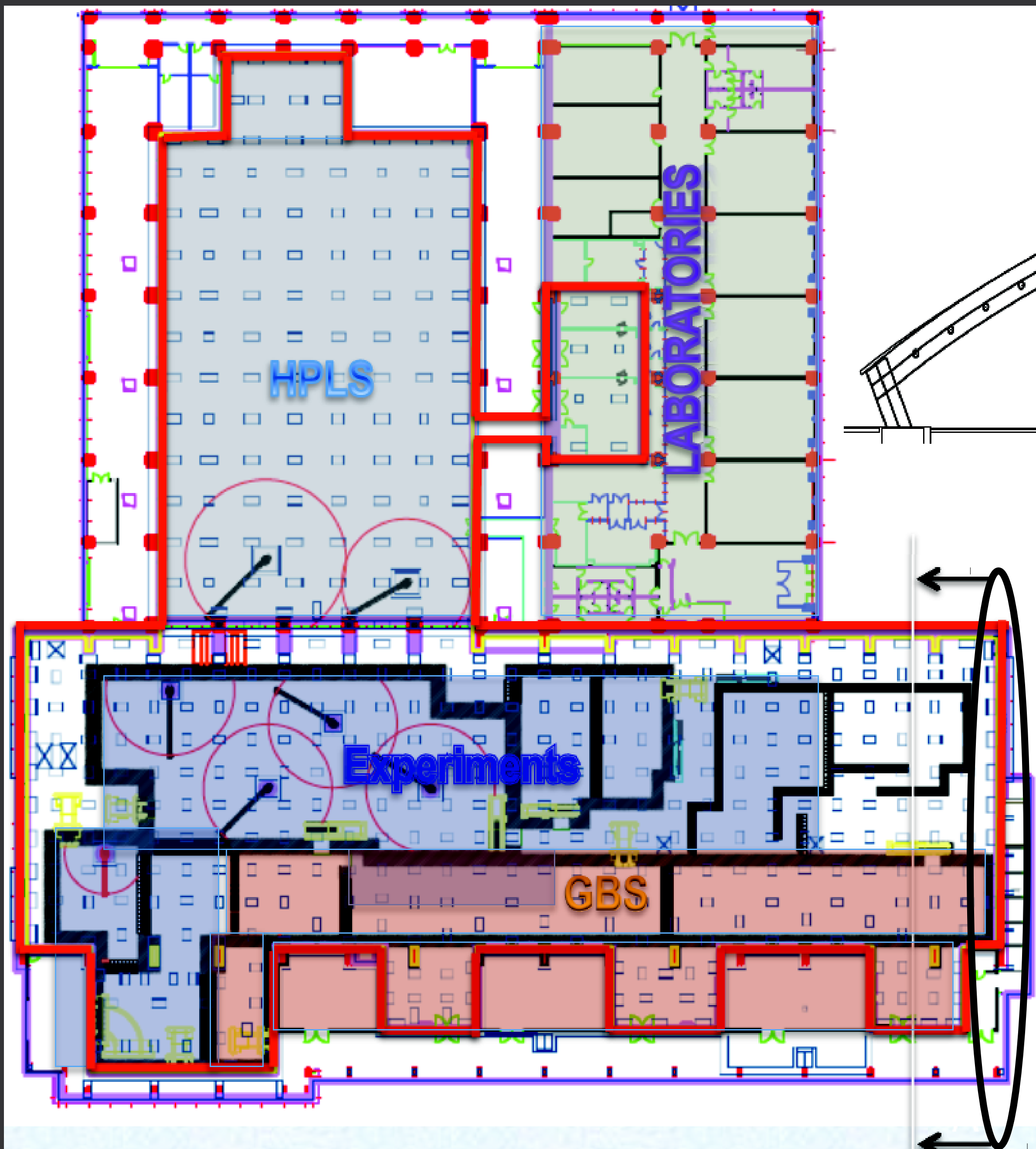


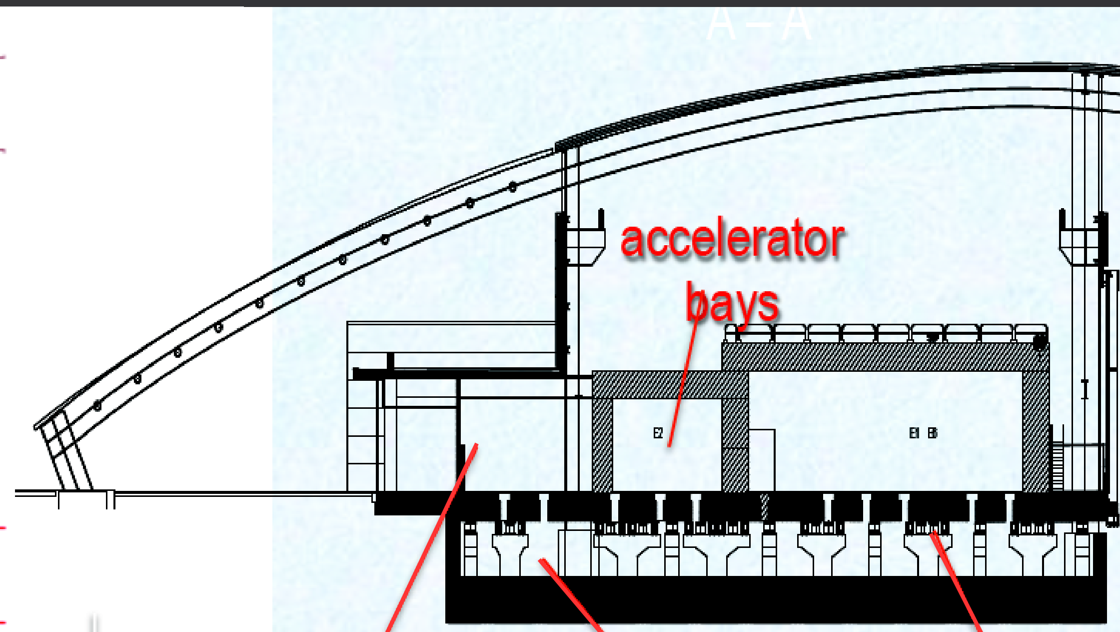


Anti-vibration platform: ±1mm @ <10Hz

**HPLS** (High Power Laser System): 2x10PW built by **Thales**, France

**GBS** (Gamma Beam System): 3.5MeV and 19.5MeV built by **EuroGammaS** consortium

# ELI-NP Gamma Beam Facility

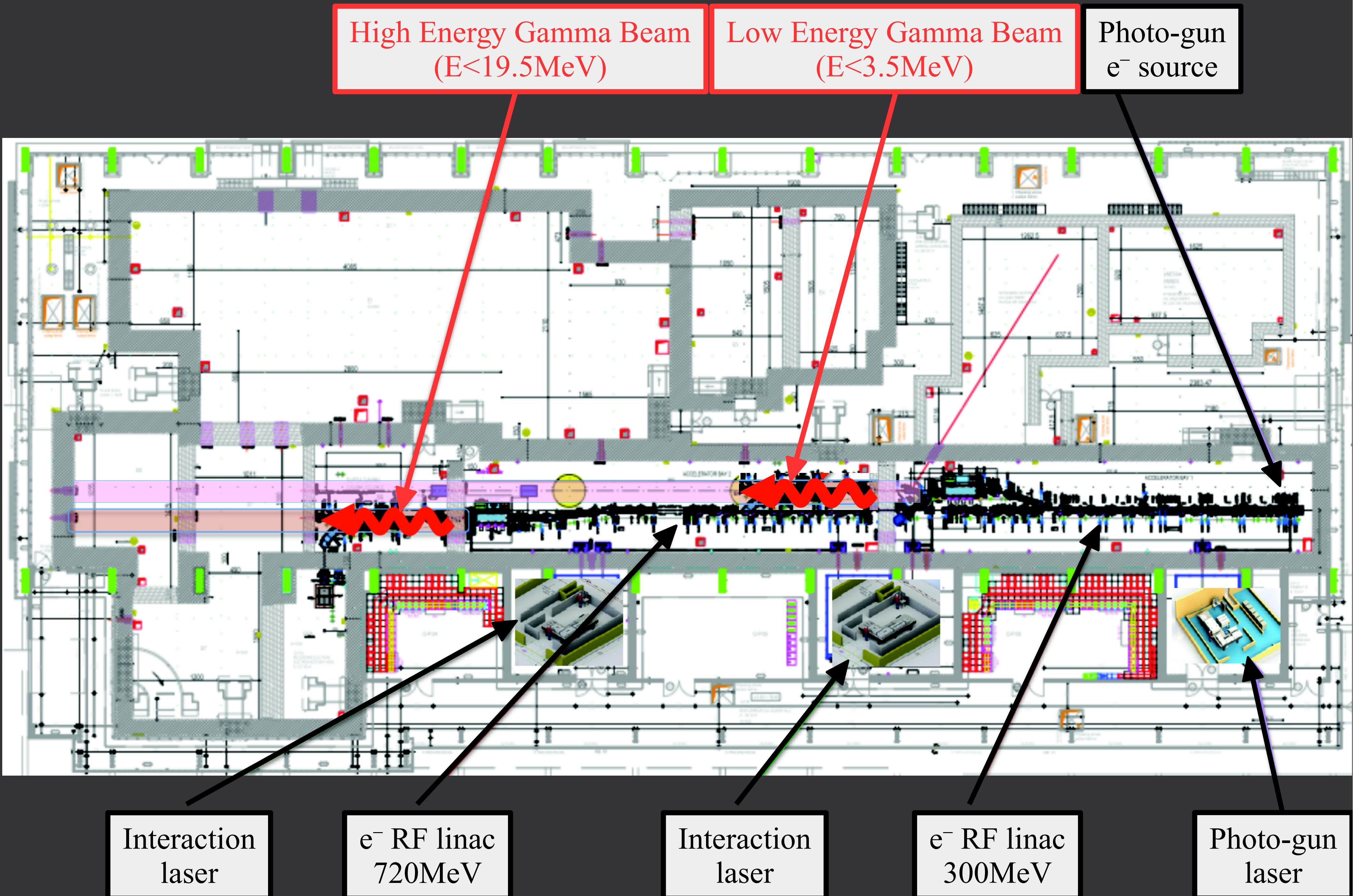

# Nuclear Astrophysics (I)

Nucleosynthesis
– primordial: at 3-20 min after Big Bang, $T \sim 10^9 K$
– stellar: helium burning at $T \sim 10^8 K$
in giant stars; s-, r- processes

# Nuclear Astrophysics (I)

Nucleosynthesis
– primordial: at 3-20 min after Big Bang, T~$10^9$K
– stellar: helium burning at T~$10^8$K
in giant stars; s-, r- processes

Thermonuclear reaction rates:

$$r_{ij} = \int \sigma_{ij} |v_i - v_j| d^3 n_i d^3 n_j$$

where number densities n(E,T) follow:
– photons: Bose-Einstein distribution
– electrons, neutrons: Fermi-Dirac distribution
– nuclei: Maxwell-Boltzmann distribution

# Nuclear Astrophysics (I)

Nucleosynthesis
– primordial: at 3-20 min after Big Bang, $T \sim 10^9$K
– stellar: helium burning at $T \sim 10^8$K
in giant stars; s-, r- processes

Thermonuclear reaction rates:

$$r_{ij} = \int \sigma_{ij} |v_i - v_j| d^3 n_i d^3 n_j$$

where number densities n(E,T) follow:
– photons: Bose-Einstein distribution
– electrons, neutrons: Fermi-Dirac distribution
– nuclei: Maxwell-Boltzmann distribution

$$r_{ij}(T) = \langle E \sigma(E) \rangle_{ij} n_i n_j$$

where <...> is the energy integral over n(E,T).

# Nuclear Astrophysics (I)

Nucleosynthesis
– primordial: at 3-20 min after Big Bang, $T\sim10^9$K
– stellar: helium burning at $T\sim10^8$K
in giant stars; s-, r- processes

Thermonuclear reaction rates:

$$r_{ij}=\int \sigma_{ij}|v_i-v_j|d^3n_i d^3n_j$$

where number densities n(E,T) follow:
– photons: Bose-Einstein distribution
– electrons, neutrons: Fermi-Dirac distribution
– nuclei: Maxwell-Boltzmann distribution

$$r_{ij}(T)=\langle E\sigma(E)\rangle_{ij} n_i n_j$$

where <...> is the energy integral over n(E,T).

However **$10^8$–$10^9$K~10-100keV!**
Sensitivity to low-energy cross-sections → extrapolations!

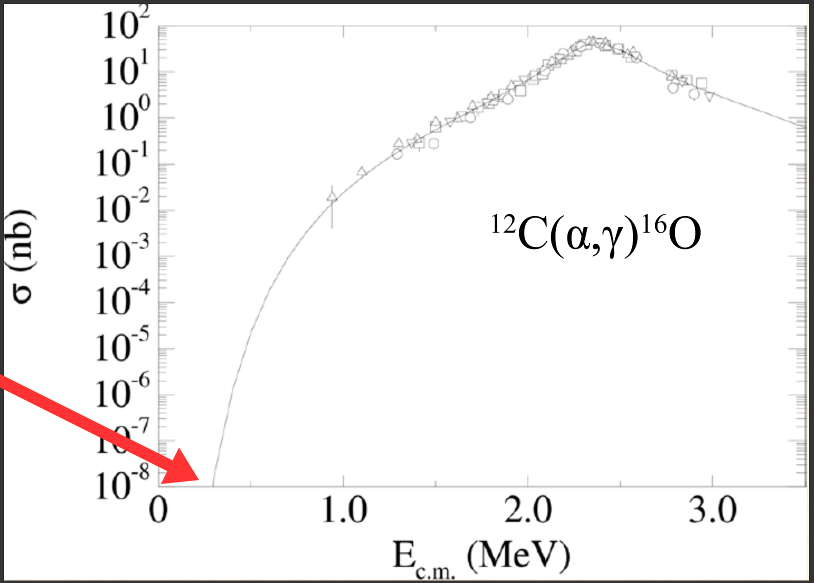

# Nuclear Astrophysics (I)

Nucleosynthesis
– primordial: at 3-20 min after Big Bang, $T\sim10^9$K
– stellar: helium burning at $T\sim10^8$K
in giant stars; s-, r- processes

Thermonuclear reaction rates:

$$r_{ij}=\int \sigma_{ij}|v_i-v_j|d^3n_i d^3n_j$$

where number densities n(E,T) follow:
– photons: Bose-Einstein distribution
– electrons, neutrons: Fermi-Dirac distribution
– nuclei: Maxwell-Boltzmann distribution

$$r_{ij}(T)=\langle E\sigma(E)\rangle_{ij} n_i n_j$$

where <...> is the energy integral over n(E,T).

However **$10^8$–$10^9$K~10-100keV!**
Sensitivity to low-energy cross-sections → extrapolations!

*C.A. Bertulani, A. Gade, Phys. Rep. 485 (2010) 195*

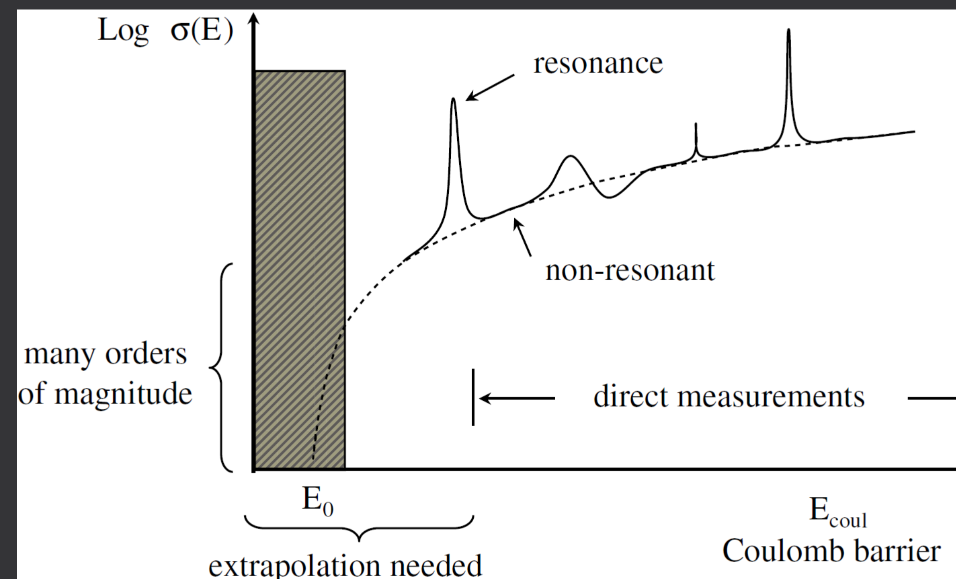


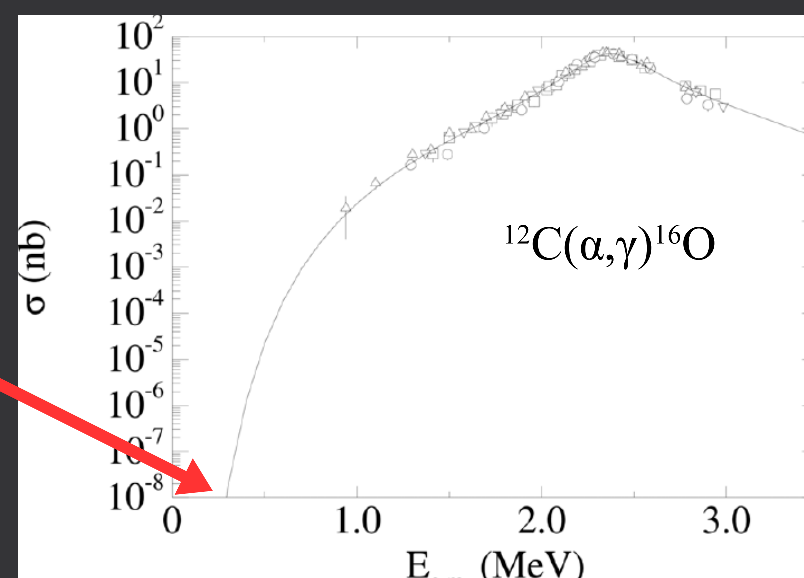

# Nuclear Astrophysics (II)

Probability to penetrate Coulomb barrier:

$$P(E) = \exp\left(-\sqrt{E_g/E}\right), E_g \equiv 2\mu c^2 \pi \alpha Z_1 Z_2$$

# Nuclear Astrophysics (II)

Probability to penetrate Coulomb barrier:

$$P(E) = \exp\left(-\sqrt{E_g/E}\right), E_g \equiv 2\mu c^2 \pi \alpha Z_1 Z_2$$

Convoluted with $n(E,T)=n_0(T,m_{12})\exp(-E/k_BT)$

→ Gamow energy window

well into σ suppression region $E<B_c$

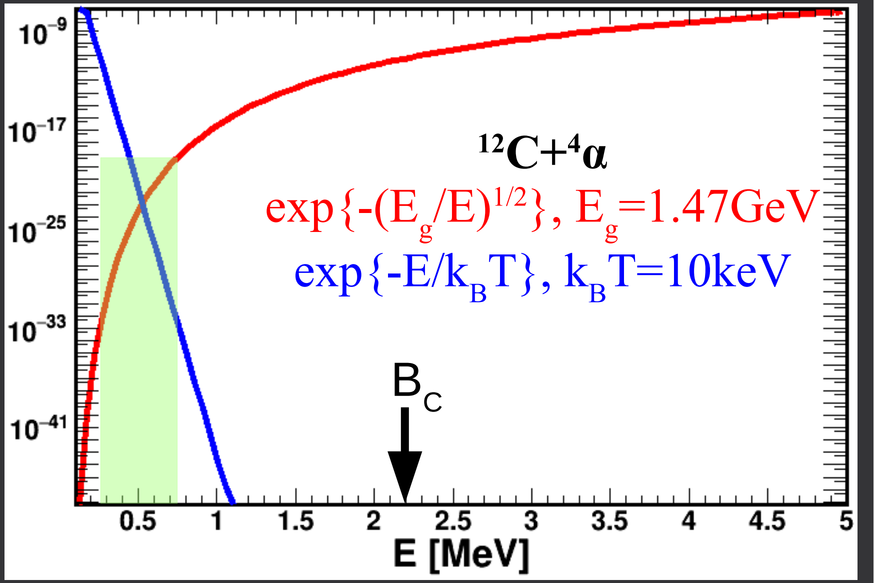

# Nuclear Astrophysics (II)

Probability to penetrate Coulomb barrier:

$$P(E)=\exp\left(-\sqrt{E_g/E}\right), E_g \equiv 2\mu c^2 \pi \alpha Z_1 Z_2$$

Convoluted with $n(E,T)=n_0(T,m_{12})\exp(-E/k_B T)$

→ Gamow energy window

well into σ suppression region $E<B_c$

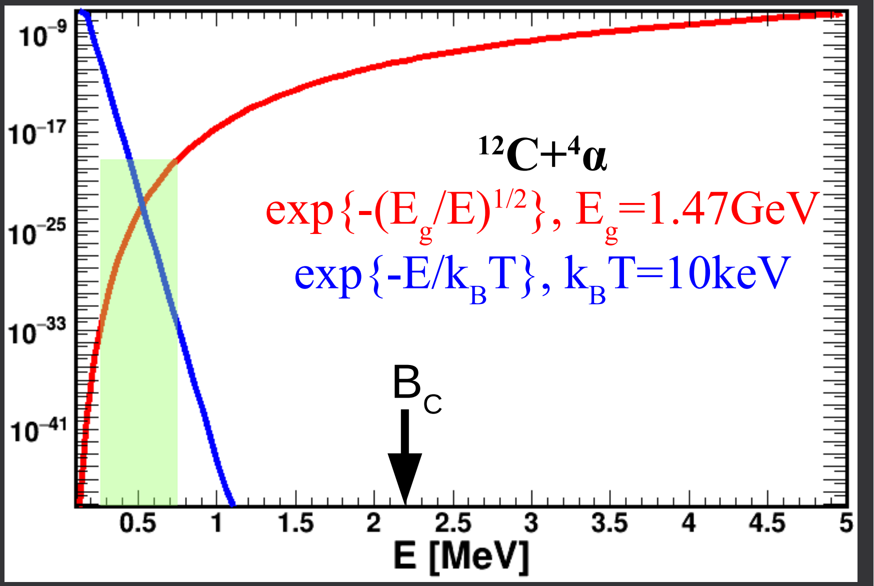


Astrophysical factor S:

$$S(E) \equiv E\sigma(E)e^{2\pi\eta}, \quad \eta=\frac{Z_1 Z_2 e^2}{\hbar v_{12}}$$

Sommerfeld parameter η factors out the barrier penetration and

$$\langle E\sigma(E)\rangle_{ij} \sim \int dE\, S(E)\exp\left(-E/k_B T - b/\sqrt{(E)}\right)$$

# Nuclear Astrophysics (II)

Probability to penetrate Coulomb barrier:

$$P(E)=\exp\left(-\sqrt{E_g/E}\right), E_g\equiv 2\mu c^2\pi\alpha Z_1 Z_2$$

Convoluted with $n(E,T)=n_0(T,m_{12})\exp(-E/k_BT)$

→ Gamow energy window

well into σ suppression region $E<B_c$

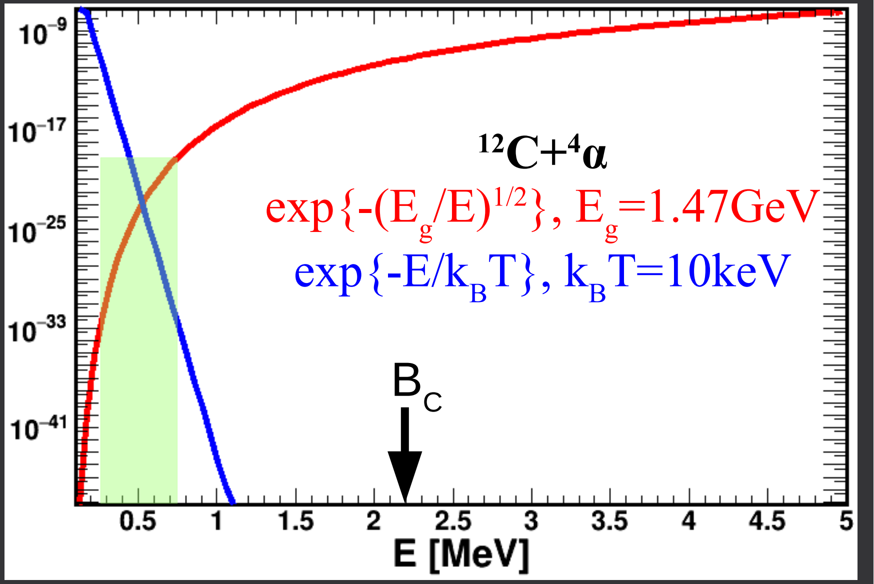


Astrophysical factor S:

$$S(E)\equiv E\sigma(E)e^{2\pi\eta},\quad \eta=\frac{Z_1 Z_2 e^2}{\hbar v_{12}}$$

Sommerfeld parameter η factors out the barrier penetration and

$$\langle E\sigma(E)\rangle_{ij}\sim\int dE\, S(E)\exp\left(-E/k_B T-b/\sqrt{(E)}\right)$$

Radiative capture b+c→γ+a from photo-dissociation γ+a→b+c via **reciprocity theorem**:

$$(2J_b+1)(2J_c+1)k_{b+c}^2\sigma_{b+c\rightarrow\gamma+a}(E_\gamma)=2(2J_a+1)k_{\gamma+a}^2\sigma_{\gamma+a\rightarrow b+c}(E_\gamma)$$

# Nuclear Astrophysics (II)

Probability to penetrate Coulomb barrier:

$$P(E)=\exp\left(-\sqrt{E_g/E}\right), E_g\equiv 2\mu c^2\pi\alpha Z_1 Z_2$$

Convoluted with $n(E,T)=n_0(T,m_{12})\exp(-E/k_BT)$

$\rightarrow$ Gamow energy window

well into $\sigma$ suppression region $E<B_c$

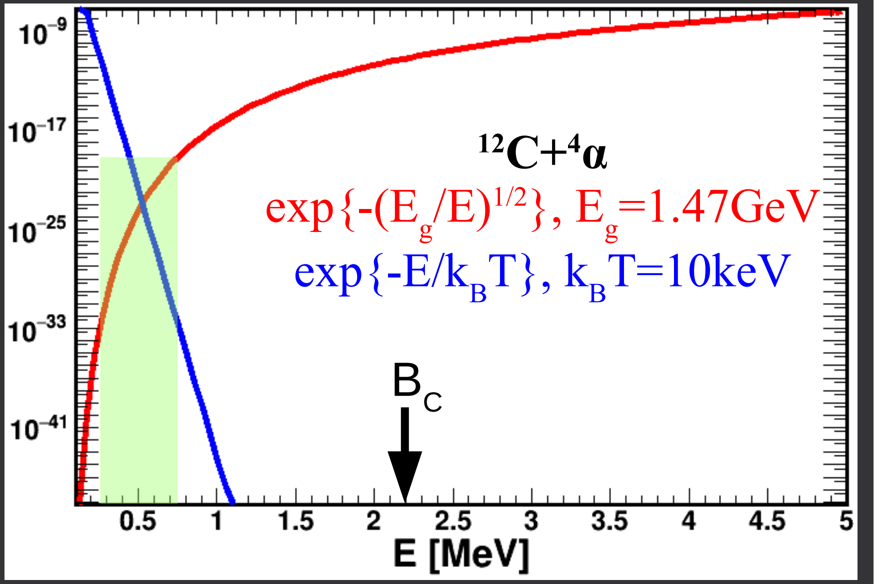


Astrophysical factor S:

$$S(E)\equiv E\sigma(E)e^{2\pi\eta},\quad \eta=\frac{Z_1 Z_2 e^2}{\hbar v_{12}}$$

Sommerfeld parameter η factors out the barrier penetration and

$$\langle E\sigma(E)\rangle_{ij}\sim\int dE\, S(E)\exp\left(-E/k_BT-b/\sqrt{(E)}\right)$$

Radiative capture b+c→γ+a from photo-dissociation γ+a→b+c via **reciprocity theorem**:

$$(2J_b+1)(2J_c+1)k^2_{b+c}\sigma_{b+c\to\gamma+a}(E_\gamma)=2(2J_a+1)k^2_{\gamma+a}\sigma_{\gamma+a\to b+c}(E_\gamma)$$

$$k^2_{\gamma,a}=k^2_\gamma=E^2_\gamma/(\hbar c)^2,\qquad k^2_{b,c}=2\mu_{bc}E_{bc}/\hbar^2=2\mu_{bc}(E_\gamma-S_n)/\hbar^2$$

# Nuclear Astrophysics (II)

Probability to penetrate Coulomb barrier:

$$P(E)=\exp\left(-\sqrt{E_g/E}\right), E_g \equiv 2\mu c^2 \pi \alpha Z_1 Z_2$$

Convoluted with $n(E,T)=n_0(T,m_{12})\exp(-E/k_B T)$
$\rightarrow$ Gamow energy window
well into $\sigma$ suppression region $E<B_c$

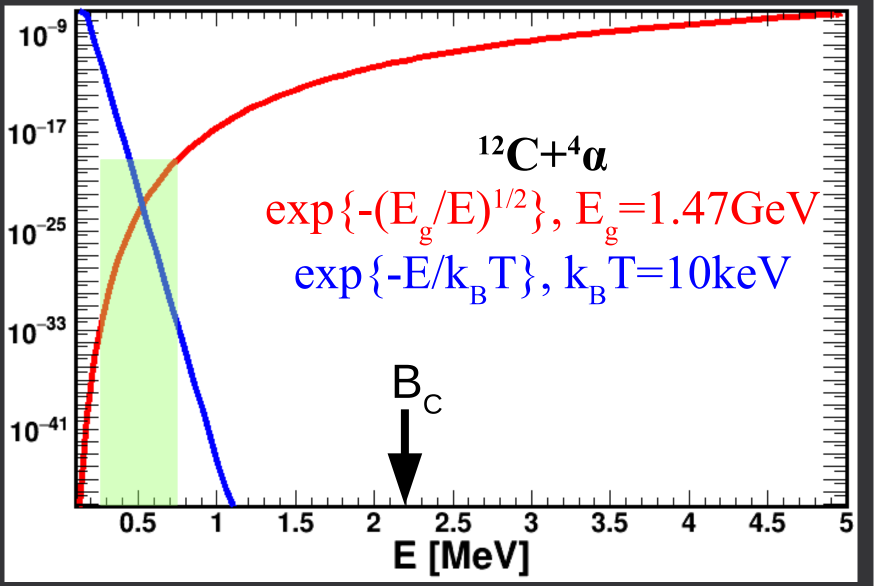


Astrophysical factor S:

$$S(E) \equiv E\sigma(E) e^{2\pi\eta}, \quad \eta = \frac{Z_1 Z_2 e^2}{\hbar v_{12}}$$

Sommerfeld parameter $\eta$ factors out the barrier penetration and

$$\langle E\sigma(E)\rangle_{ij} \sim \int dE\, S(E) \exp\left(-E/k_B T - b/\sqrt{(E)}\right)$$

Radiative capture $b+c \rightarrow \gamma+a$ from photo-dissociation $\gamma+a \rightarrow b+c$ via **reciprocity theorem**:

$$(2J_b+1)(2J_c+1) k_{b+c}^2 \sigma_{b+c\rightarrow\gamma+a}(E_\gamma) = 2(2J_a+1) k_{\gamma+a}^2 \sigma_{\gamma+a\rightarrow b+c}(E_\gamma)$$

$$k_{\gamma,a}^2 = k_\gamma^2 = E_\gamma^2/(\hbar c)^2, \qquad k_{b,c}^2 = 2\mu_{bc} E_{bc}/\hbar^2 = 2\mu_{bc}(E_\gamma - S_n)/\hbar^2$$

$$(2J_b+1)(2J_c+1) 2\mu_{bc} c^2 (E_\gamma - S) \sigma_{b+c\rightarrow\gamma+a}(E_\gamma) = 2(2J_a+1) E_\gamma^2 \sigma_{\gamma+a\rightarrow b+c}(E_\gamma)$$

where $S=(m_b+m_c-m_a)c^2$ and $\mu_{bc}=m_b m_c/(m_b+m_c)$

# Nuclear Astrophysics (II)

Probability to penetrate Coulomb barrier:

$$P(E) = \exp\left(-\sqrt{E_g/E}\right), E_g \equiv 2\mu c^2 \pi \alpha Z_1 Z_2$$

Convoluted with $n(E,T) = n_0(T, m_{12}) \exp(-E/k_B T)$

→ Gamow energy window

well into σ suppression region $E < B_c$

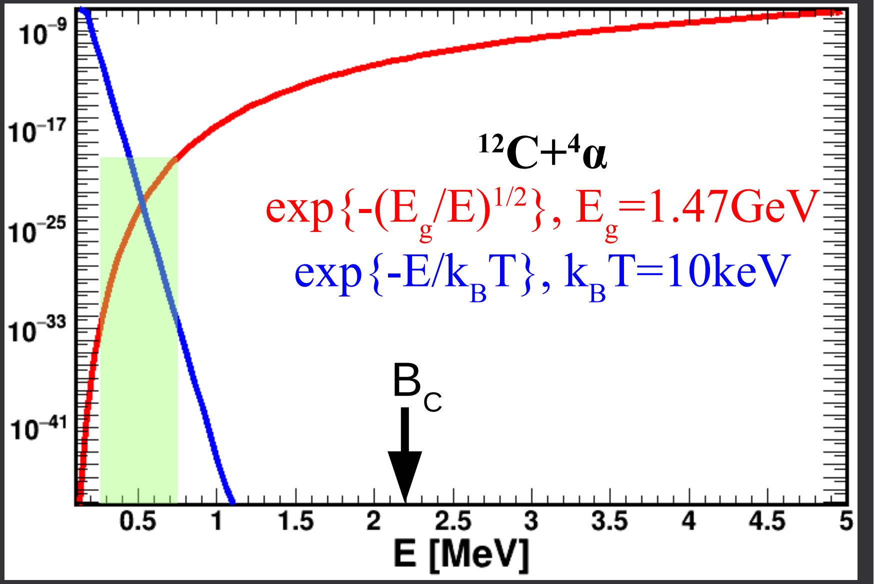


Astrophysical factor S:

$$S(E) \equiv E\sigma(E) e^{2\pi\eta}, \quad \eta = \frac{Z_1 Z_2 e^2}{\hbar v_{12}}$$

Sommerfeld parameter η factors out the barrier penetration and

$$\langle E\sigma(E)\rangle_{ij} \sim \int dE\, S(E) \exp\left(-E/k_B T - b/\sqrt{(E)}\right)$$

Radiative capture b+c→γ+a from photo-dissociation γ+a→b+c via **reciprocity theorem**:

$$(2J_b+1)(2J_c+1)k^2_{b+c}\sigma_{b+c\to\gamma+a}(E_\gamma) = 2(2J_a+1)k^2_{\gamma+a}\sigma_{\gamma+a\to b+c}(E_\gamma)$$

$$k^2_{\gamma,a} = k^2_\gamma = E^2_\gamma/(\hbar c)^2, \qquad k^2_{b,c} = 2\mu_{bc}E_{bc}/\hbar^2 = 2\mu_{bc}(E_\gamma - S_n)/\hbar^2$$

$$(2J_b+1)(2J_c+1)2\mu_{bc}c^2(E_\gamma - S)\sigma_{b+c\to\gamma+a}(E_\gamma) = 2(2J_a+1)E^2_\gamma\sigma_{\gamma+a\to b+c}(E_\gamma)$$

where $S = (m_b + m_c - m_a)c^2$ and $\mu_{bc} = m_b m_c/(m_b + m_c)$

Example $^7$Li(γ,α)t: $J_\alpha=0$, $J_t=1/2$, $J_{Li7}=3/2$, $\mu_{\alpha t}c^2 \approx 1.6$GeV, $S \approx 2.65$MeV

→ $\sigma_{\gamma Li} \approx 75 \cdot \sigma_{\alpha t}$ at $E_\gamma$=5MeV, $\sigma_{\gamma Li} \approx 59 \cdot \sigma_{\alpha t}$ at $E_\gamma$=10MeV

$$\sigma_{\gamma+Li7\to\alpha+t} = 800\frac{E_\gamma - 2.65}{E^2_\gamma}\sigma_{\alpha+t\to\gamma+Li7}$$

# Nuclear Astrophysics (III)

**Cosmological Li problem**

– Big-Bang Nucleosynthesis calculates primordial abundances of light elements D, $^3$He, $^4$He, Li, Be
– good agreement between calculated and observed abundances for all, except $^7$Li:
  – calculated $^7$Li abundance at WMAP baryonic density: $^7\mathrm{Li/H} = (5.24 \pm 0.71) \cdot 10^{-10}$
  – measured $^7$Li abundance in low metallicity stars: $^7\mathrm{Li/H} = (1.58 \pm 0.31) \cdot 10^{-10}$

# Nuclear Astrophysics (III)

## Cosmological Li problem

– Big-Bang Nucleosynthesis calculates primordial abundances of light elements D, $^3He$, $^4He$, Li, Be

– good agreement between calculated and observed abundances for all, except $^7Li$:

  – calculated $^7Li$ abundance at WMAP baryonic density: $^7Li/H = (5.24 \pm 0.71) \cdot 10^{-10}$

  – measured $^7Li$ abundance in low metallicity stars: $^7Li/H = (1.58 \pm 0.31) \cdot 10^{-10}$

– different α capture reactions dominate depending on baryonic density $\Omega_B$: $^3He(\alpha,\gamma)$ vs. $^3H(\alpha,\gamma)$

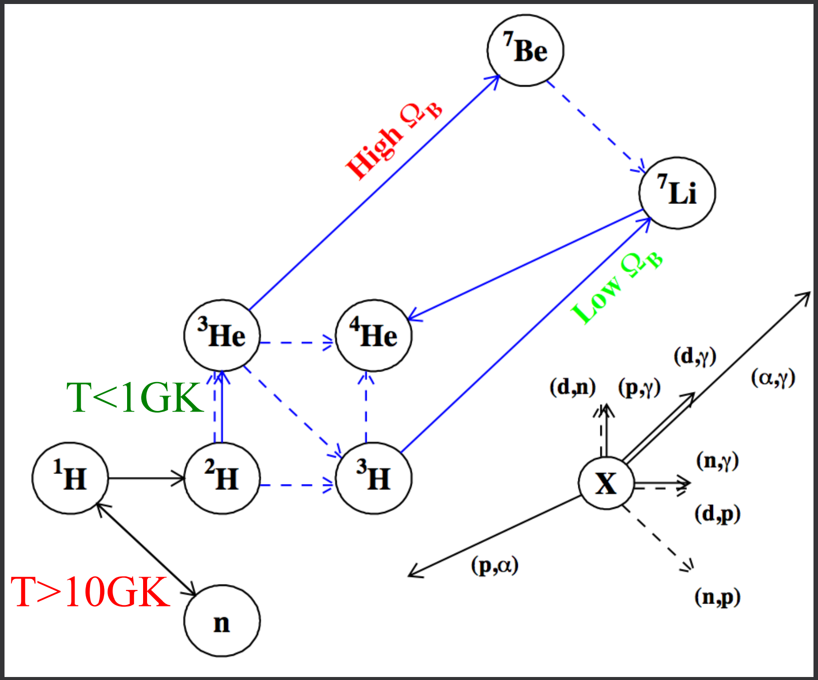

# Nuclear Astrophysics (III)

## Cosmological Li problem

– Big-Bang Nucleosynthesis calculates primordial abundances of light elements D, $^3He$, $^4He$, Li, Be
– good agreement between calculated and observed abundances for all, except $^7Li$:
  – calculated $^7Li$ abundance at WMAP baryonic density: $^7Li/H = (5.24 \pm 0.71) \cdot 10^{-10}$
  – measured $^7Li$ abundance in low metallicity stars: $^7Li/H = (1.58 \pm 0.31) \cdot 10^{-10}$
– different α capture reactions dominate depending on baryonic density $\Omega_B$: $^3He(\alpha,\gamma)$ vs. $^3H(\alpha,\gamma)$
– data on $^3H(\alpha,\gamma)^7Li$: lacking above 1MeV, conflicting below 1MeV

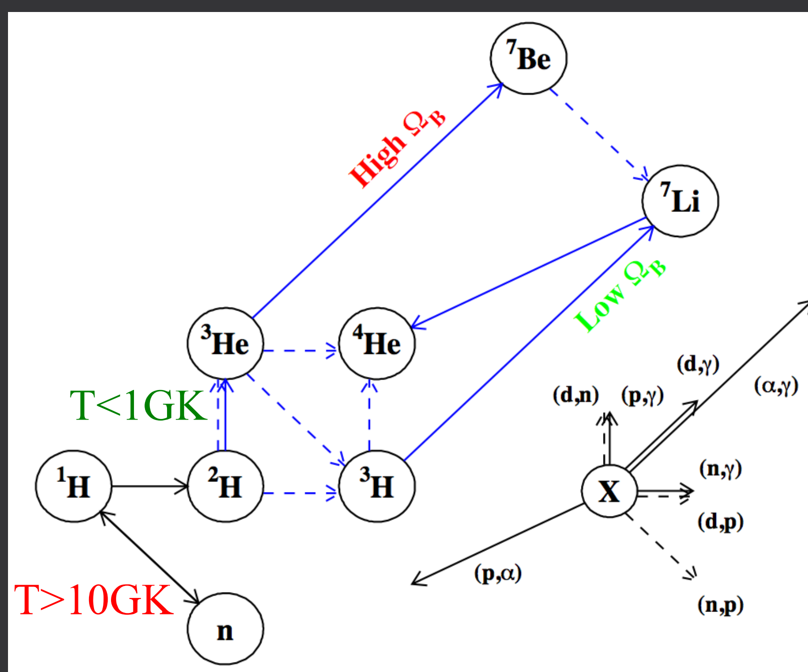


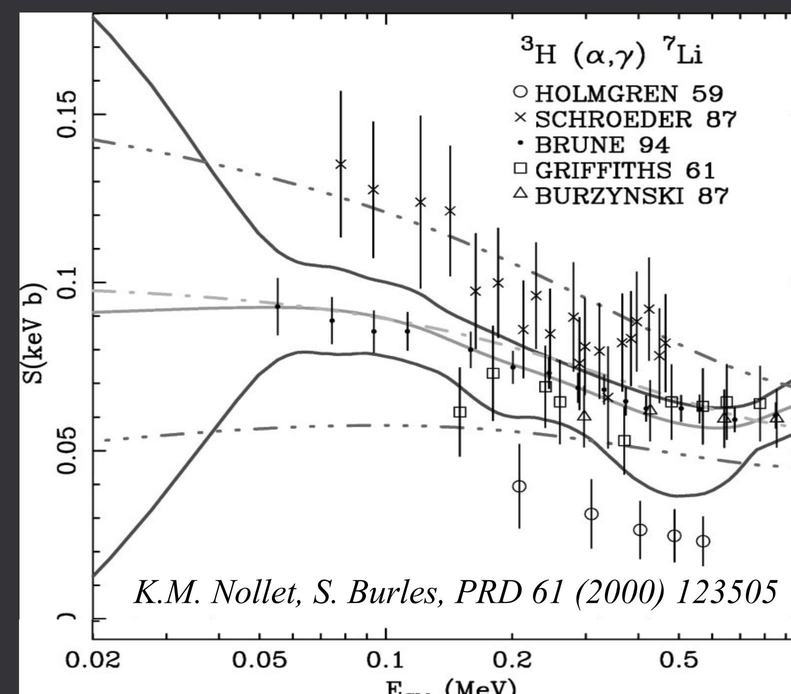

# Nuclear Astrophysics (IV)

**ELISSA (INFN Catania & ELI-NP)**

– array of position sensitive silicon strip detectors
– high energy resolution (~50keV at 5.8MeV) and detection efficiency (>95%)
– small sensitivity to main background channels ($\gamma$, $e^{\pm}$, n)

# Nuclear Astrophysics (IV)

## ELISSA (INFN Catania & ELI-NP)

– array of position sensitive silicon strip detectors
– high energy resolution (~50keV at 5.8MeV) and detection efficiency (>95%)
– small sensitivity to main background channels ($\gamma$, $e^{\pm}$, n)
– 3 rings of 12 position sensitive X3 silicon-strip detectors (1000 µm) by Micron
– 2 end cap detectors from 4 QQQ3 segmented detectors by Micron
– 320 channels readout with standard analog DAQ

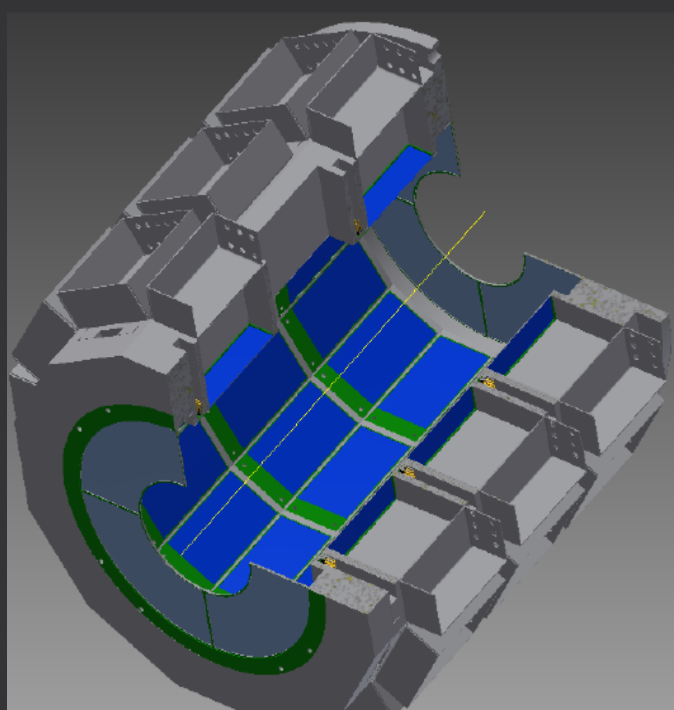

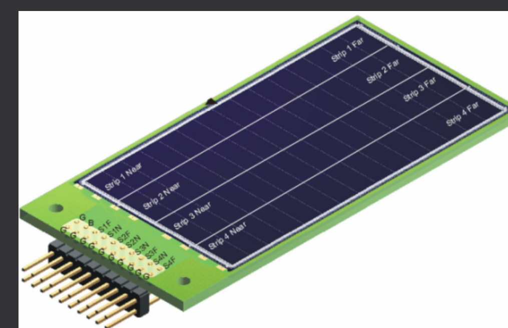

# Nuclear Astrophysics (IV)

## ELISSA (INFN Catania & ELI-NP)

– array of position sensitive silicon strip detectors
– high energy resolution (~50keV at 5.8MeV) and detection efficiency (>95%)
– small sensitivity to main background channels ($\gamma$, $e^{\pm}$, n)
– 3 rings of 12 position sensitive X3 silicon-strip detectors (1000 μm) by Micron
– 2 end cap detectors from 4 QQQ3 segmented detectors by Micron
– 320 channels readout with standard analog DAQ
– $^{7}$Li($\gamma$,$\alpha$)t: reconstruction of reaction kinematics
– p-process reactions: $^{24}$Mg($\gamma$,$\alpha$)$^{20}$Ne, $^{96}$Ru($\gamma$,$\alpha$)$^{92}$Mo

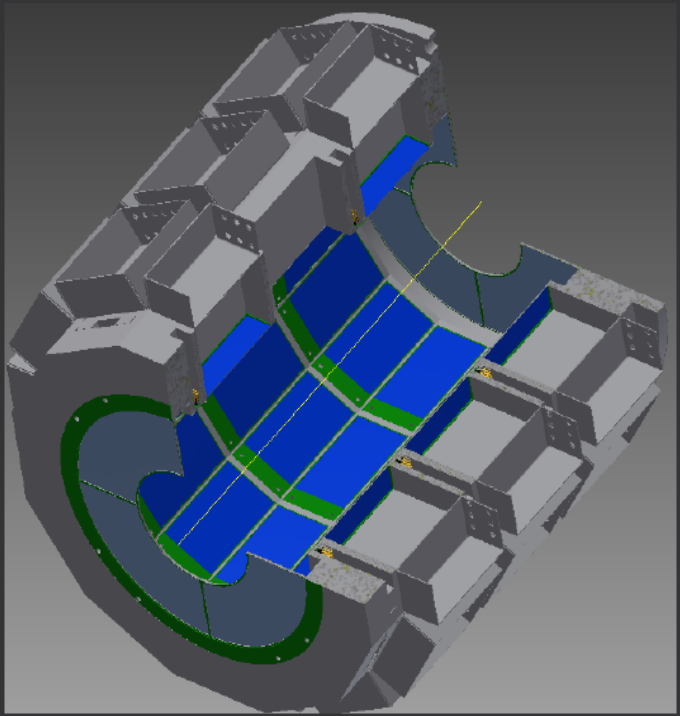

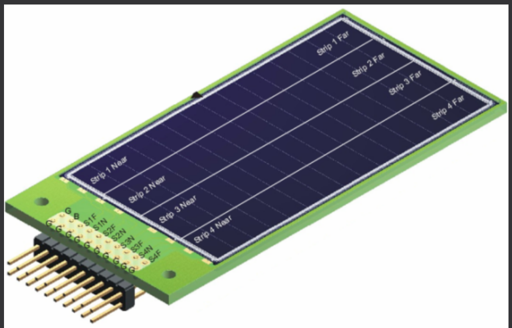

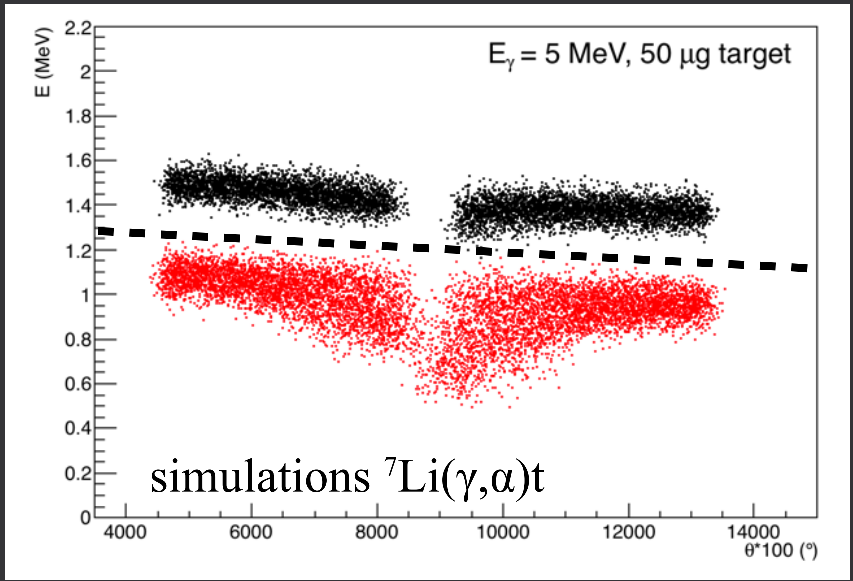

# Nuclear Astrophysics (V)

**Process $^{12}C(\alpha,\gamma)^{16}O$**

– relative rates of these reactions determine the $^{12}C/^{16}O$ ratio at the end of He burning

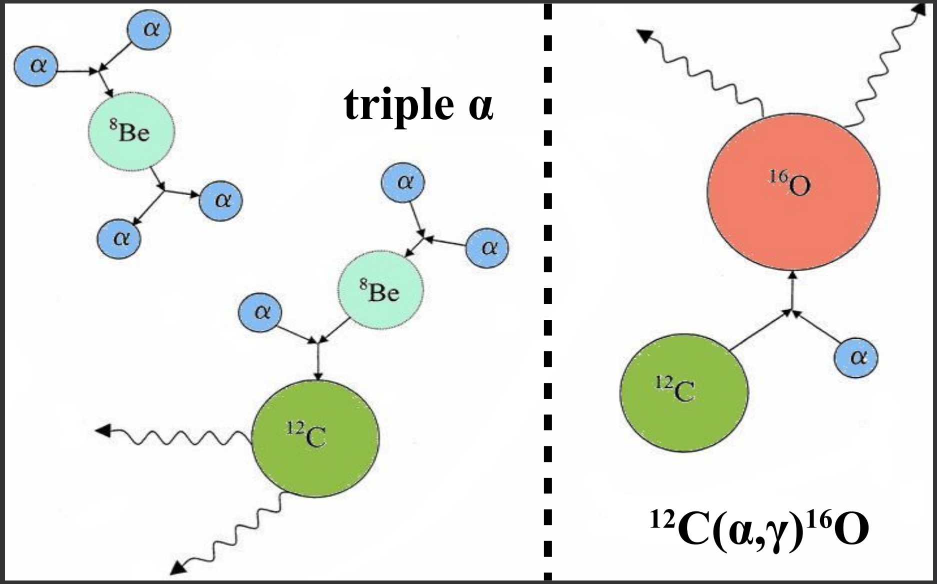


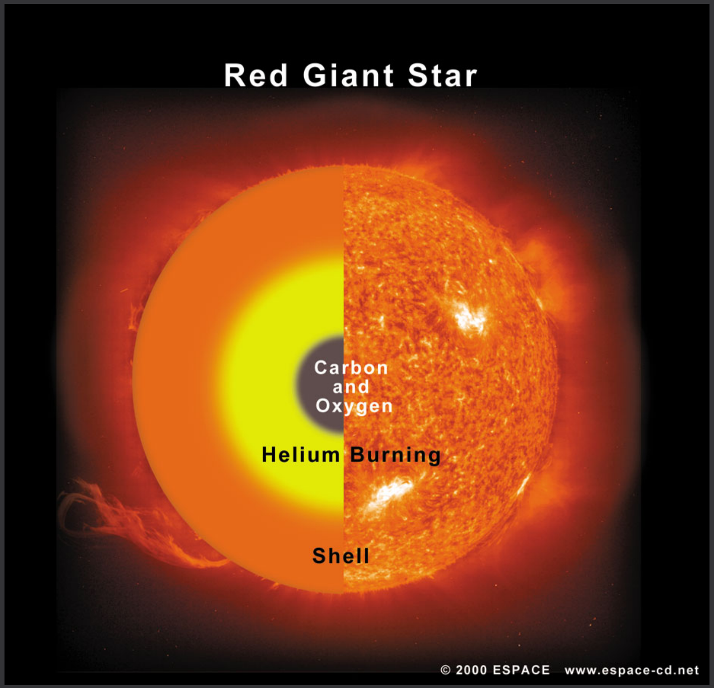

# Nuclear Astrophysics (V)

**Process $^{12}C(\alpha,\gamma)^{16}O$**

– relative rates of these reactions determine the $^{12}C/^{16}O$ ratio at the end of He burning

– L. Buchmann, Astro. J. Lett. 468 (1996) 127: S(300keV)≈170±20 keV·b

– high sensitivity...

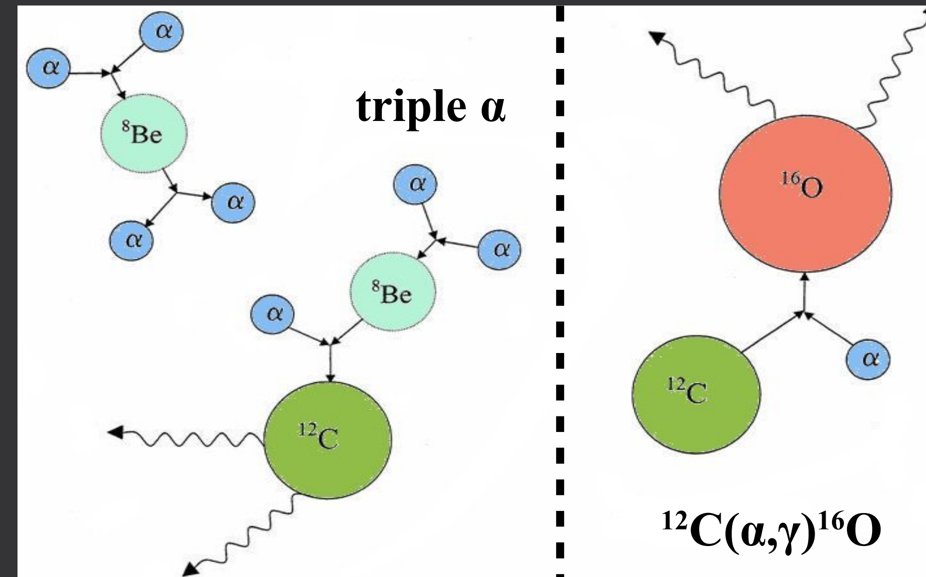


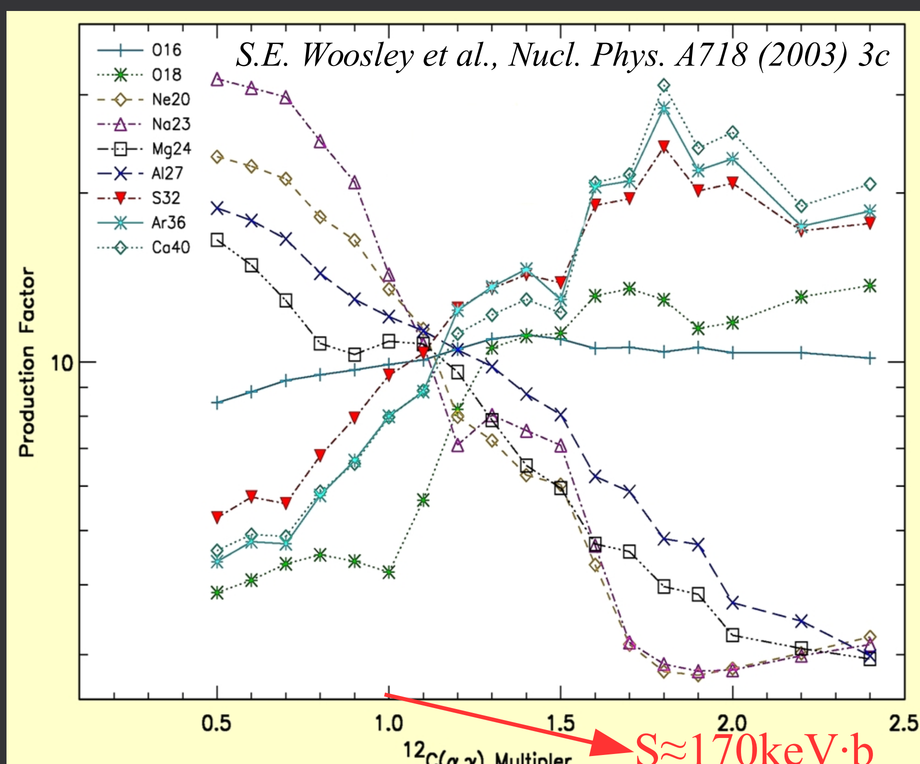


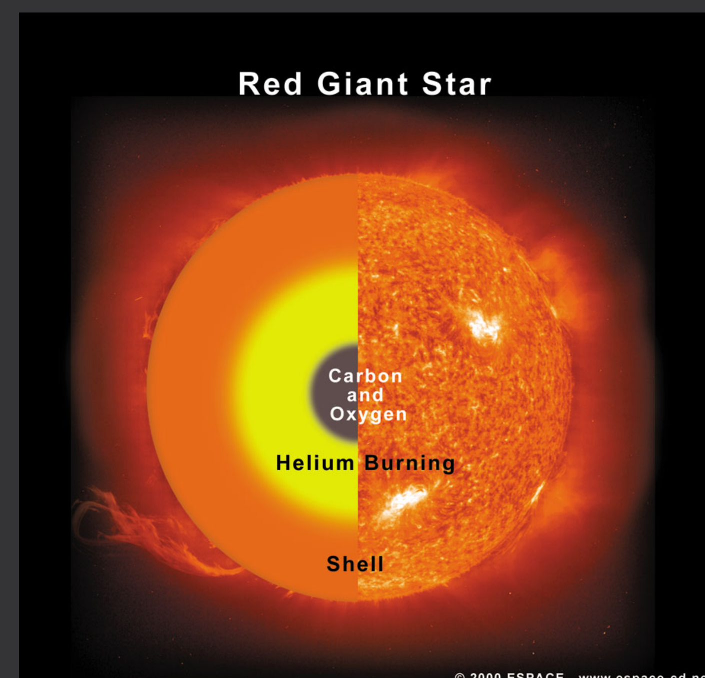

# Nuclear Astrophysics (V)

**Process $^{12}C(\alpha,\gamma)^{16}O$**

– relative rates of these reactions determine the $^{12}C/^{16}O$ ratio at the end of He burning
– L. Buchmann, Astro. J. Lett. 468 (1996) 127: $S(300 keV) \approx 170 \pm 20$ keV·b
– high sensitivity...
– on a poorly determined parameter

| Result @ 300 keV | Method & Source |
|---|---|
| $S_{E1}$ = 79(21) keV b | $^{16}N(\beta\alpha)$, Buchmann at al. (1994) |
| $S_{E1}$ = 101(17) keV b | sub-coulomb α transfer, Brune et al. (1999) |
| $S_{E1}$ = 80(20) keV b | elastic scattering, Tischhauser et al. (2002) |
| $S_{E2}$ = 120(60) keV b | compilation, NACRE (1999) |
| $S_{E2}$ = 42(20) keV b | sub-coulomb α transfer, Brune et al. (1999) |
| $S_{E2}$ = 85(30) keV b | direct measurement, Kunz et al. (2002) |
| $S_{E2}$ = 53(15) keV b | elastic scattering, Tischhauser et al. (2002) |
| $S_{total}$~ 170 keV b | Buchmann (1999) |

# Nuclear Astrophysics (VI)

**eTPC (University of Warsaw & ELI-NP)**
– active target Time Projection Chamber with electronic readout

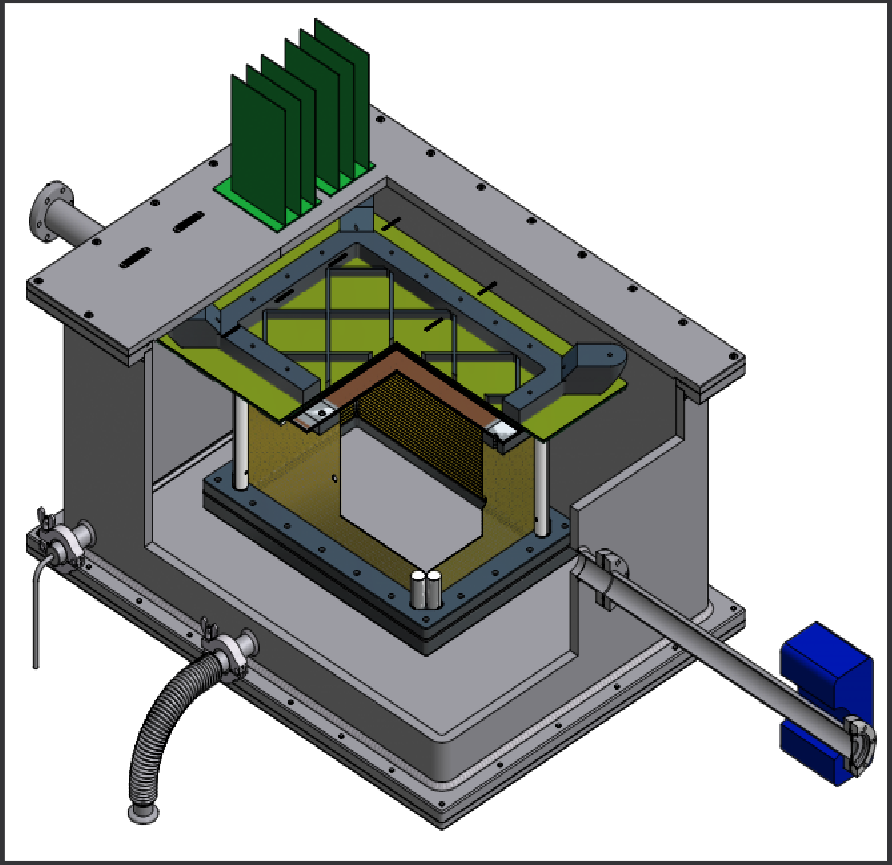

# Nuclear Astrophysics (VI)

**eTPC (University of Warsaw & ELI-NP)**

– active target Time Projection Chamber with electronic readout
– electron multiplication by a sequence of 35x20cm$^2$ GEM (Gas Electron Multipliers) foils
– the charge will be read by a u-v-w readout (grids crossing at 60°) mounted on a circuit board

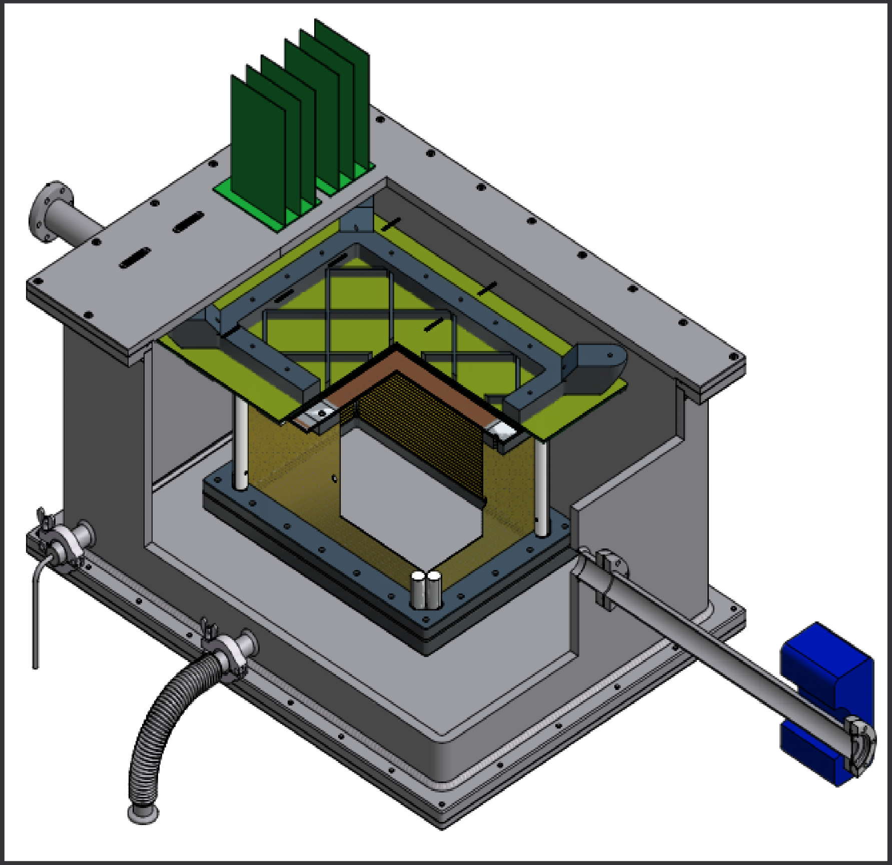

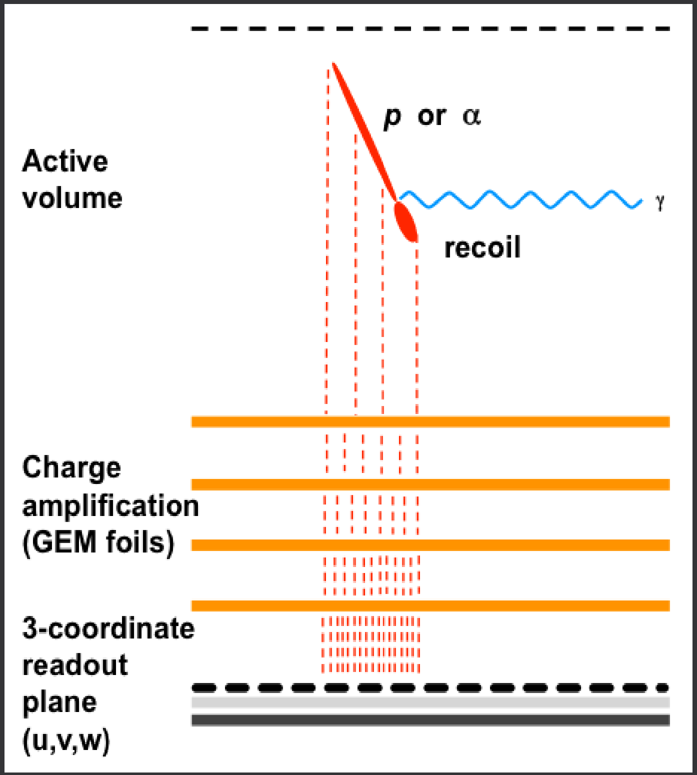

# Nuclear Astrophysics (VI)

**eTPC (University of Warsaw & ELI-NP)**

– active target Time Projection Chamber with electronic readout
– electron multiplication by a sequence of 35x20cm$^2$ GEM (Gas Electron Multipliers) foils
– the charge will be read by a u-v-w readout (grids crossing at 60°) mounted on a circuit board
– $^{16}O(\gamma,\alpha)^{12}C$: $CO_2$ gas at 100mbar, $E_\gamma \sim 8MeV$
– $^{19}F(\gamma,p)^{18}O$: $CF_4$ gas at 100mbar, $E_\gamma \sim 8MeV$
– $^{22}Ne(\gamma,\alpha)^{18}O$: $^{22}Ne$ gas at 100mbar, $E_\gamma \sim 10MeV$

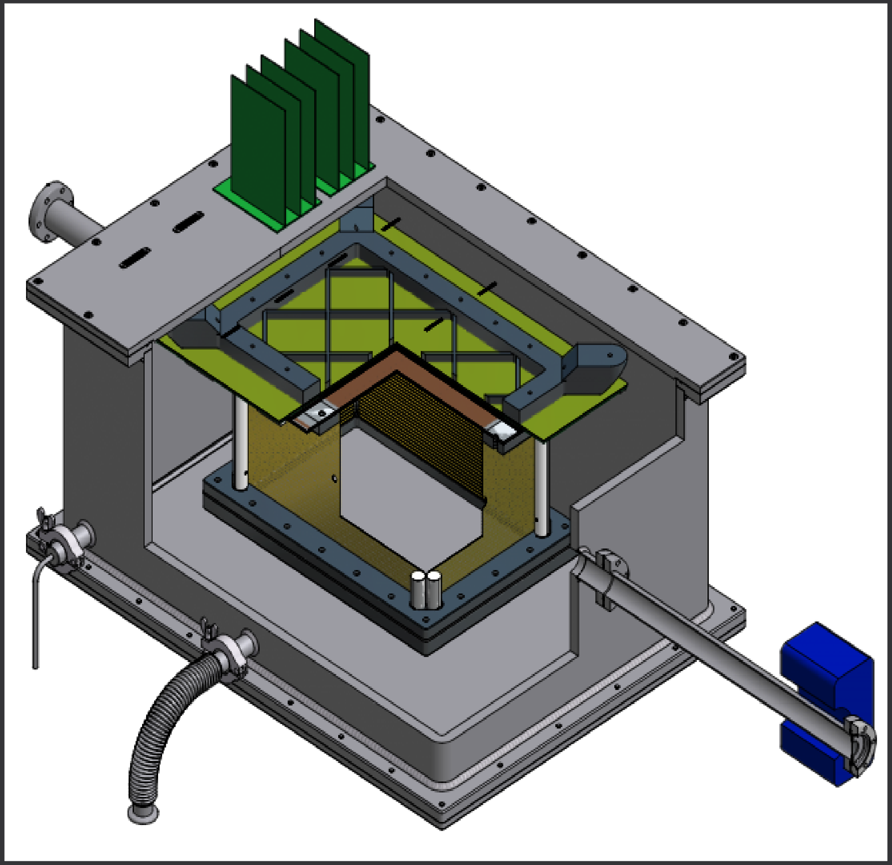

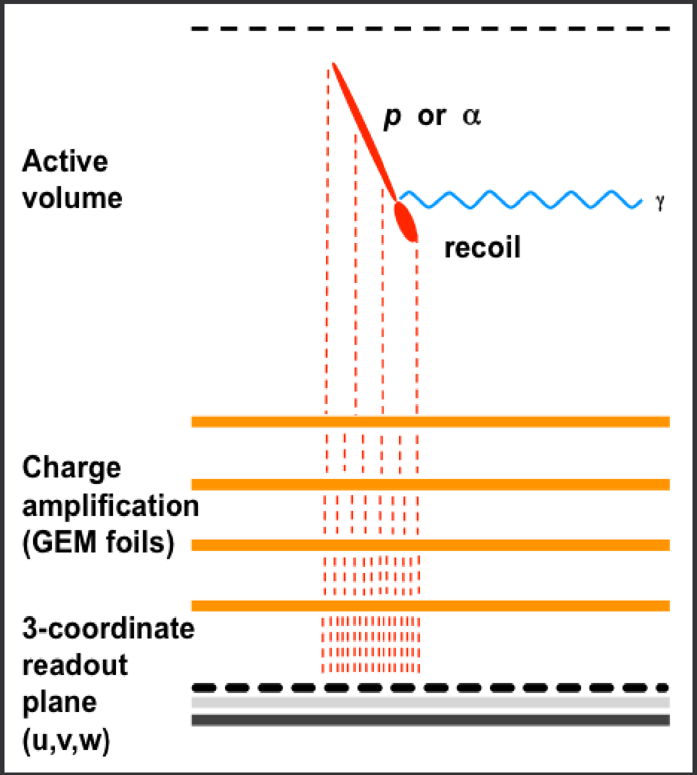

# Exotic nuclei (I)

**Neutron-rich nuclei extracted from RIBs created via actinide photo-fission**

# Exotic nuclei (I)

**Neutron-rich nuclei extracted from RIBs created via actinide photo-fission**
– nuclear EOS $e=e(\rho,\delta)$: energy per nucleon as function of nucleon density and relative neutron excess

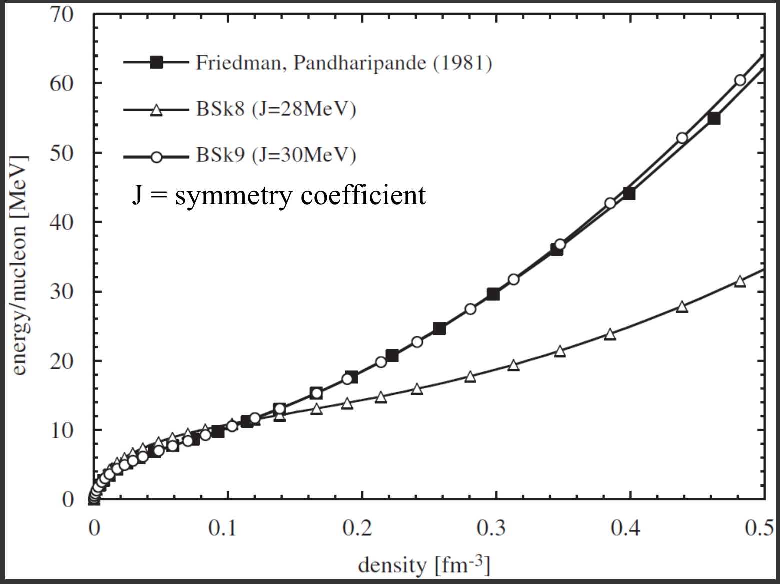

# Exotic nuclei (I)

**Neutron-rich nuclei extracted from RIBs created via actinide photo-fission**

– nuclear EOS $e=e(\rho,\delta)$: energy per nucleon as function of nucleon density and relative neutron excess

– r-process nucleosynthesis: masses, mass&charge $\rho(r)$, $\tau_\beta$ lifetime, β-delayed $P_n$

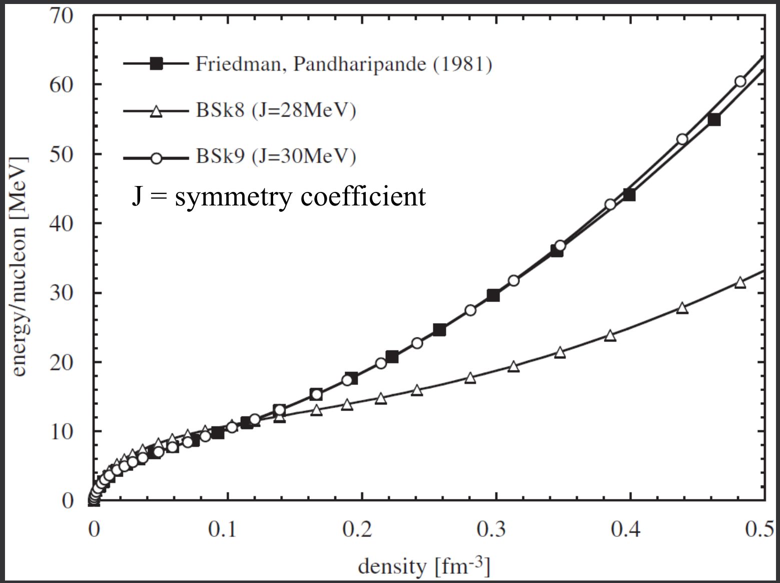

# Exotic nuclei (I)

**Neutron-rich nuclei extracted from RIBs created via actinide photo-fission**

– nuclear EOS $e=e(\rho,\delta)$: energy per nucleon as function of nucleon density and relative neutron excess
– r-process nucleosynthesis: masses, mass&charge $\rho(r)$, $\tau_\beta$ lifetime, β-delayed $P_n$
– tests of nuclear structure models: above + α–/β–/γ–spectroscopy, nuclear moments, charge radii, etc.
– region of sudden deformation onset A~100; region of doubly-magic $^{132}Sn$

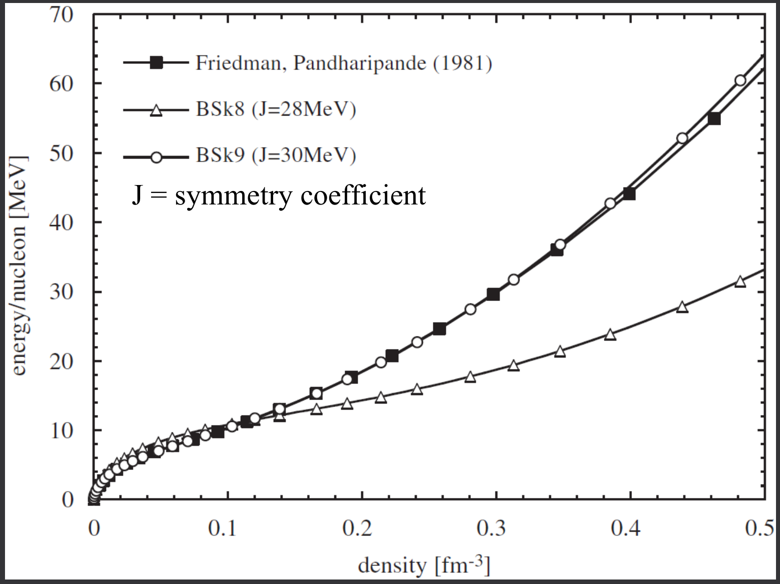

# Exotic nuclei (I)

**Neutron-rich nuclei extracted from RIBs created via actinide photo-fission**

– nuclear EOS ***e=e(ρ,δ)***: energy per nucleon as function of nucleon density and relative neutron excess
– r-process nucleosynthesis: masses, mass&charge ρ(r), $\tau_\beta$ lifetime, β-delayed $P_n$
– tests of nuclear structure models: above + α–/β–/γ–spectroscopy, nuclear moments, charge radii, etc.
– region of sudden deformation onset A~100; region of doubly-magic $^{132}$Sn

r-process nucleosynthesis: rapid neutron capture
– $\tau_\beta > \tau_{n\gamma} \sim 1/r_{n\gamma} \sim 1/(n_n \sigma_{n\gamma})$ at high neutron density (n,γ) more likely than β-decay (and than (γ,n))
– heavier nuclei build-up along isotopic chain → neutron-rich isotopes

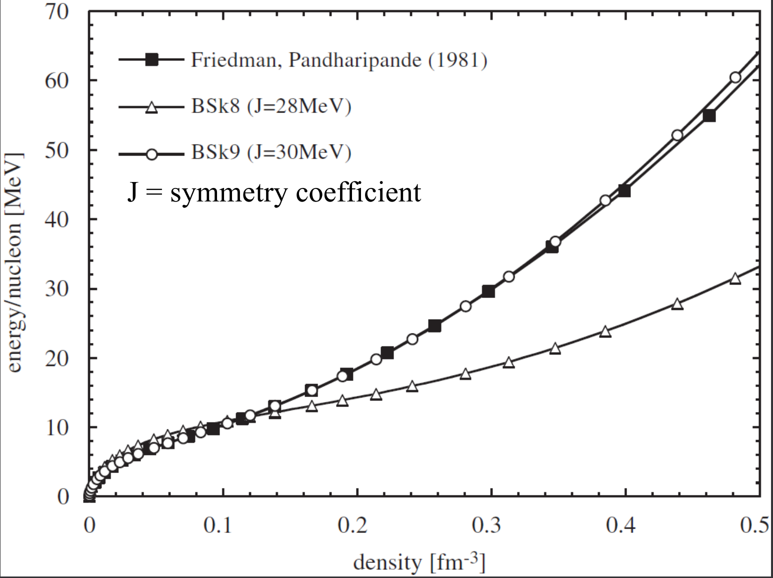


M. Arnould et al., Phys. Rep. 450 (2007) 97

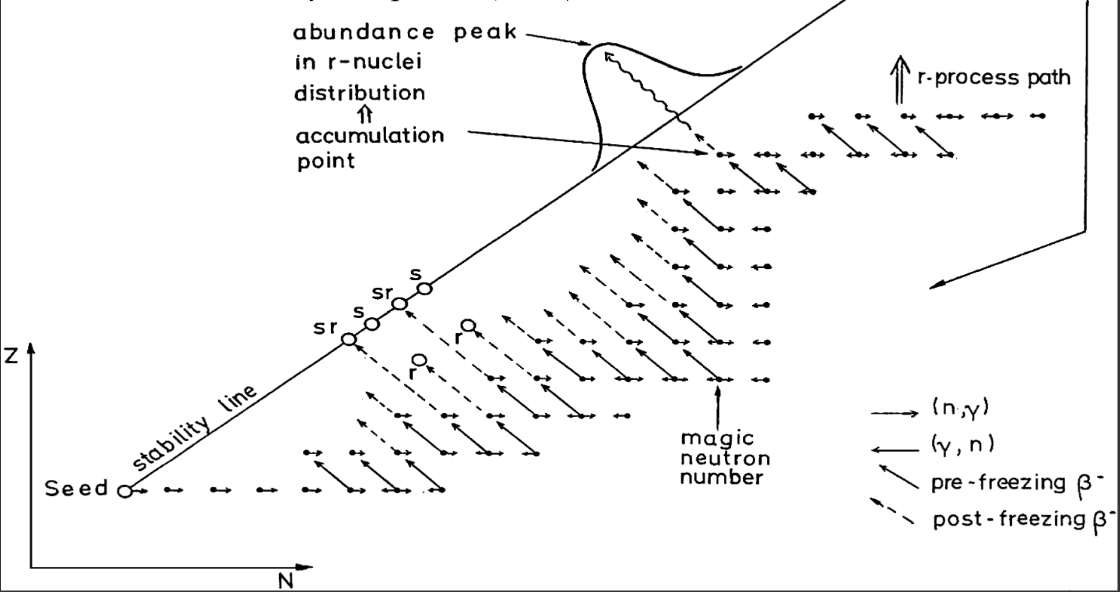

# Exotic nuclei (I)

**Neutron-rich nuclei extracted from RIBs created via actinide photo-fission**

– nuclear EOS ***e=e(ρ,δ)***: energy per nucleon as function of nucleon density and relative neutron excess
– r-process nucleosynthesis: masses, mass&charge ρ(r), $\tau_\beta$ lifetime, β-delayed $P_n$
– tests of nuclear structure models: above + α–/β–/γ–spectroscopy, nuclear moments, charge radii, etc.
– region of sudden deformation onset A~100; region of doubly-magic $^{132}$Sn

r-process nucleosynthesis: rapid neutron capture
– $\tau_\beta > \tau_{n\gamma} \sim 1/r_{n\gamma} \sim 1/(n_n \sigma_{n\gamma})$ at high neutron density (n,γ) more likely than β-decay (and than (γ,n))
– heavier nuclei build-up along isotopic chain → neutron-rich isotopes
– $\tau_\beta$ decreases away from stability line and $\tau_{\gamma n}$ decreases towards neutron dripline
– the isotopic chain stops and $\beta^-$-decay (n→p) moves the process to next isotopic chain

$$r_{\gamma,n}(T) \sim \langle \sigma v \rangle_{n,\gamma} \exp(-S_n / k_B T)$$

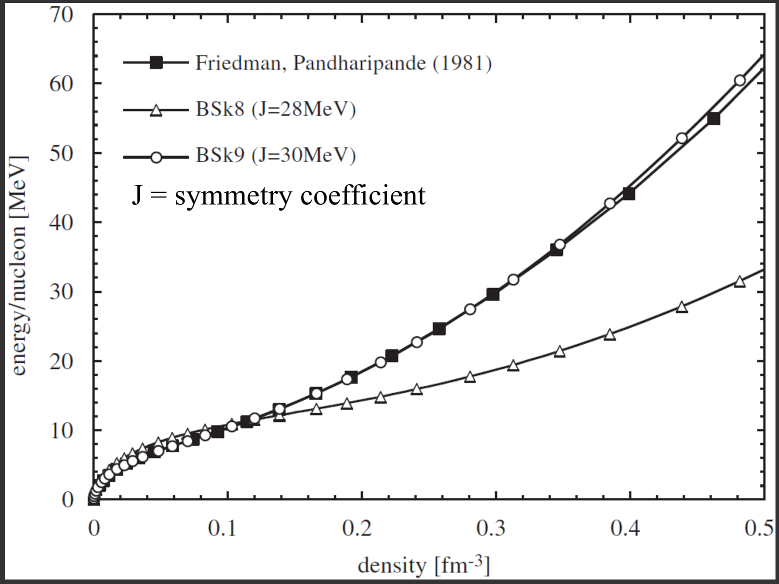


M. Arnould et al., Phys. Rep. 450 (2007) 97

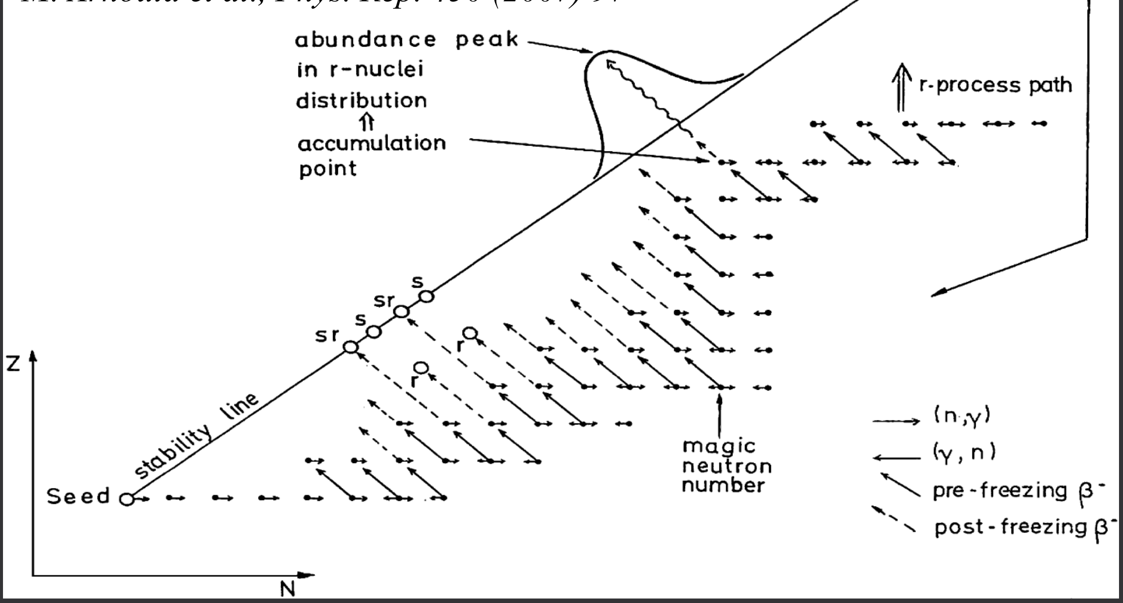

# Exotic nuclei (I)

**Neutron-rich nuclei extracted from RIBs created via actinide photo-fission**

– nuclear EOS $e = e(\rho,\delta)$: energy per nucleon as function of nucleon density and relative neutron excess
– r-process nucleosynthesis: masses, mass&charge $\rho(r)$, $\tau_\beta$ lifetime, β-delayed $P_n$
– tests of nuclear structure models: above + α–/β–/γ–spectroscopy, nuclear moments, charge radii, etc.
– region of sudden deformation onset A~100; region of doubly-magic $^{132}$Sn

r-process nucleosynthesis: rapid neutron capture
– $\boldsymbol{\tau_\beta > \tau_{n\gamma} \sim 1/r_{n\gamma} \sim 1/(n_n \sigma_{n\gamma})}$ at high neutron density (n,γ) more likely than β-decay (and than (γ,n))
– heavier nuclei build-up along isotopic chain → neutron-rich isotopes
– $\tau_\beta$ decreases away from stability line and $\tau_{\gamma n}$ decreases towards neutron dripline
– the isotopic chain stops and $\beta^-$-decay (n→p) moves the process to next isotopic chain
– close to neutron drip line, β-delayed neutron emission possible
– when neutron shell is filled: $S_n$ stays low and r-process path moves along constant N → **waiting points**

$$r_{\gamma,n}(T) \sim \langle \sigma v \rangle_{n,\gamma} \exp(-S_n/k_B T)$$

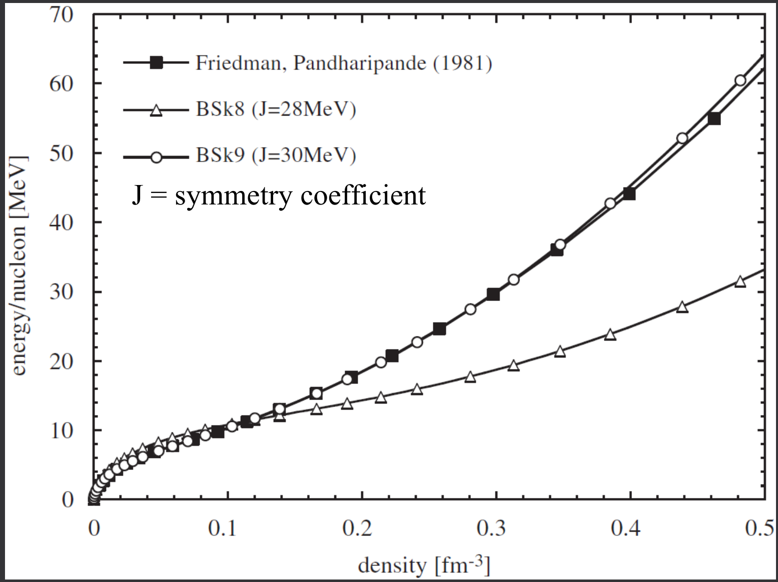


*M. Arnould et al., Phys. Rep. 450 (2007) 97*

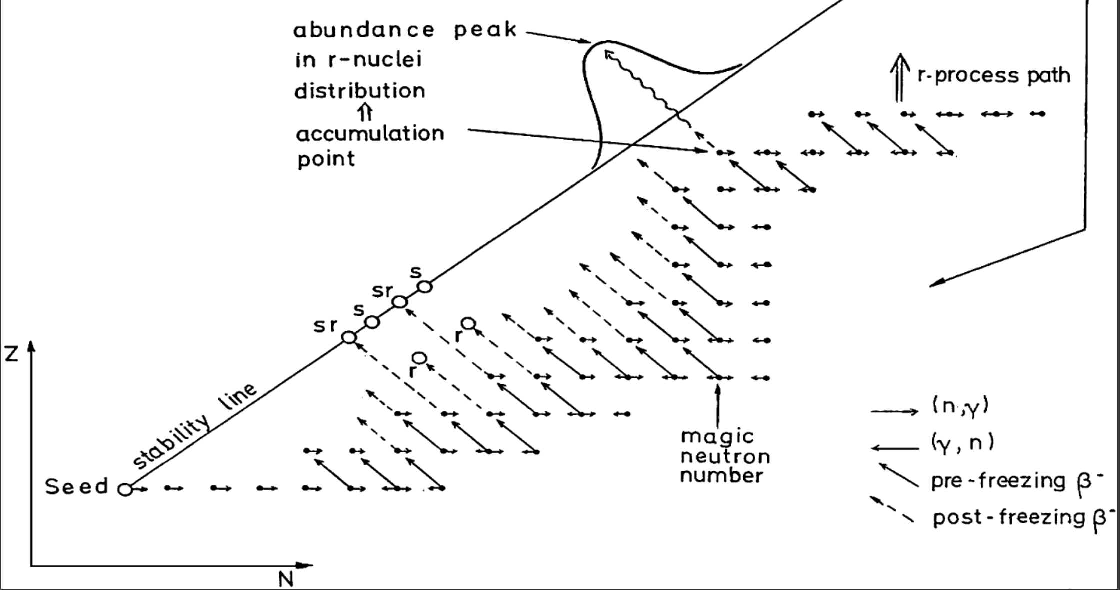

# Exotic nuclei (II)

– r-process: half of elements above Fe (the other half: s-process)
– unclear reaction path in nuclide chart: $^{80}$Zn(Z=30,N=50), $^{130}$Cd(Z=48,N=82)
– unclear astronomical site: probably in supernovae core colapse

# Exotic nuclei (II)

– r-process: half of elements above Fe (the other half: s-process)
– unclear reaction path in nuclide chart: $^{80}$Zn(Z=30,N=50), $^{130}$Cd(Z=48,N=82)
– unclear astronomical site: probably in supernovae core colapse

RIBs (Radioctive Ion Beams) with neutron-rich nuclei:
– fragmentation or fission reactions

*M. Thoennessen, Rep. Prog. Phys. 76 (2013) 056301*

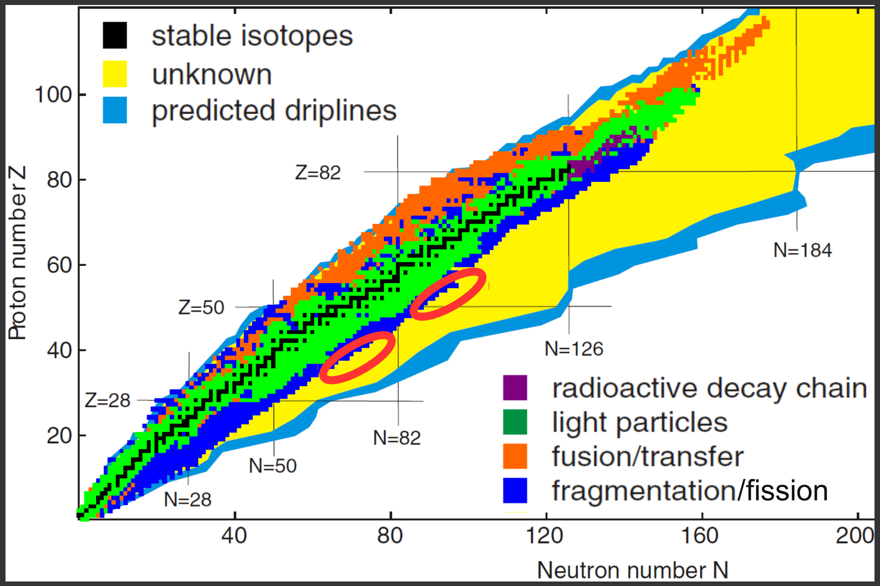

# Exotic nuclei (II)

– r-process: half of elements above Fe (the other half: s-process)
– unclear reaction path in nuclide chart: $^{80}$Zn(Z=30,N=50), $^{130}$Cd(Z=48,N=82)
– unclear astronomical site: probably in supernovae core colapse

RIBs (Radioctive Ion Beams) with neutron-rich nuclei:
– fragmentation or fission reactions
– **in-flight fragment separation**:
  - high energy beam fragmentation on thin target (+Coulex fission)
  - produces high energy RIBs → access to ~μs isomers but poorer beam quality (emittance, purity)
  - GSI (Germany), NSCL/MSU (USA), GANIL (France), FNLR (Russia), RIBF/RIKEN (Japan)

*M. Thoennessen, Rep. Prog. Phys. 76 (2013) 056301*

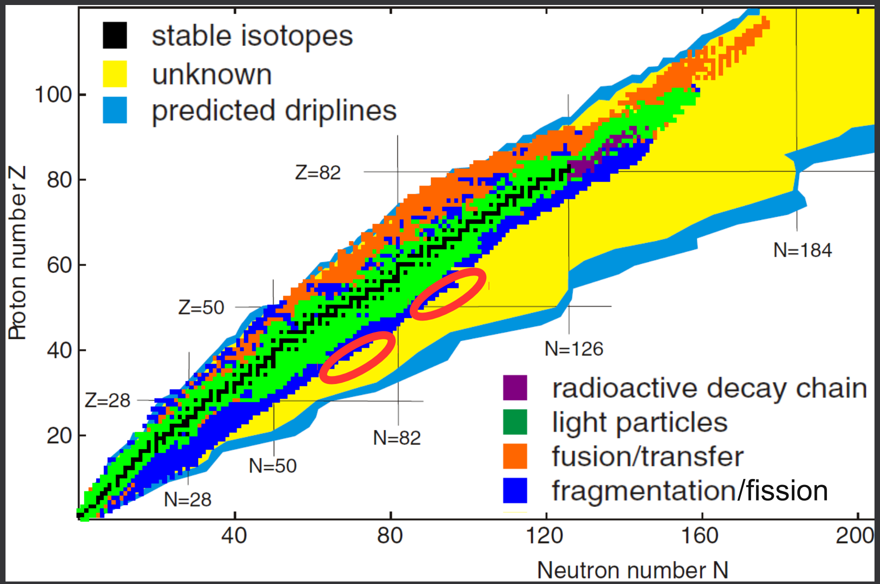


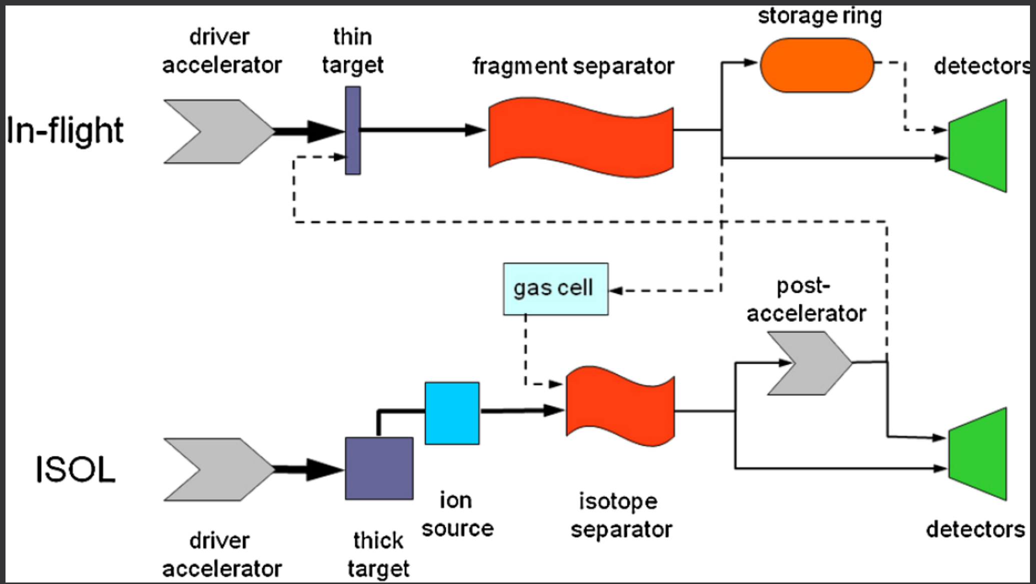

# Exotic nuclei (II)

– r-process: half of elements above Fe (the other half: s-process)
– unclear reaction path in nuclide chart: $^{80}$Zn(Z=30,N=50), $^{130}$Cd(Z=48,N=82)
– unclear astronomical site: probably in supernovae core colapse

RIBs (Radioctive Ion Beams) with neutron-rich nuclei:
– fragmentation or fission reactions
– **in-flight fragment separation**:
 - high energy beam fragmentation on thin target (+Coulex fission)
 - produces high energy RIBs → access to ~μs isomers but poorer beam quality (emittance, purity)
 - GSI (Germany), NSCL/MSU (USA), GANIL (France), FNLR (Russia), RIBF/RIKEN (Japan)
– **isotope separation on-line (ISOL)**:
 - various primary beams (ions, protons, neutrons, gammas) on thick targets in gas catchers
 - produces low energy RIBs → ms isomers but better beam quality (emittance, purity, bunching)
 - JYFL (Jyvaskyla), ISOLDE (CERN), ISAC (TRIUMF), CARIBU (ANL), SPIRAL (GANIL)

*M. Thoennessen, Rep. Prog. Phys. 76 (2013) 056301*

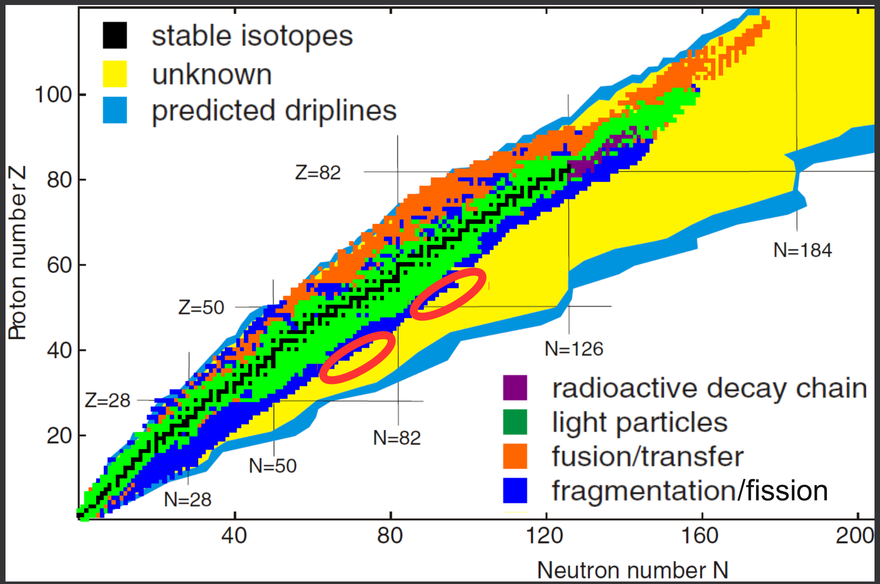


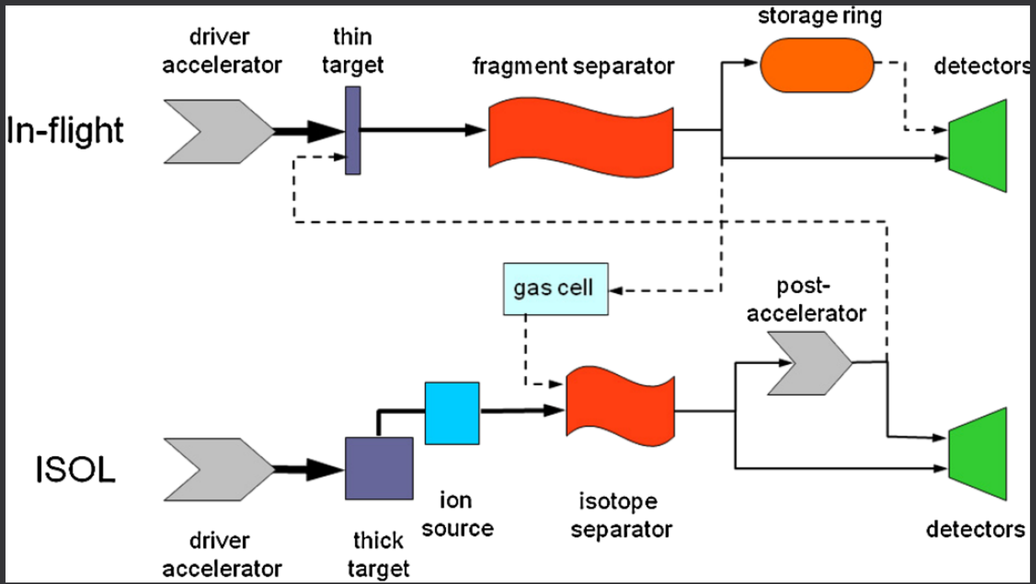

# Exotic nuclei (III)

– fragmentation and spallation produce more proton rich isotopes
– fission produces more neutron rich isotopes

*M. Pfützner et al., Rev. Mod. Phys. 84 (2012) 567*

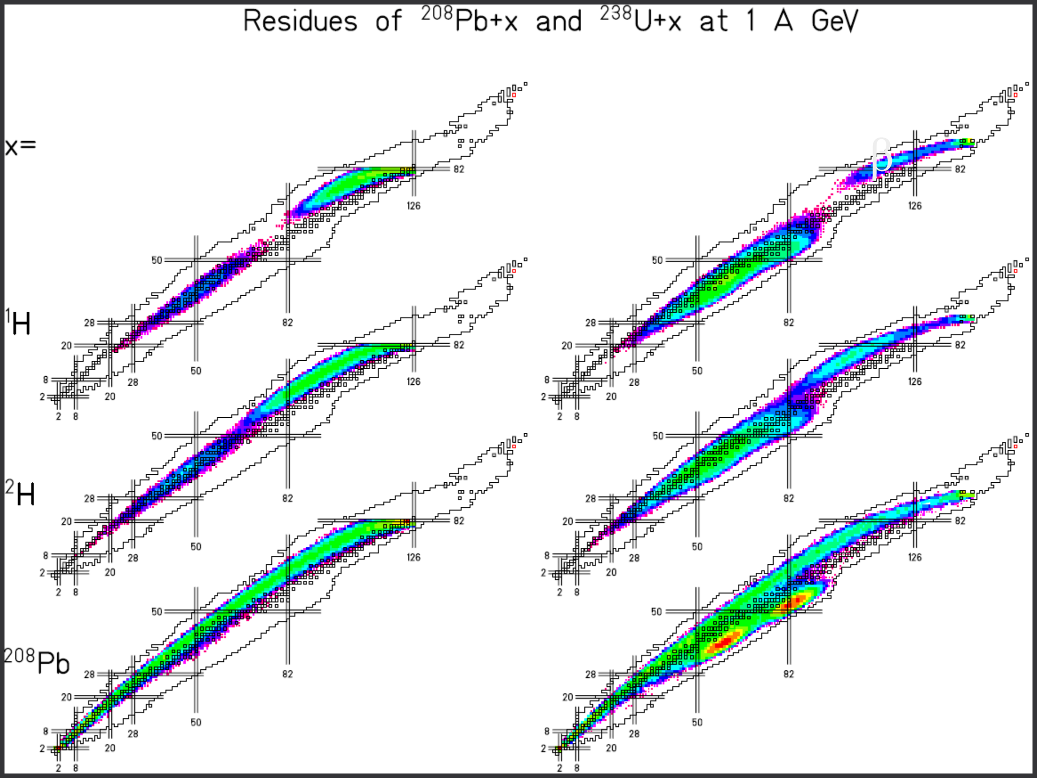

# Exotic nuclei (III)

– fragmentation and spallation produce more proton rich isotopes
– fission produces more neutron rich isotopes

ISOLDE (CERN): r-process waiting point at (Z=50,N=82)
p-induced $^{238}U$ fission → magnetic separation
→ RILIS (resonance ionization laser ion source)
→ neutron-rich $^{131,132}Cd$ and $\beta^-$-decay daughter $^{131,132}In$
→ β-delayed neutron data: $^{3}He$ counters + plastic scintillators

*M. Pfützner et al., Rev. Mod. Phys. 84 (2012) 567*

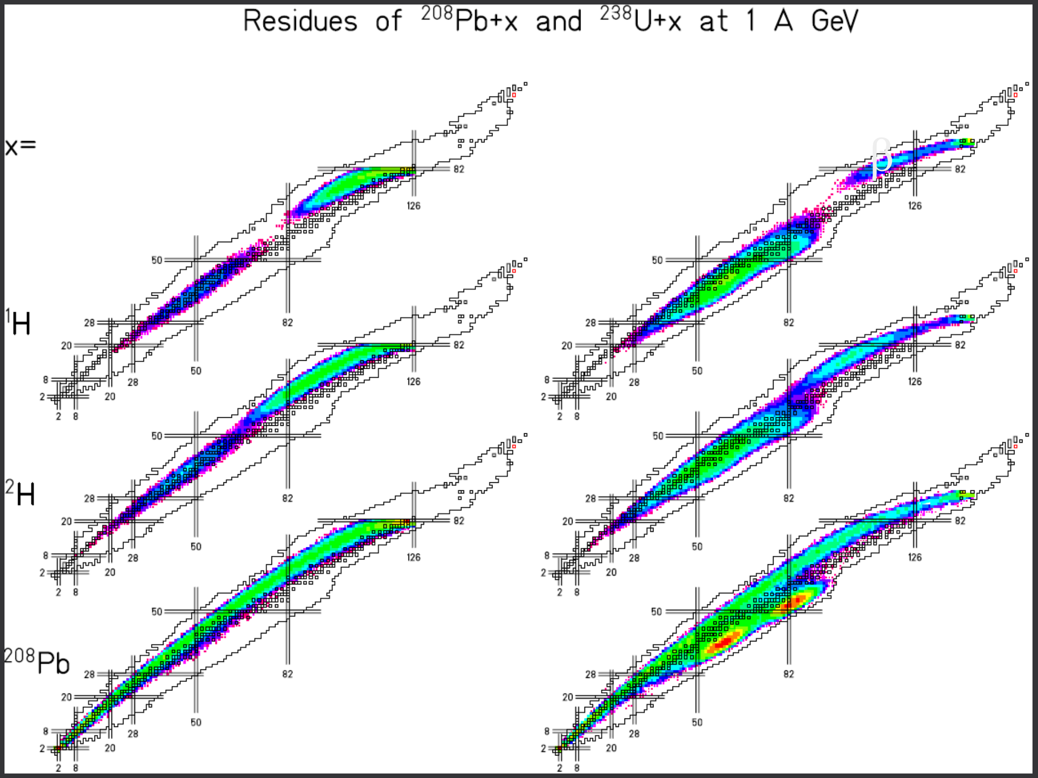

# Exotic nuclei (III)

– fragmentation and spallation produce more proton rich isotopes
– fission produces more neutron rich isotopes

ISOLDE (CERN): r-process waiting point at (Z=50,N=82)
p-induced $^{238}U$ fission → magnetic separation
→ RILIS (resonance ionization laser ion source)
→ neutron-rich $^{131,132}Cd$ and $\beta^-$-decay daughter $^{131,132}In$
→ β-delayed neutron data: $^3He$ counters + plastic scintillators

*M. Hannawald et al., Phys. Rev. C62 (2000) 054301*

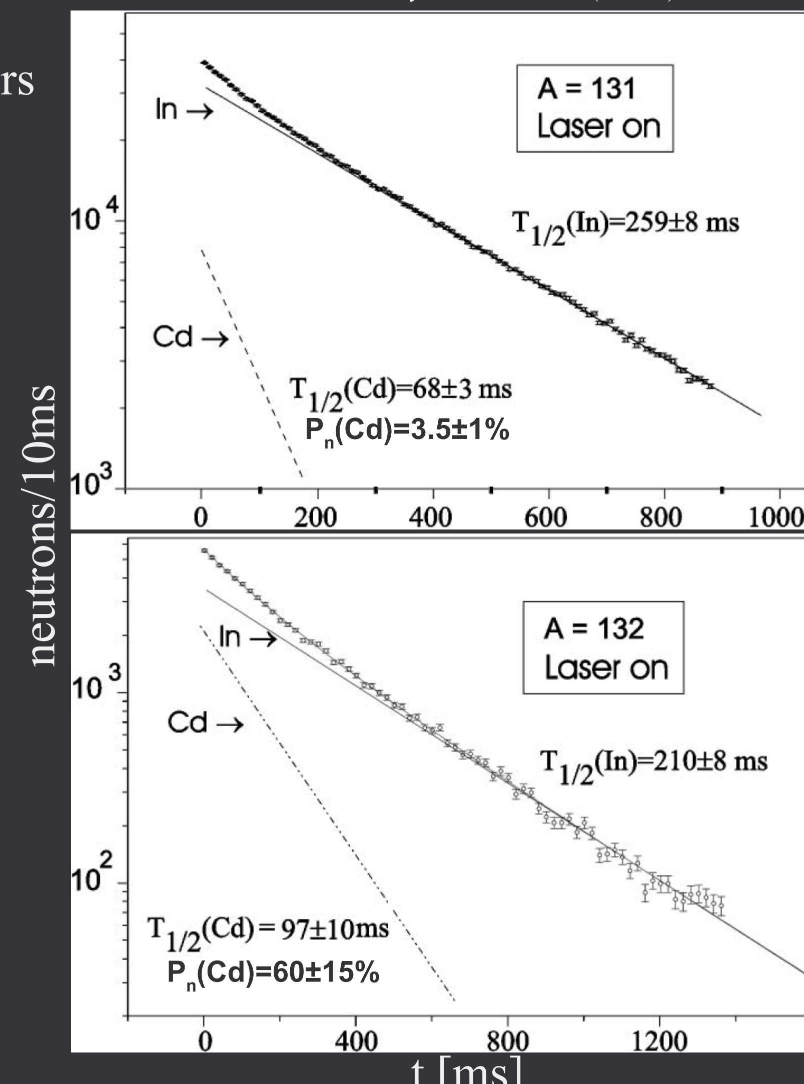


*M. Pfützner et al., Rev. Mod. Phys. 84 (2012) 567*

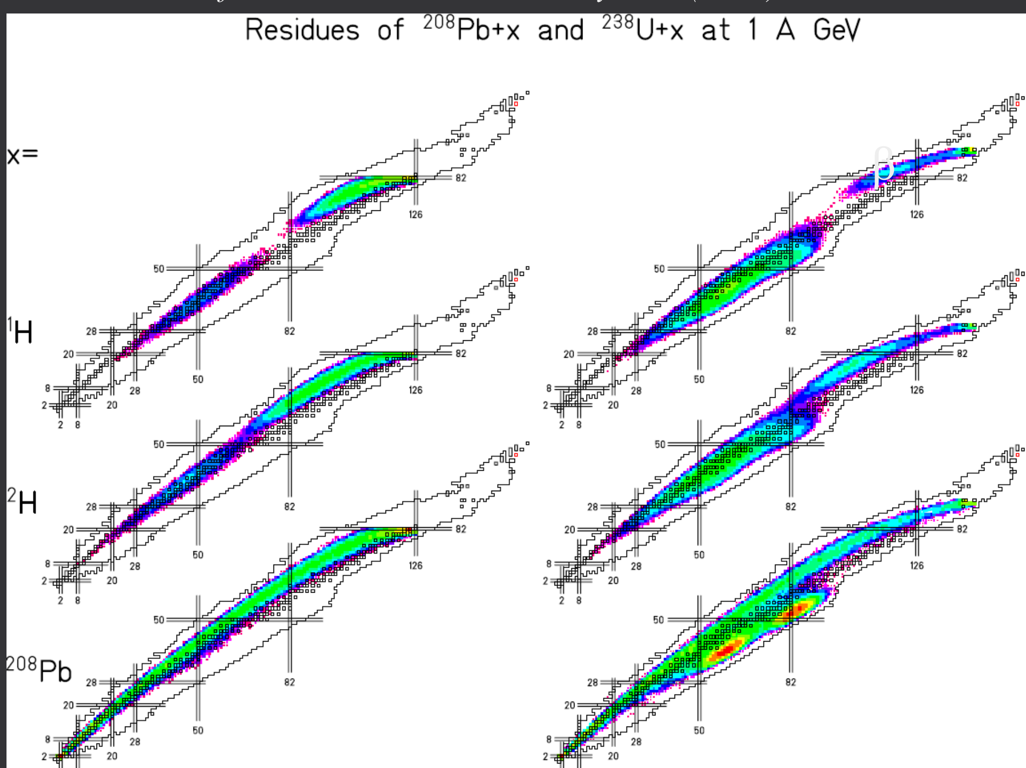

# Exotic nuclei (IV)

**IGISOL @ ELI-NP**:
– collimate beam in 10-18 MeV → cover **GDR**
– actinide thick target → **photofission**

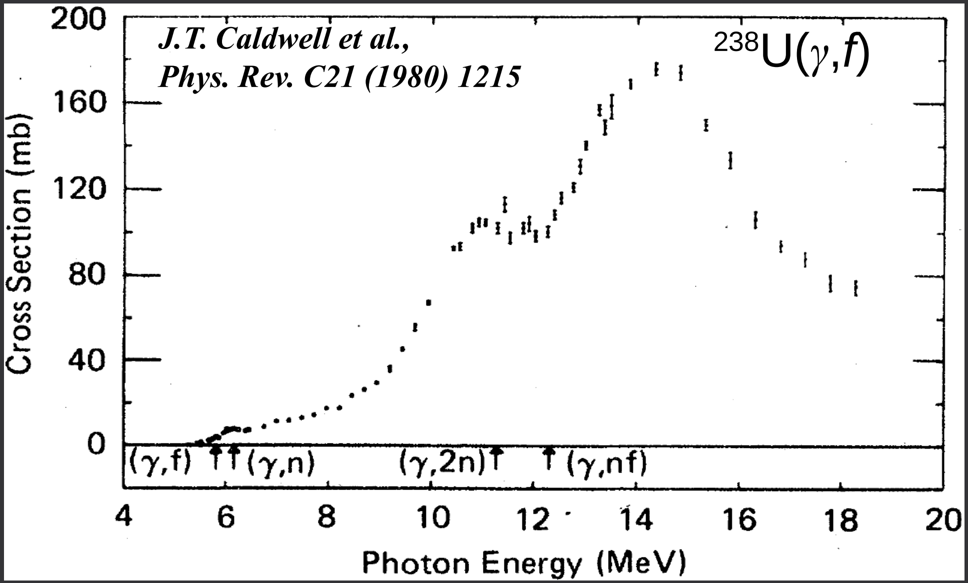


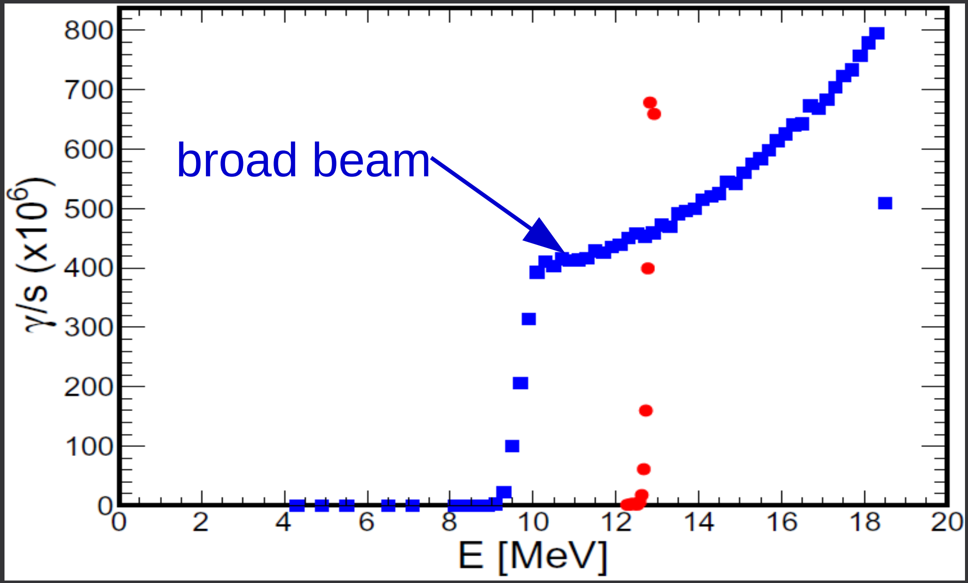

# Exotic nuclei (IV)

**IGISOL @ ELI-NP**:

– collimate beam in 10-18 MeV → cover **GDR**
– actinide thick target → **photofission**
– target in gas catcher + electric drift → **RIB**
– mass spectrometer → **neutron-rich** isotopes

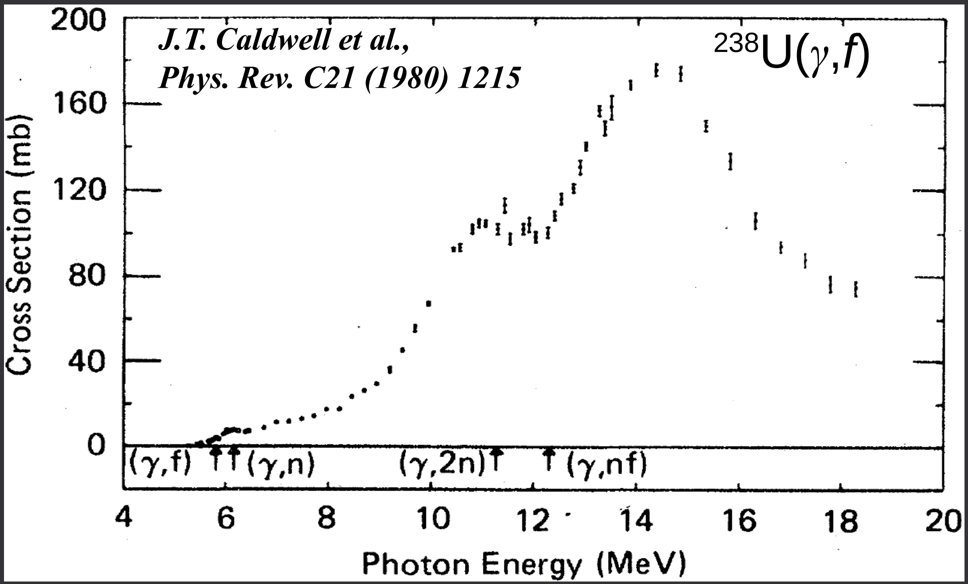


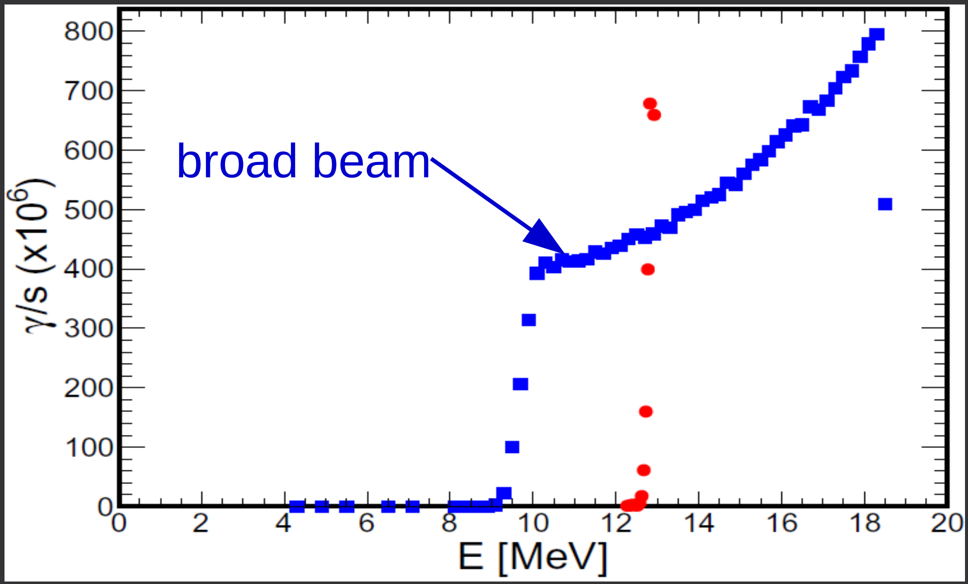

# Exotic nuclei (IV)

**IGISOL @ ELI-NP**:

– collimate beam in 10-18 MeV → cover **GDR**
– actinide thick target → **photofission**
– target in gas catcher + electric drift → **RIB**
– mass spectrometer → **neutron-rich** isotopes
– **refractory** elements: light region Zr-Mo-Rh and heavy rare-earths region around Ce
– complex **detection** systems: α, β, γ decays, electromagnetic moments, rms charge radii

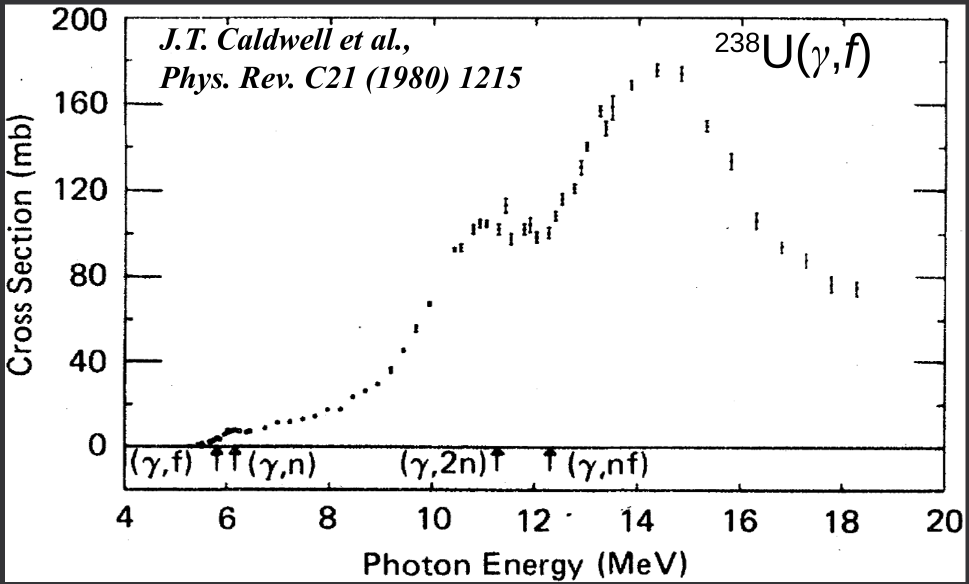


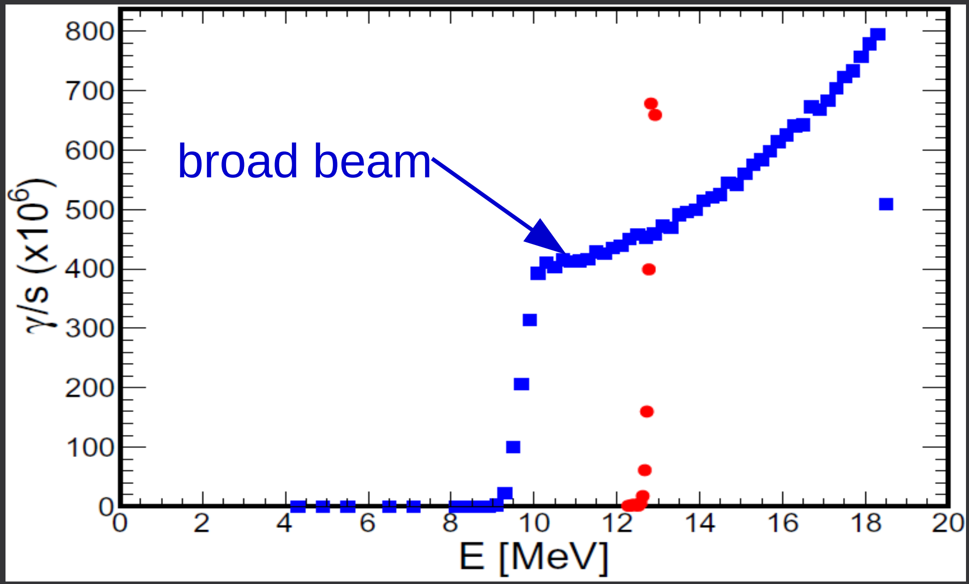

# Exotic nuclei (IV)

**IGISOL @ ELI-NP**:
- collimate beam in 10-18 MeV → cover **GDR**
- actinide thick target → **photofission**
- target in gas catcher + electric drift → **RIB**
- mass spectrometer → **neutron-rich** isotopes
- **refractory** elements: light region Zr-Mo-Rh and heavy rare-earths region around Ce
- complex **detection** systems: α, β, γ decays, electromagnetic moments, rms charge radii

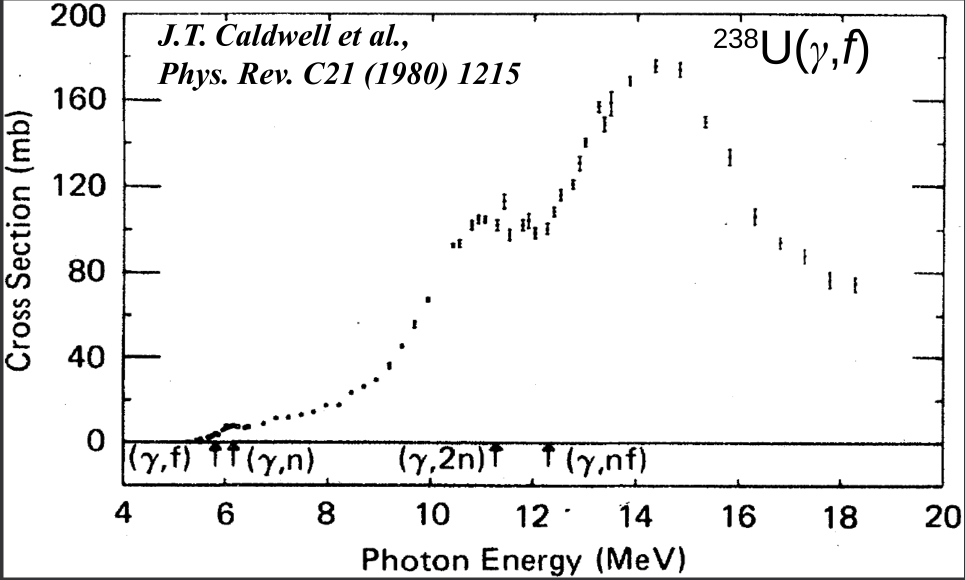


**$^{238}U$ ($^{232}Th$) target**:
- thick because σ(γ,f)~1b
- sliced in many thin foils: fast extraction, refractory isotopes
- tilted foils:
  (1) avoid hitting neighboring foils
  (2) same thickness, longer γ pathlength

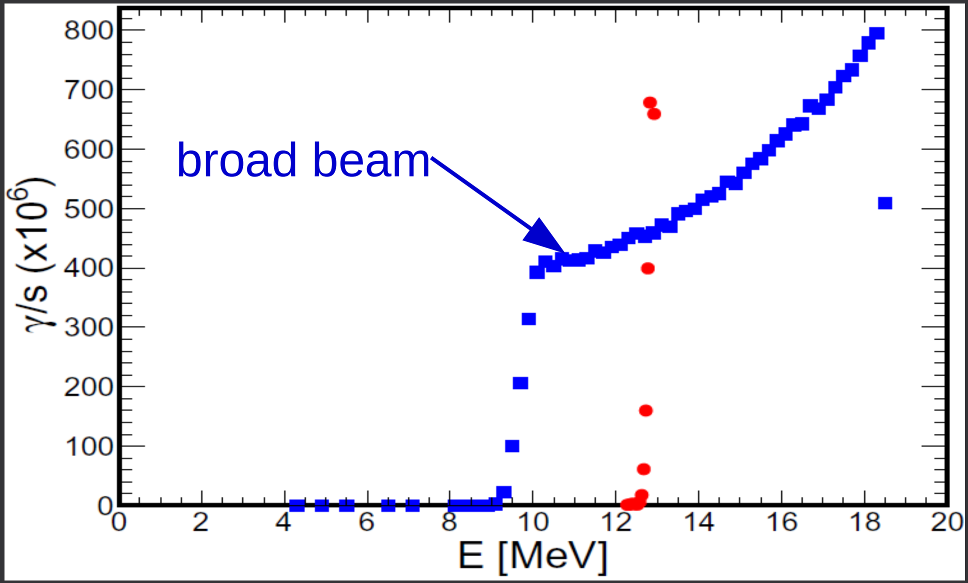

# Exotic nuclei (V)

**IGISOL beamline** (collaboration with GSI/Giessen):

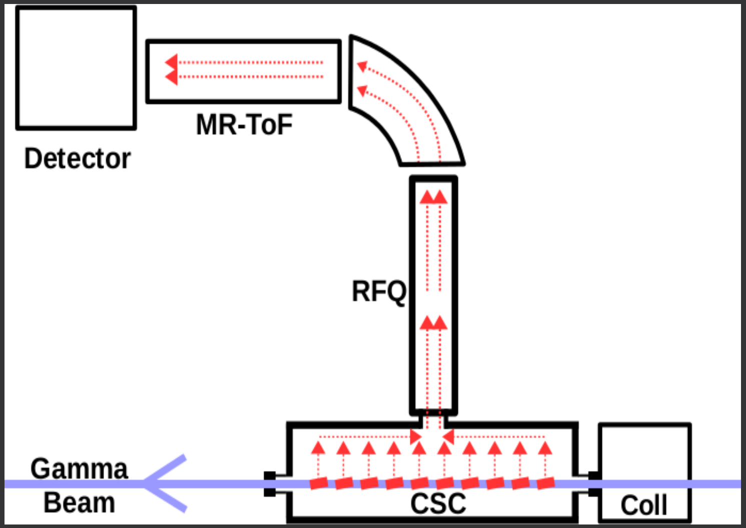

# Exotic nuclei (V)

**IGISOL beamline** (collaboration with GSI/Giessen):

CSC (Cryogenic Stopping Cell):
– gas catcher (He/Ar) with electric drift fields
– low T (~80K) to freeze impurities

RFQ (Radio Frequency Quadrupole):
– beam formation (cooling, mass filtering, CID, bunching)

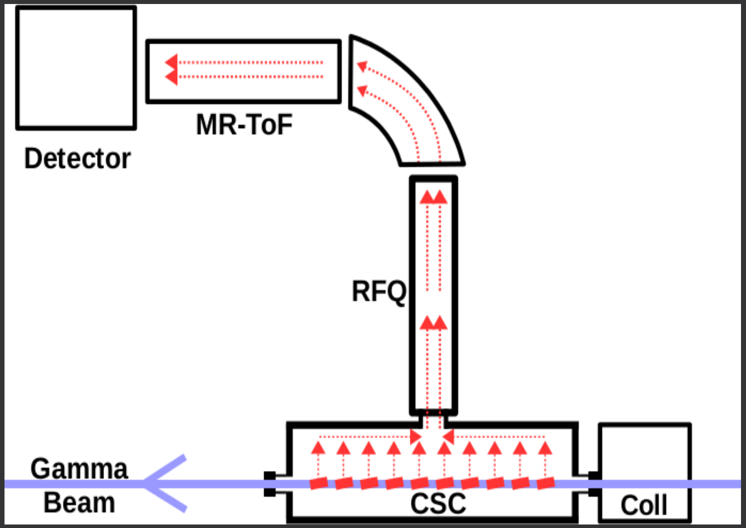

# Exotic nuclei (V)

**IGISOL beamline** (collaboration with GSI/Giessen):

CSC (Cryogenic Stopping Cell):
– gas catcher (He/Ar) with electric drift fields
– low T (~80K) to freeze impurities

RFQ (Radio Frequency Quadrupole):
– beam formation (cooling, mass filtering, CID, bunching)

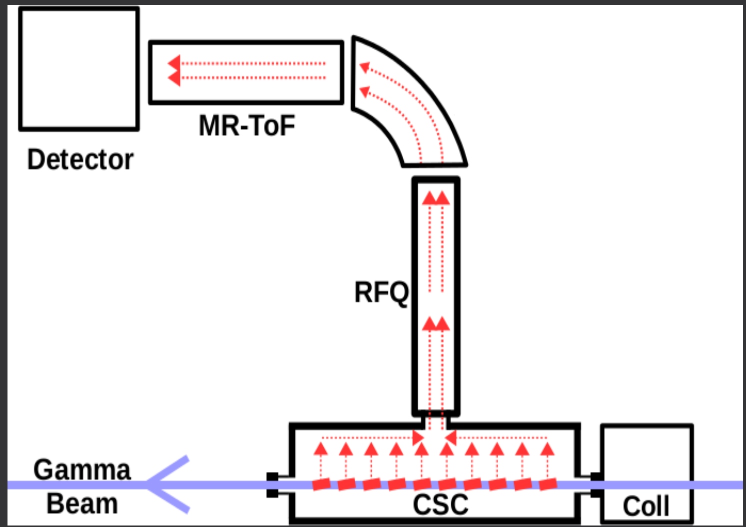


*T. Dickel et al., NIM B 376 (2016) 216*

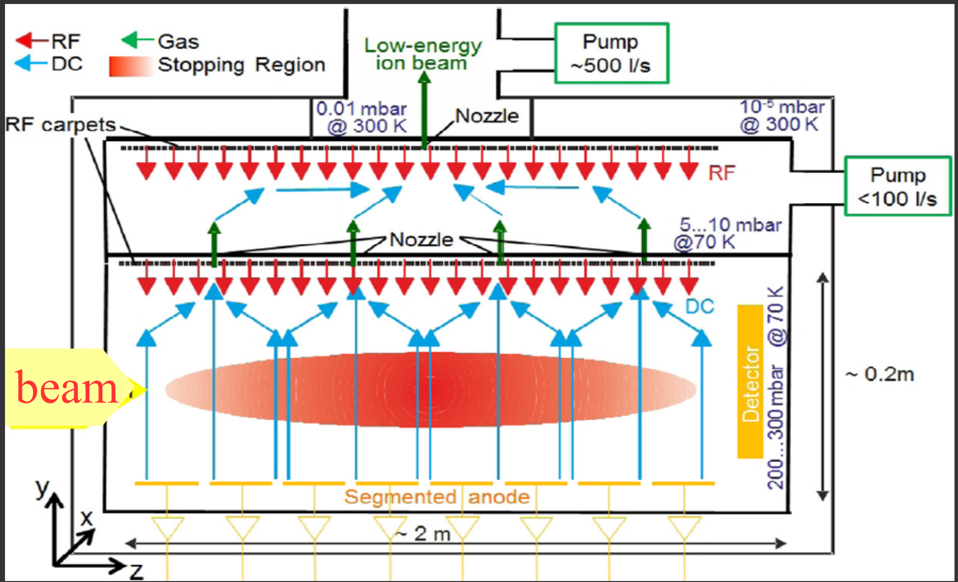

# Exotic nuclei (V)

**IGISOL beamline** (collaboration with GSI/Giessen):

CSC (Cryogenic Stopping Cell):
– gas catcher (He/Ar) with electric drift fields
– low T (~80K) to freeze impurities

RFQ (Radio Frequency Quadrupole):
– beam formation (cooling, mass filtering, CID, bunching)

MR-ToF (Multiple Reflection Time-of-Flight):
– high resolution mass spectrometer: $m/\Delta m = 10^5 - 10^6$
– α spectroscopy

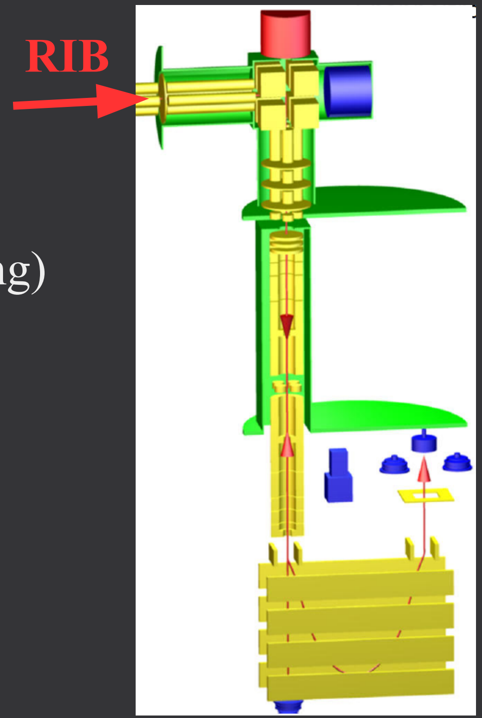


**MR-ToF**

| N | t [ms] | m/Δm |
|---|---|---|
| 260 | 5 | $2\cdot10^5$ |
| 520 | 10 | $4\cdot10^5$ |
| 1040 | 20 | $6\cdot10^5$ |

*T. Dickel et al., NIM B 376 (2016) 216*

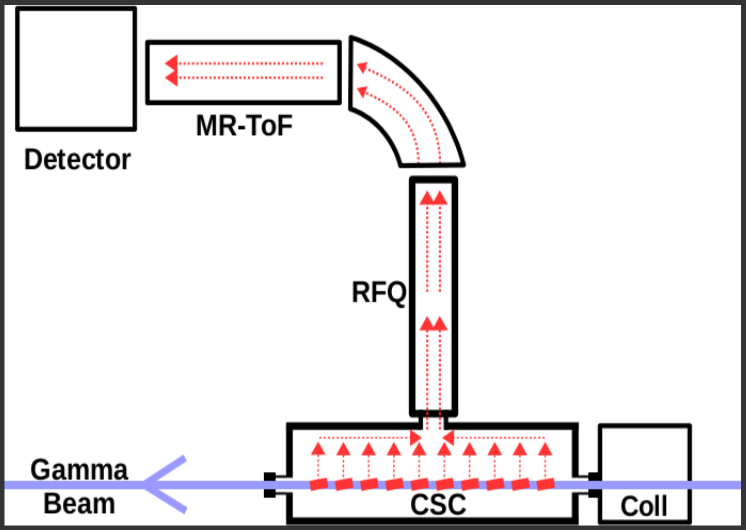


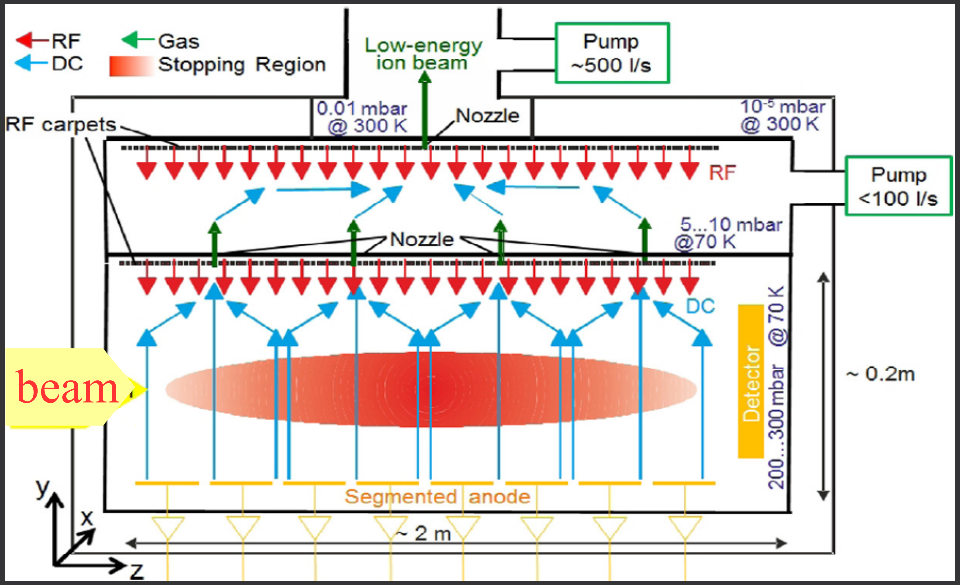

# Exotic nuclei (V)

**IGISOL beamline** (collaboration with GSI/Giessen):

CSC (Cryogenic Stopping Cell):
– gas catcher (He/Ar) with electric drift fields
– low T (~80K) to freeze impurities

RFQ (Radio Frequency Quadrupole):
– beam formation (cooling, mass filtering, CID, bunching)

MR-ToF (Multiple Reflection Time-of-Flight):
– high resolution mass spectrometer: $m/\Delta m = 10^5 - 10^6$
– α spectroscopy

**Detection systems** (collaboration with IPN Orsay):

β-decay tape station:
– β, γ decays and correlations
– HPGe (energy resolution), $LaBr_3$ (timing resolution)

colinear laser spectroscopy:
– electromagnetic moments, rms charge radii

RIB

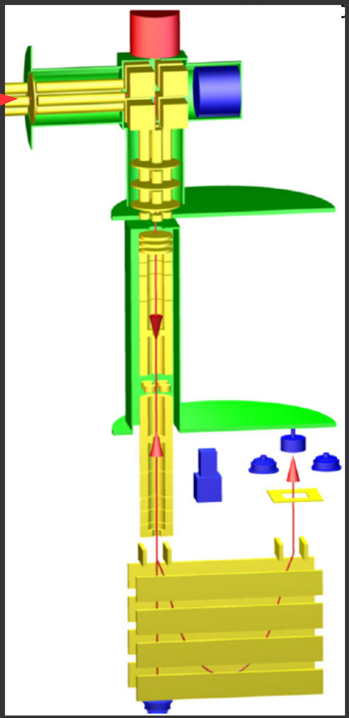

**MR-ToF**

| N | t [ms] | m/Δm |
|---|---|---|
| 260 | 5 | $2 \cdot 10^5$ |
| 520 | 10 | $4 \cdot 10^5$ |
| 1040 | 20 | $6 \cdot 10^5$ |

*T. Dickel et al., NIM B 376 (2016) 216*

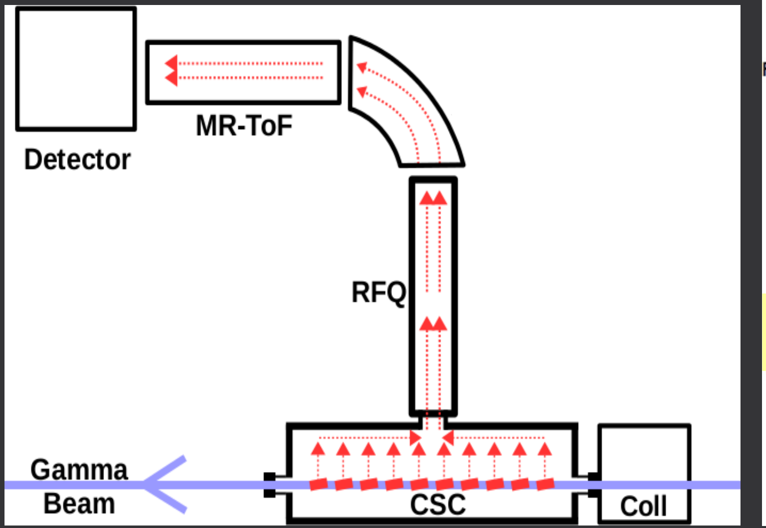


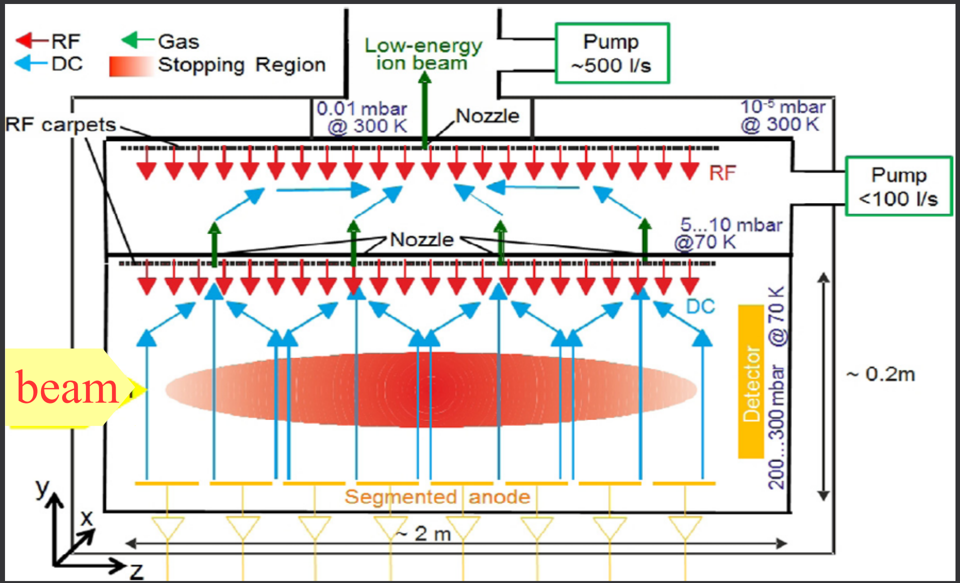

# Exotic nuclei (VI)

Geant4 simulations: photofission implemented

*P. Constantin, D.L. Balabanski, P.V. Cuong NIM B 372 (2016) 78*

# Exotic nuclei (VI)

Geant4 simulations: photofission implemented

*P. Constantin, D.L. Balabanski, P.V. Cuong NIM B 372 (2016) 78*

For day-one rate of $5 \cdot 10^{10} \gamma$/s:

**$10^7$ fissions/s**

Optimal beam: ***x*20**

# Exotic nuclei (VI)

Geant4 simulations: photofission implemented

*P. Constantin, D.L. Balabanski, P.V. Cuong NIM B 372 (2016) 78*

For day-one rate of $5 \cdot 10^{10}\gamma$/s:

**$10^7$ fissions/s**

Optimal beam: ***x*20**

Geant4 stopping (same as SRIM):

*J.F. Ziegler and J.M. Manoyan, NIM B 35 (1988) 215*

# Exotic nuclei (VI)

Geant4 simulations: photofission implemented

*P. Constantin, D.L. Balabanski, P.V. Cuong NIM B 372 (2016) 78*

For day-one rate of $5\cdot10^{10}\gamma$/s:

**$10^7$ fissions/s**

Optimal beam: ***x*20**

Geant4 stopping (same as SRIM):

*J.F. Ziegler and J.M. Manoyan, NIM B 35 (1988) 215*

Not so good for low v, high Z ions in high-Z media.

Two new q=Q/Z parameterizations:

*K. Shima et al., Nucl. Instr. Meth. 200 (1982) 605*

*G. Schiwietz, P.L. Grande, Nucl. Instr. Meth. B 175–177 (2001) 125*

# Exotic nuclei (VI)

Geant4 simulations: photofission implemented

*P. Constantin, D.L. Balabanski, P.V. Cuong NIM B 372 (2016) 78*

For day-one rate of $5 \cdot 10^{10} \gamma/s$:

**$10^7$ fissions/s**

Optimal beam: ***x*20**

Geant4 stopping (same as SRIM):

*J.F. Ziegler and J.M. Manoyan, NIM B 35 (1988) 215*

Not so good for low v, high Z ions in high-Z media.

Two new q=Q/Z parameterizations:

*K. Shima et al., Nucl. Instr. Meth. 200 (1982) 605*

*G. Schiwietz, P.L. Grande, Nucl. Instr. Meth. B 175–177 (2001) 125*

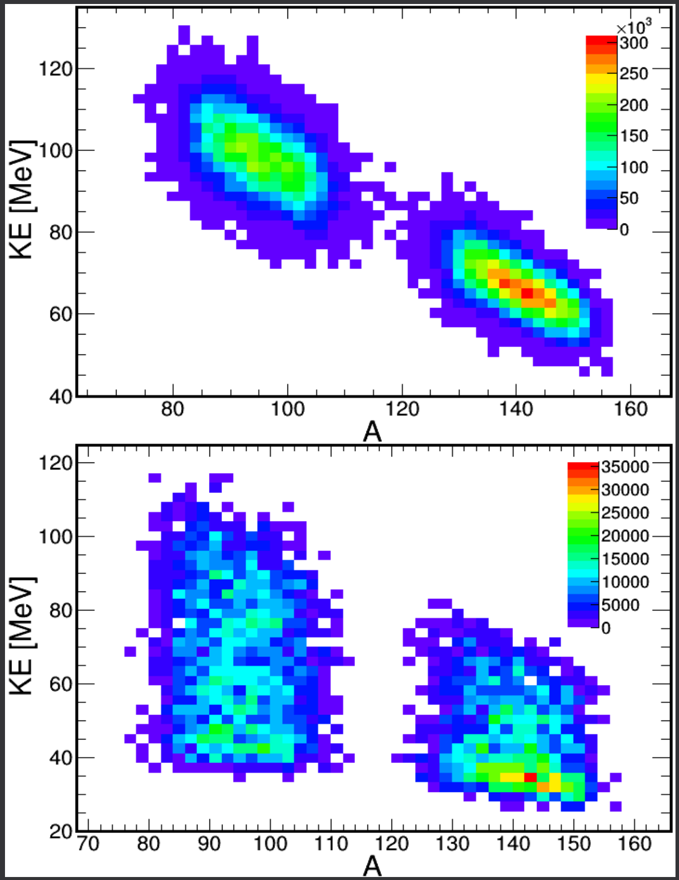

# Exotic nuclei (VI)

Geant4 simulations: photofission implemented

*P. Constantin, D.L. Balabanski, P.V. Cuong NIM B 372 (2016) 78*

For day-one rate of $5 \cdot 10^{10}\gamma$/s:

**$10^7$ fissions/s**

Optimal beam: ***x*20**

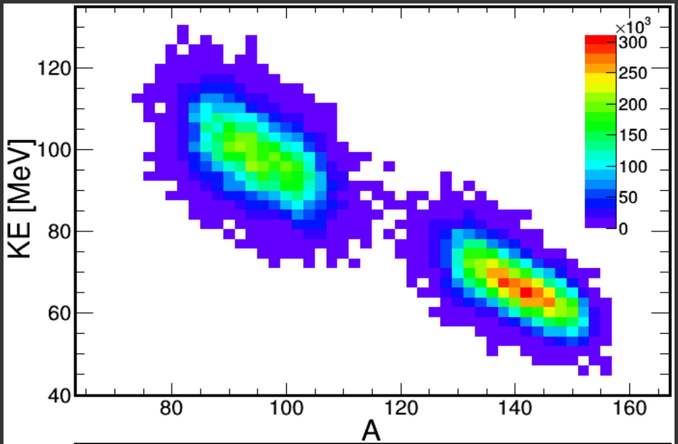


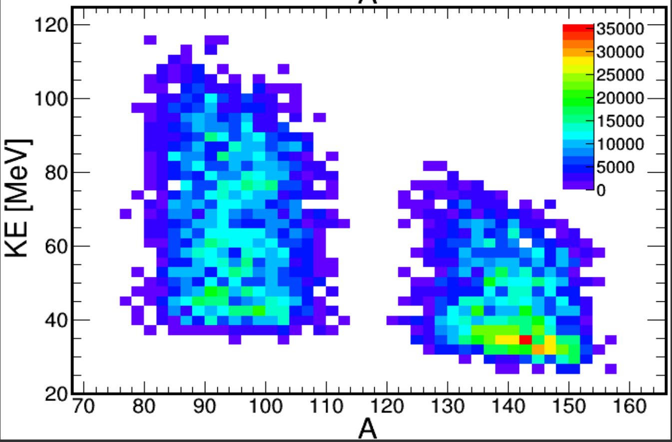


Geant4 stopping (same as SRIM):

*J.F. Ziegler and J.M. Manoyan, NIM B 35 (1988) 215*

Not so good for low v, high Z ions in high-Z media.

Two new q=Q/Z parameterizations:

*K. Shima et al., Nucl. Instr. Meth. 200 (1982) 605*

*G. Schiwietz, P.L. Grande, Nucl. Instr. Meth. B 175–177 (2001) 125*

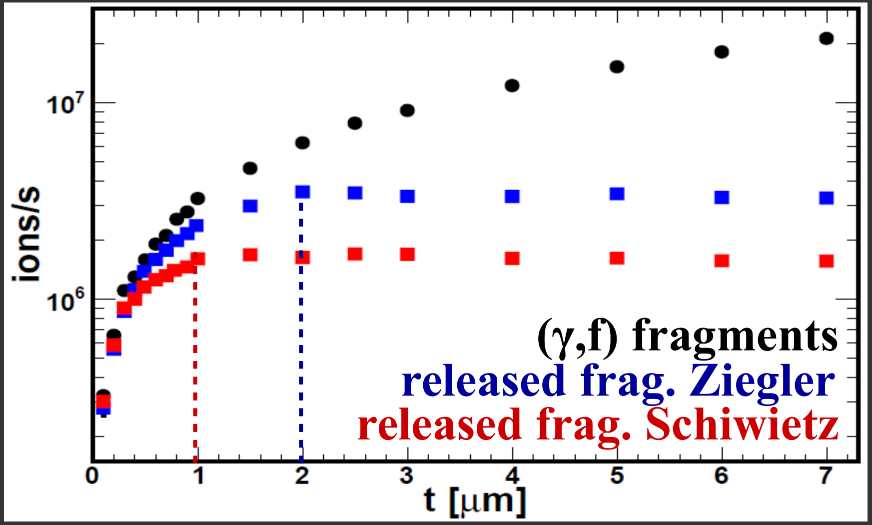

# Exotic nuclei (VI)

Geant4 simulations: photofission implemented

*P. Constantin, D.L. Balabanski, P.V. Cuong NIM B 372 (2016) 78*

For day-one rate of $5\cdot10^{10}\gamma$/s:

**$10^7$ fissions/s**

Optimal beam: ***x20***

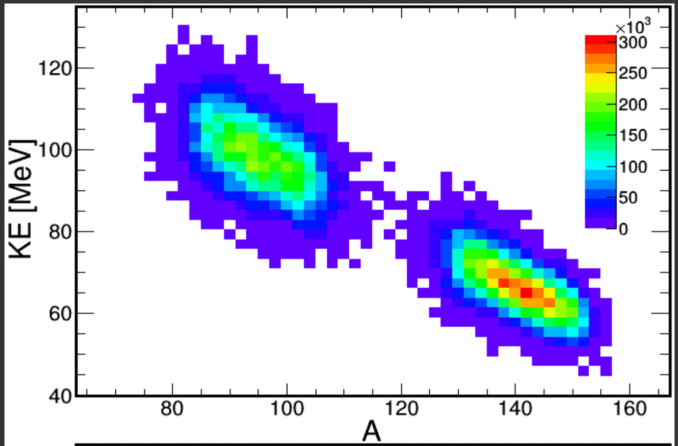


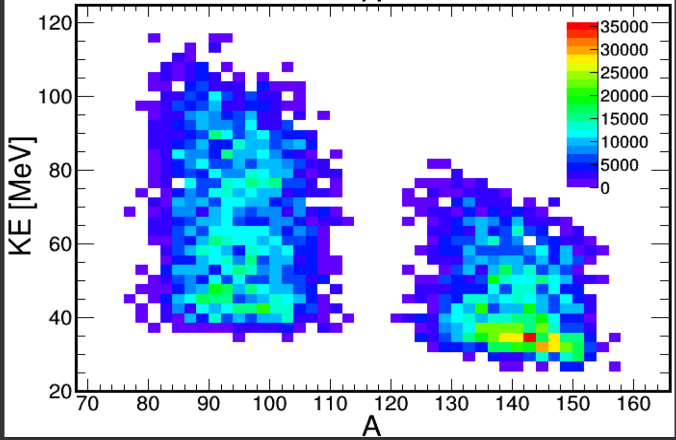


Geant4 stopping (same as SRIM):

*J.F. Ziegler and J.M. Manoyan, NIM B 35 (1988) 215*

Not so good for low v, high Z ions in high-Z media.

Two new q=Q/Z parameterizations:

*K. Shima et al., Nucl. Instr. Meth. 200 (1982) 605*

*G. Schiwietz, P.L. Grande, Nucl. Instr. Meth. B 175–177 (2001) 125*

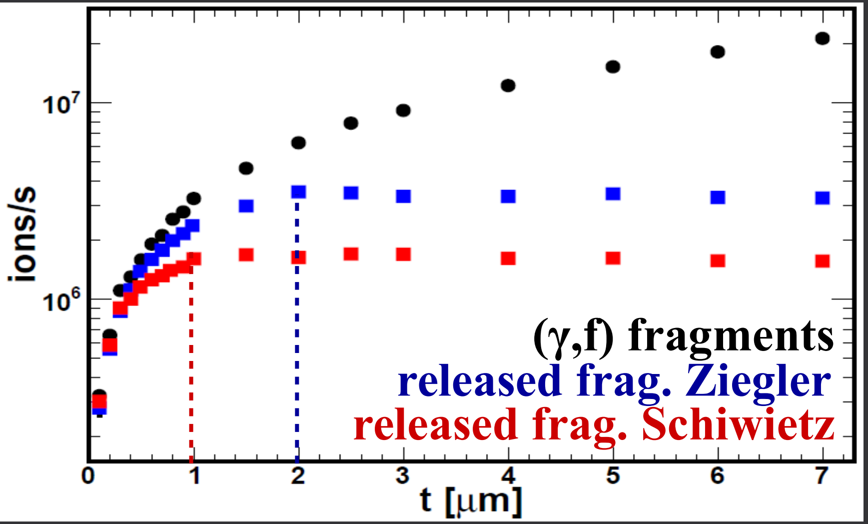


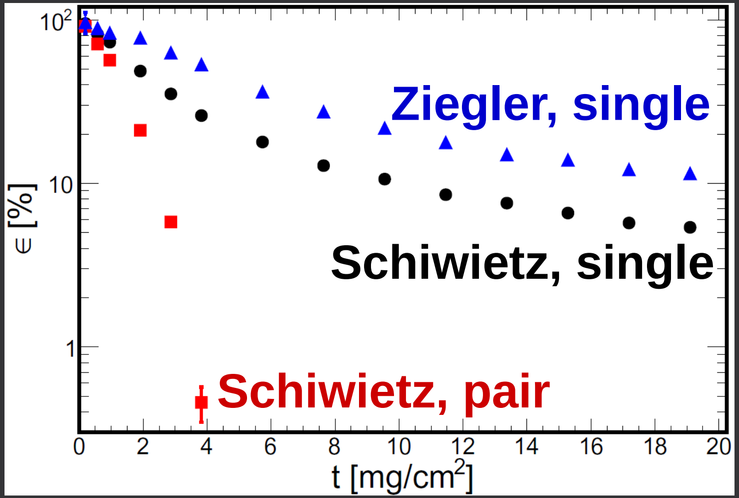

# Exotic nuclei (VI)

Geant4 simulations: photofission implemented

*P. Constantin, D.L. Balabanski, P.V. Cuong NIM B 372 (2016) 78*

For day-one rate of $5\cdot10^{10}\gamma$/s:

**$10^7$ fissions/s → $2\cdot10^6$ frag/s**

Optimal beam: ***x*20 → $4\cdot10^7$ frag/s**

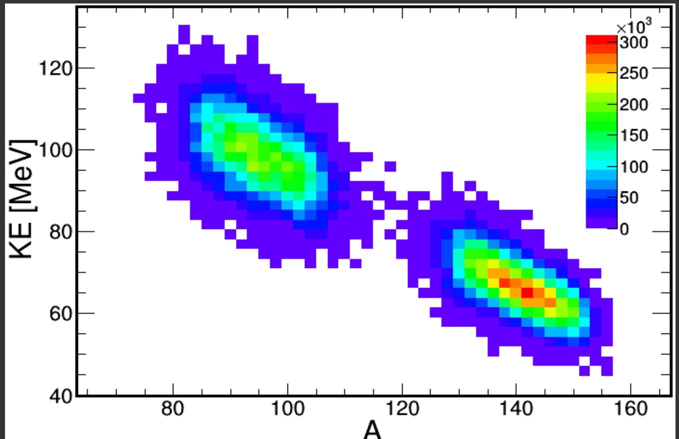


Geant4 stopping (same as SRIM):

*J.F. Ziegler and J.M. Manoyan, NIM B 35 (1988) 215*

Not so good for low v, high Z ions in high-Z media.

Two new q=Q/Z parameterizations:

*K. Shima et al., Nucl. Instr. Meth. 200 (1982) 605*

*G. Schiwietz, P.L. Grande, Nucl. Instr. Meth. B 175–177 (2001) 125*

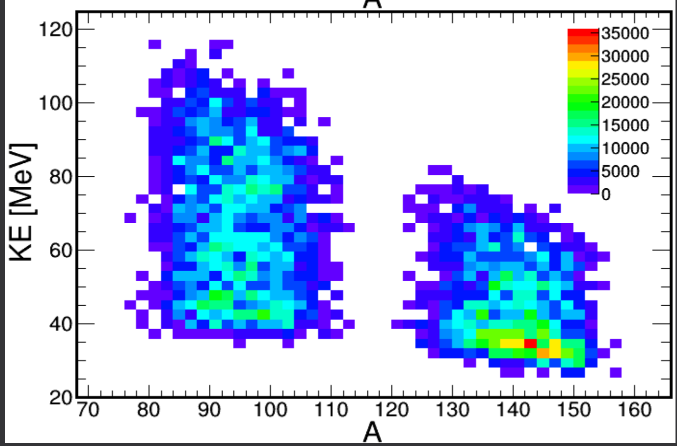


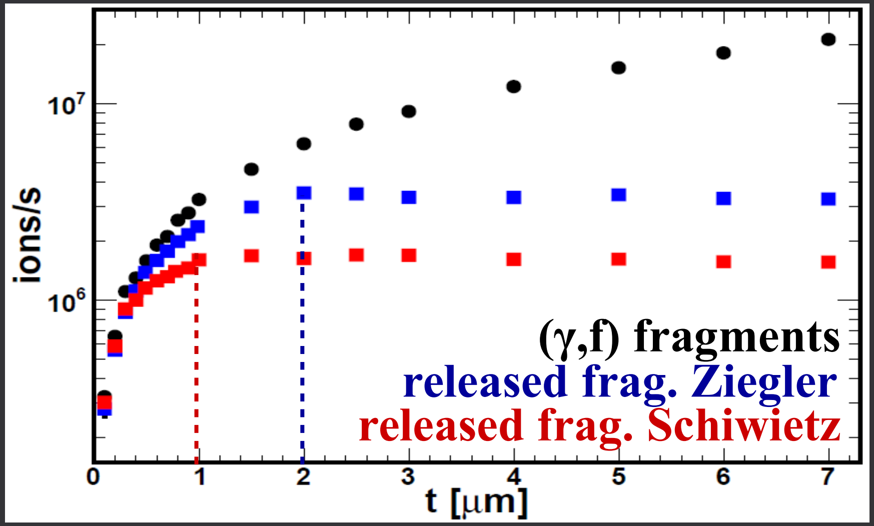


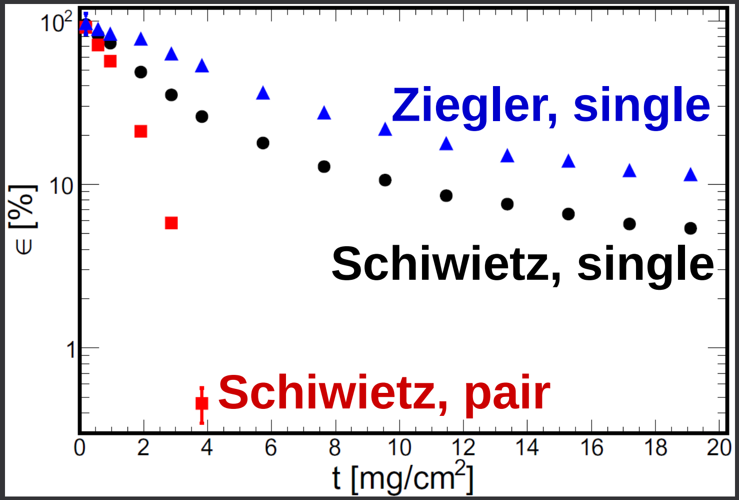

# Exotic nuclei (VII)

Geant4: fragment slowing down in the CSC gas
He, T=70K, p=300mbar ($\rho$=0.206mg/cm$^3$) → >95% of fragments stop in 11.3cm → **width~25cm**

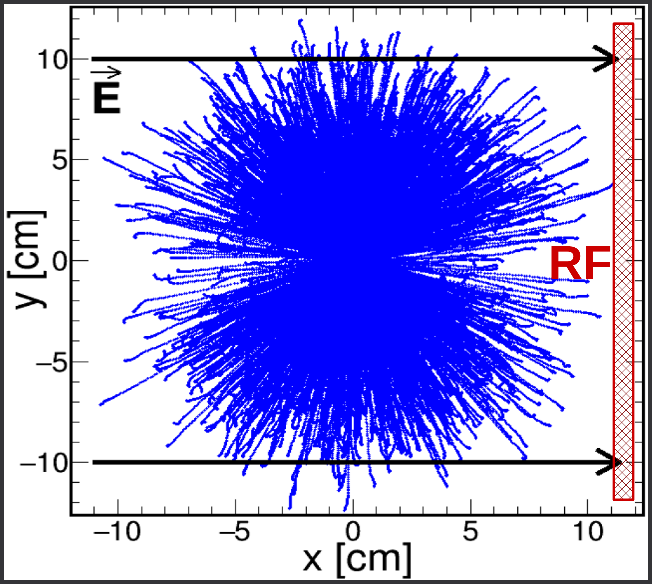

# Exotic nuclei (VII)

Geant4: fragment slowing down in the CSC gas
He, T=70K, p=300mbar (ρ=0.206mg/cm$^3$) → >95% of fragments stop in 11.3cm → **width~25cm**

**Space charge** = He$^+$ cloud by fragment (>90%) and e$^+$/e$^-$ (<10%) induced ionization of He gas:
field saturation ($V_{induced} \approx V_{applied}$), strong e-ion recombination,
weak plasma ($n_+ \approx n_- << n_0$) = injection-recombination equil.

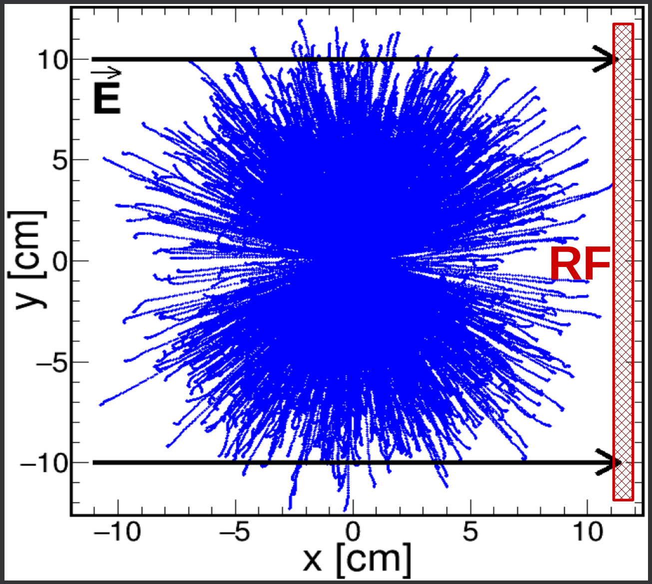

# Exotic nuclei (VII)

Geant4: fragment slowing down in the CSC gas
He, T=70K, p=300mbar ($\rho$=0.206mg/cm$^3$) → >95% of fragments stop in 11.3cm → **width~25cm**

**Space charge** = $He^+$ cloud by fragment (>90%) and $e^+/e^-$ (<10%) induced ionization of He gas:
field saturation ($V_{induced} \approx V_{applied}$), strong e-ion recombination,
weak plasma ($n_+ \approx n_- \ll n_0$) = injection-recombination equil.

SIMION 8.1 simulation in 3 steps:

1) solves the static Poisson equation: $\epsilon \nabla^2 \Phi(x, y) = -e\tau_i Q(x, y)$

with Q(x,y) from Geant4 and DC extraction time: **$\tau_i$[s]= 1.32/E[V/cm]**

2) drifts 4000 photofission fragments from Geant4 thru $\Phi$(x,y)

3) solves Poisson eq. dynamically (PIC simulation) → extraction efficiency $\varepsilon$ and time $\tau$

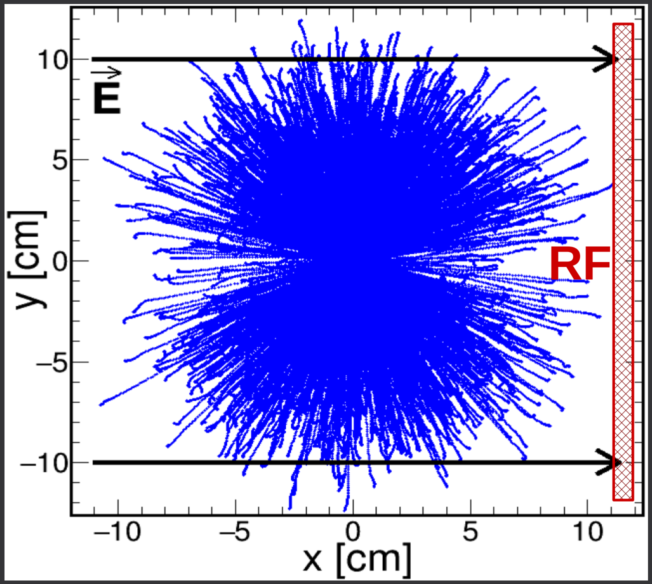

# Exotic nuclei (VII)

Geant4: fragment slowing down in the CSC gas
He, T=70K, p=300mbar (ρ=0.206mg/cm³) → >95% of fragments stop in 11.3cm → **width~25cm**

**Space charge** = $He^{+}$ cloud by fragment (>90%) and $e^{+}/e^{-}$ (<10%) induced ionization of He gas:
field saturation ($V_{induced} \approx V_{applied}$), strong e-ion recombination,
weak plasma ($n_{+} \approx n_{-} << n_{0}$) = injection-recombination equil.

SIMION 8.1 simulation in 3 steps:
1) solves the static Poisson equation: $$\epsilon \nabla^2 \Phi(x,y) = -e\tau_i Q(x,y)$$

with Q(x,y) from Geant4 and DC extraction time: **$\tau_i$[s]= 1.32/E[V/cm]**
2) drifts 4000 photofission fragments from Geant4 thru Φ(x,y)
3) solves Poisson eq. dynamically (PIC simulation) → extraction efficiency ε and time τ

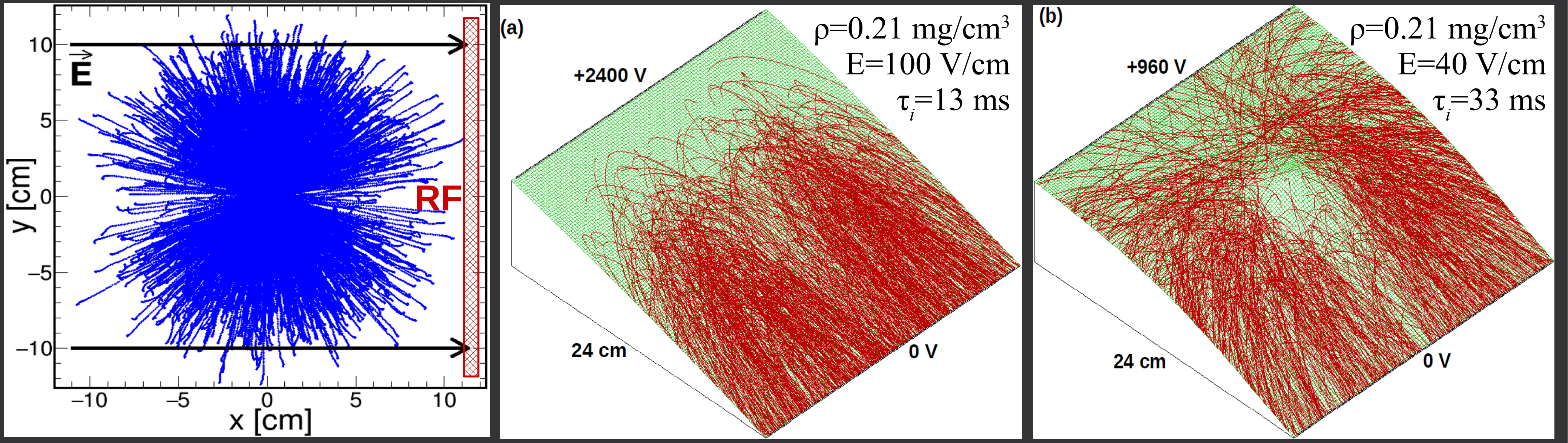


**ε = 89% <τ> = 6.8ms** **ε = 67% <τ> = 17ms**

**IF τ<9.5ms: PULSED REGIME!**

# Photofission (I)

- BW≈0.3% → ΔE≈15keV below fission barrier: resolve isomeric fission transmission resonances in the 2nd and 3rd minima of isomeric fission

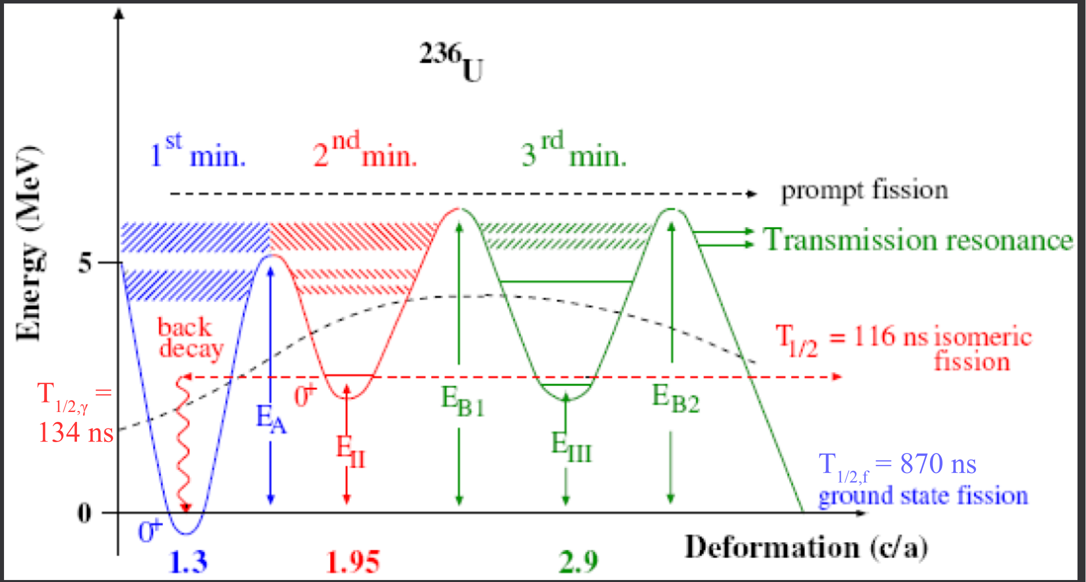

# Photofission (I)

- BW≈0.3% → ΔE≈15keV below fission barrier: resolve isomeric fission transmission resonances in the 2nd and 3rd minima of isomeric fission
- sub-mm beam spot and low backgrounds: high-resolution fragment angular distributions, resonance spin and parity
- ternary fission cross-section dependence on $E_\gamma$

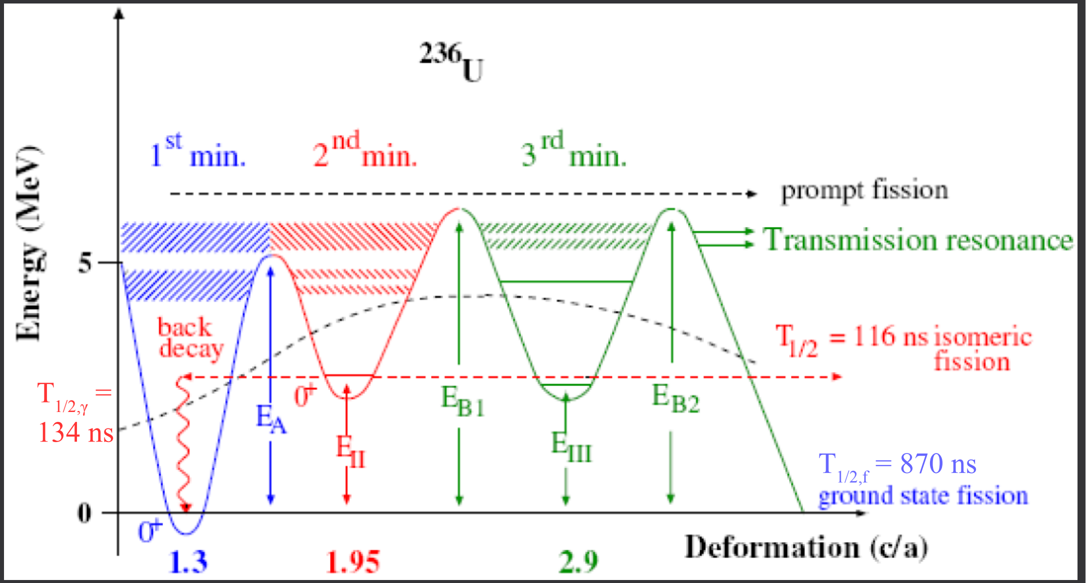

# Photofission (I)

- ✓ BW≈0.3% → ΔE≈15keV below fission barrier: resolve isomeric fission transmission resonances in the 2nd and 3rd minima of isomeric fission
- ✓ sub-mm beam spot and low backgrounds: high-resolution fragment angular distributions, resonance spin and parity
- ✓ ternary fission cross-section dependence on $E_\gamma$

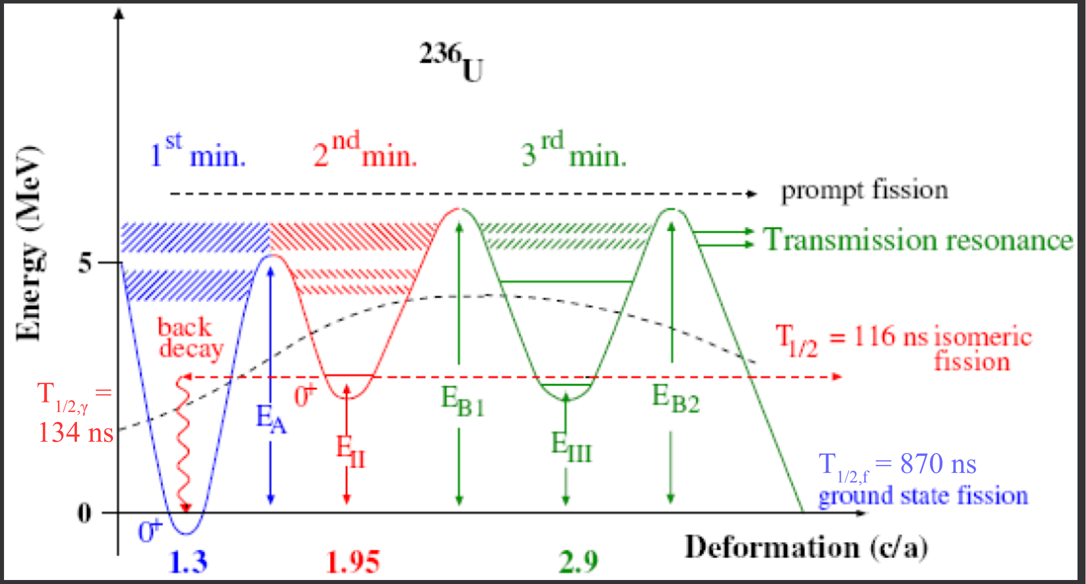


1st minimum → macroscopic (LDM) deformation

2nd minimum → microscopic shell corrections that vary periodically with $\beta_2$

3rd minimum → complex (quadrupole/octupole) mixing

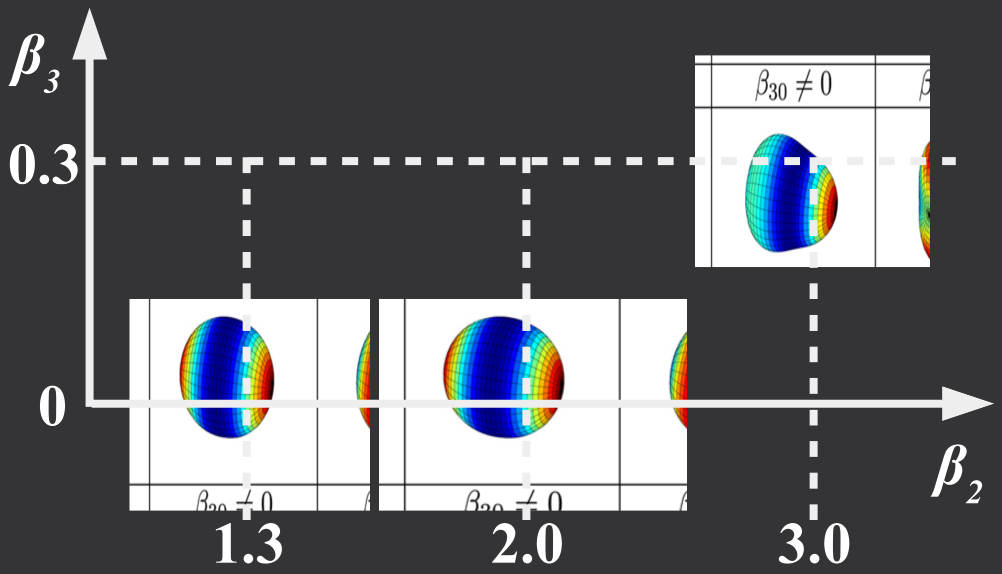

# Photofission (I)

- BW≈0.3% → ΔE≈15keV below fission barrier: resolve isomeric fission transmission resonances in the 2nd and 3rd minima of isomeric fission
- sub-mm beam spot and low backgrounds: high-resolution fragment angular distributions, resonance spin and parity
- ternary fission cross-section dependence on $E_\gamma$

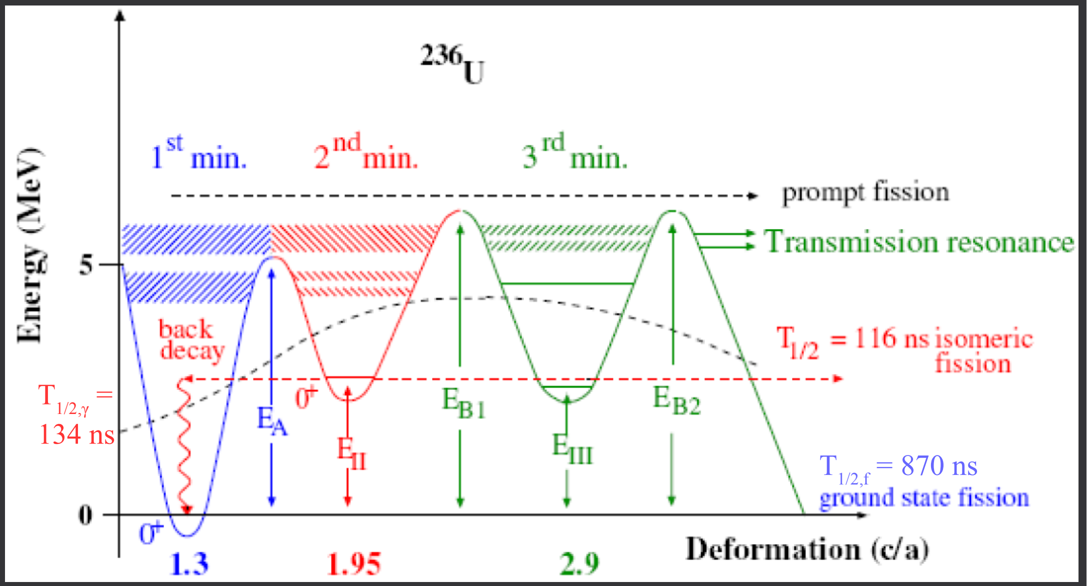


1st minimum → macroscopic (LDM) deformation
2nd minimum → microscopic shell corrections that vary periodically with $\beta_2$
3rd minimum → complex (quadrupole/octupole) mixing

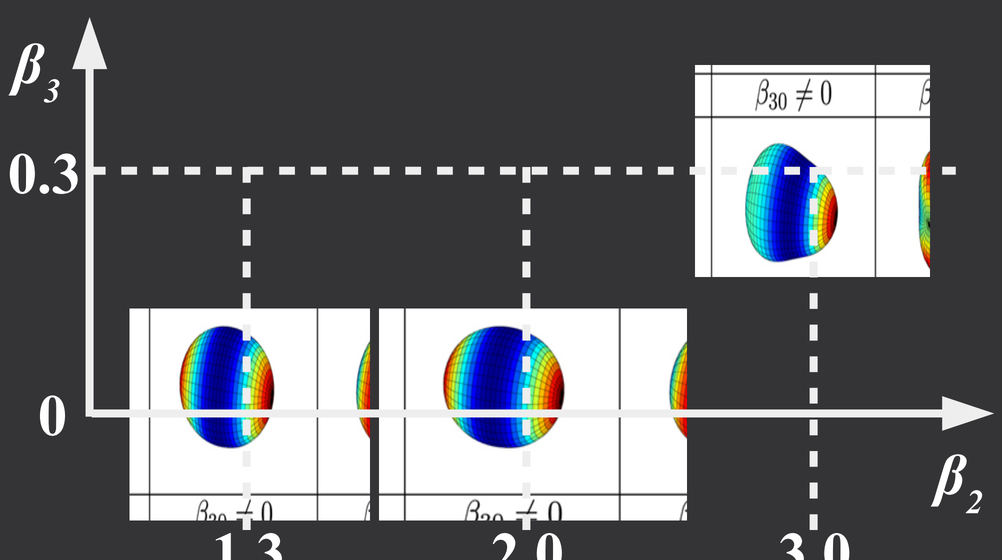


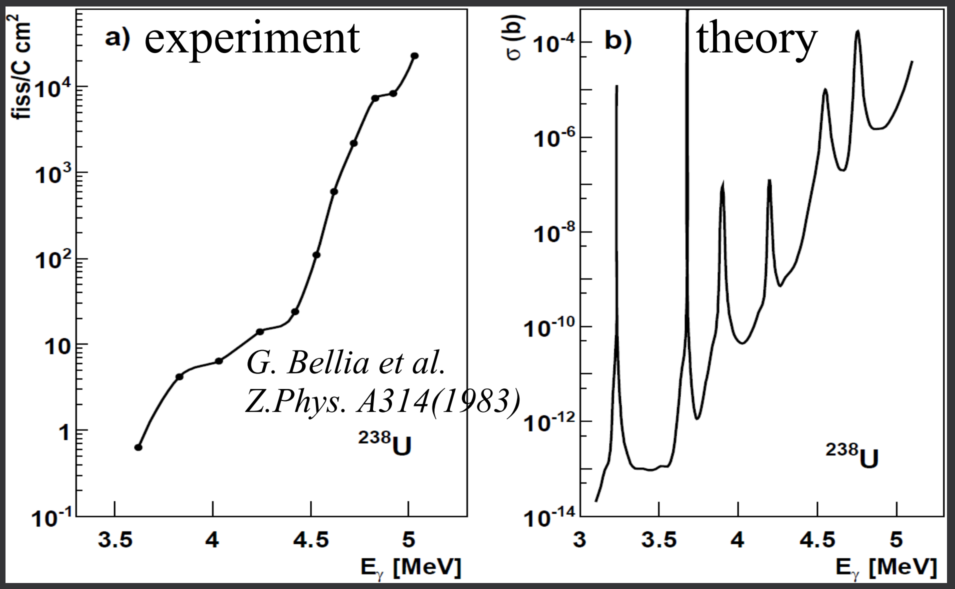


$^{238}$U photofission: experiment vs. theory

# Photofission (II)

Two setups developed at MTA-Atomki (Debrecen):
– **4 Bragg Ionization Chambers** (P10 gas at 1 atm)
– **each with 8 Double Side Silicon Strip detectors**
→ target 0.8mg/cm$^2$, beam $E_\gamma$=5.8MeV and BW=0.3%:
3 binary f/s and 11 ternary f/h
→ full fragment kinematics: KE, Z, A, angle
→ ternary fission fragments

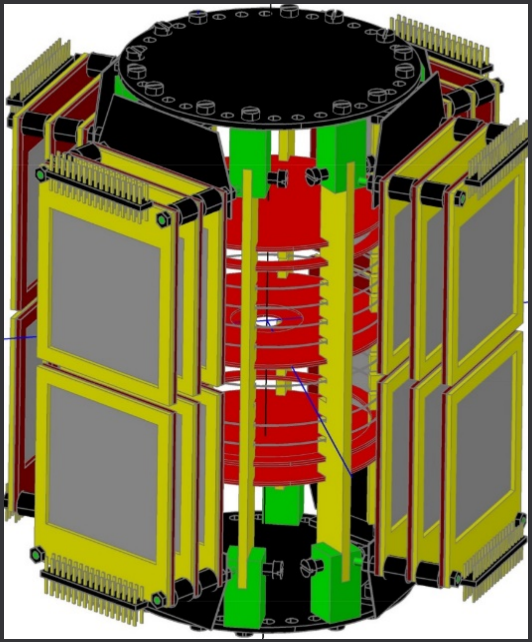

# Photofission (II)

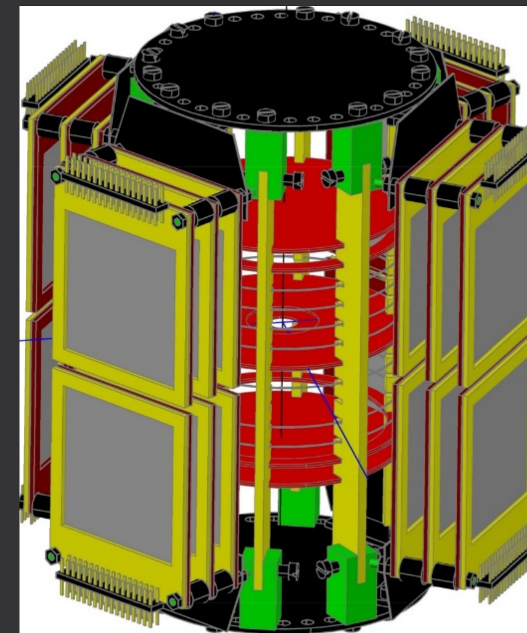

Two setups developed at MTA-Atomki (Debrecen):

– **4 Bragg Ionization Chambers** (P10 gas at 1 atm)

– **each with 8 Double Side Silicon Strip detectors**

→ target 0.8mg/cm$^2$, beam $E_\gamma$=5.8MeV and BW=0.3%:

3 binary f/s and 11 ternary f/h

→ full fragment kinematics: KE, Z, A, angle

→ ternary fission fragments

**3 modules with 4 Thick GEMs**

→ target 20mg/cm$^2$, beam BW=0.3%:

$E_\gamma$=5.8MeV: 900 binary f/s and 1 ternary f/s

$E_\gamma$=13MeV: 7000 binary f/s and 7 ternary f/s

$E_\gamma$=19MeV: 4200 binary f/s and 4 ternary f/s

→ fragment angular distribution: rotational bands

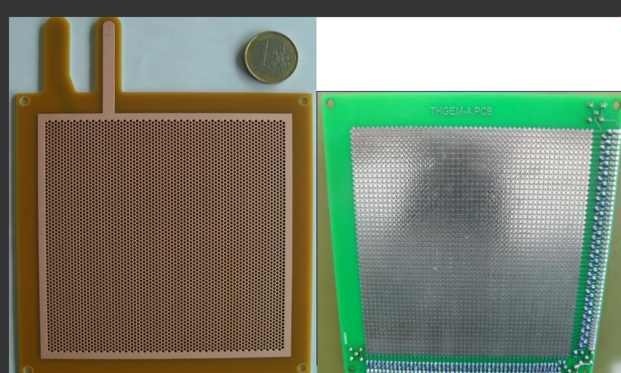

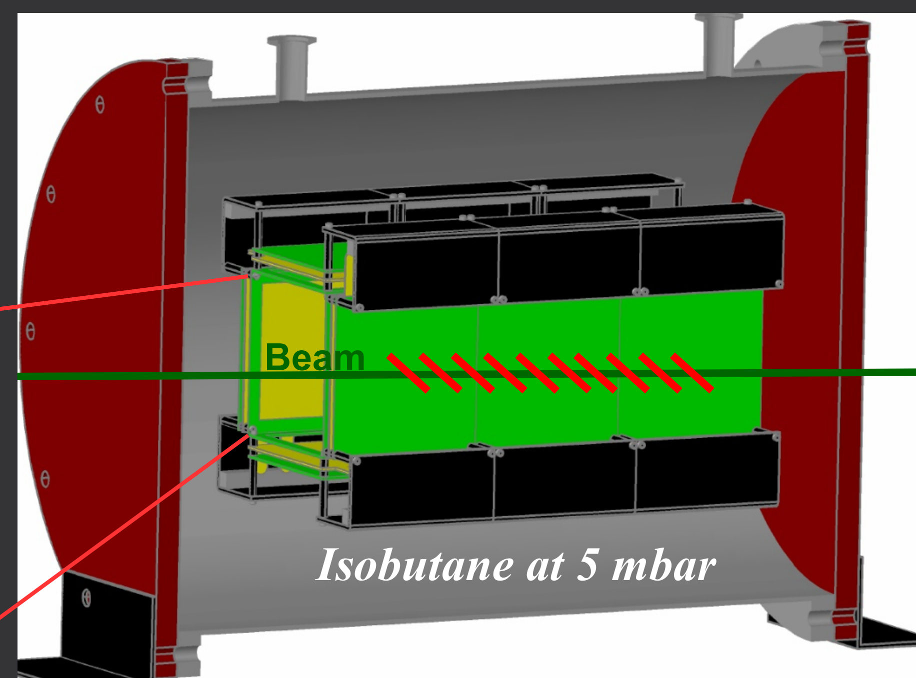

# Nuclear Resonance Fluorescence (I)

– $E_\gamma < S_n$: various collective resonances

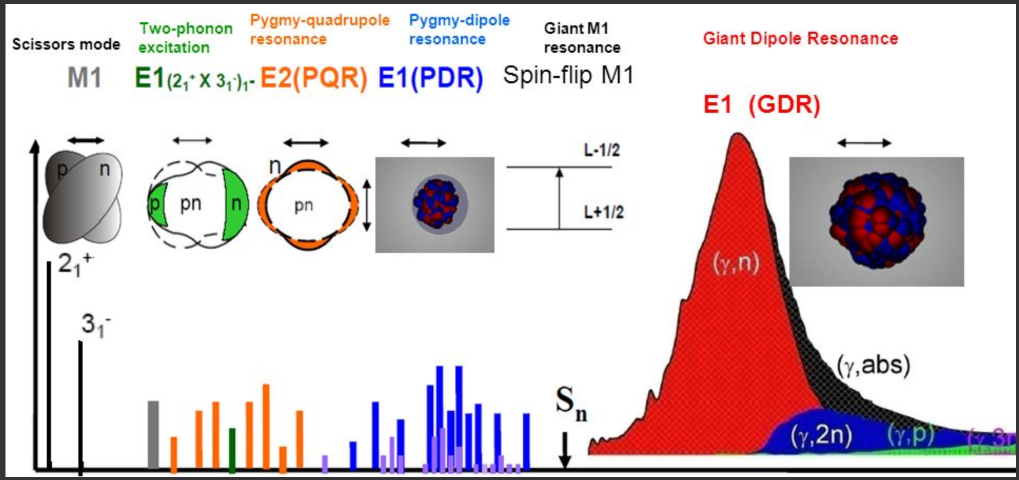

# Nuclear Resonance Fluorescence (I)

– $E_\gamma < S_n$: various collective resonances

– Breigt-Wigner cross-section:

$$\sigma(E) = g\,\frac{\pi}{2}\left(\frac{\hbar c}{E_r}\right)\frac{\Gamma_0 \Gamma}{(E - E_r)^2 + (\Gamma/2)^2}$$

$\Gamma = \Sigma_f \Gamma_f$ (total width), $\Gamma_0$(g.s. width)

$g \equiv (2J_f+1)/(2J_0+1)$

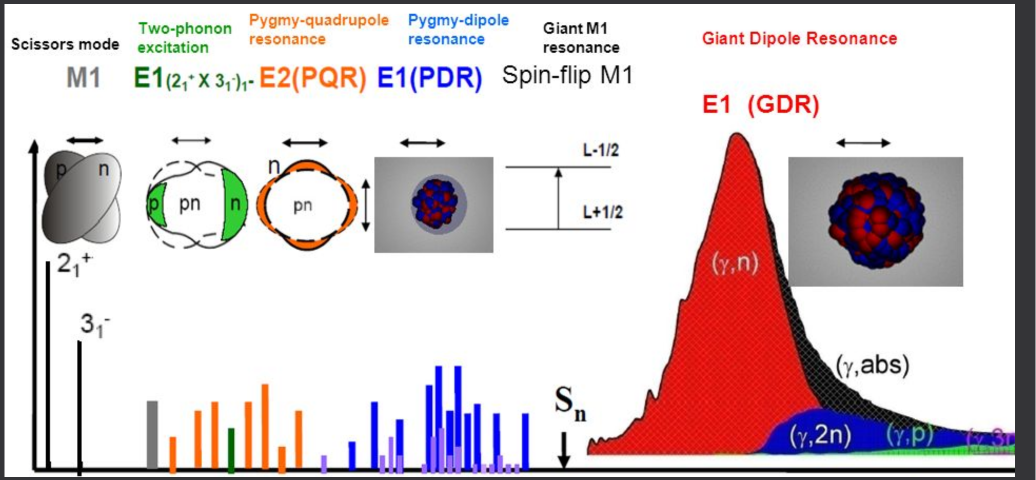


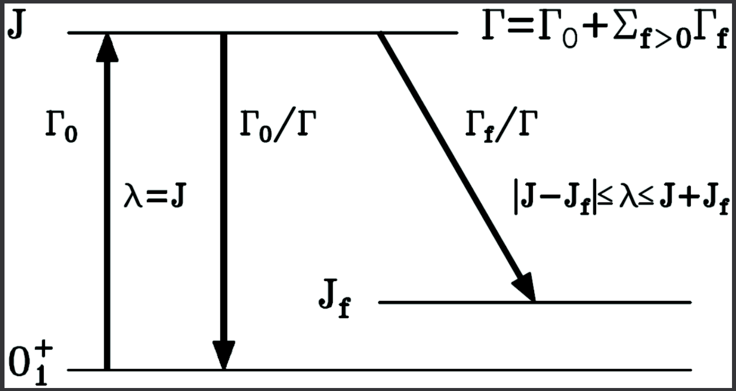

# Nuclear Resonance Fluorescence (I)

– $E_\gamma < S_n$: various collective resonances

– Breigt-Wigner cross-section:

$$\sigma(E) = g\frac{\pi}{2}\left(\frac{\hbar c}{E_r}\right)\frac{\Gamma_0\Gamma}{(E-E_r)^2+(\Gamma/2)^2}$$

$\Gamma = \Sigma_f \Gamma_f$ (total width), $\Gamma_0$(g.s. width)

$g \equiv (2J_f+1)/(2J_0+1)$

– Doppler broadening (thermal motion):

$$\sigma_D(E) \approx \frac{\sqrt{(\pi)}}{2}\sigma(E)\frac{\Gamma}{\Delta}\exp\left(-\frac{(E-E_r)^2}{\Delta^2}\right)$$

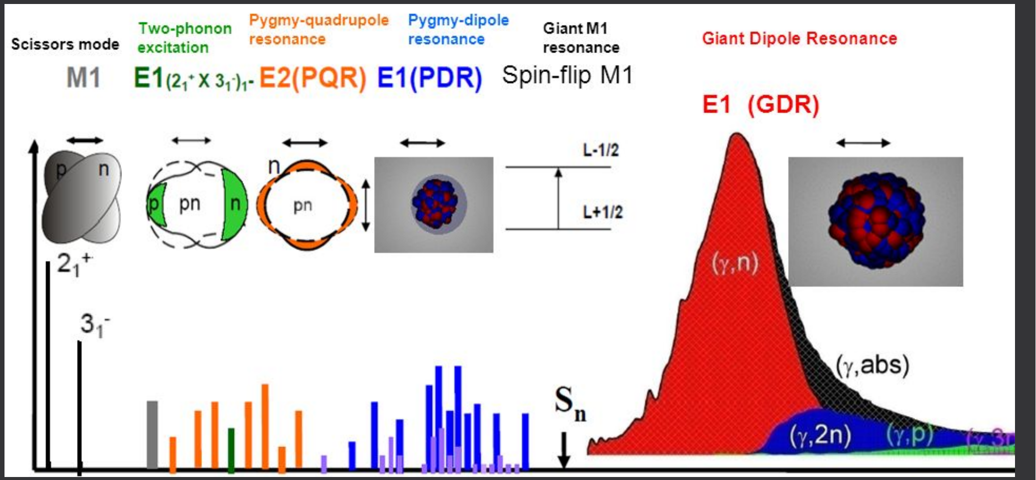


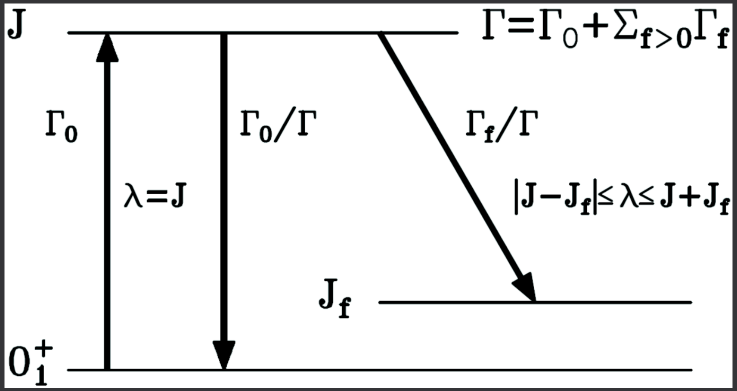

# Nuclear Resonance Fluorescence (I)

– $E_\gamma < S_n$: various collective resonances
– Breigt-Wigner cross-section:

$$\sigma(E) = g\frac{\pi}{2}\left(\frac{\hbar c}{E_r}\right)\frac{\Gamma_0 \Gamma}{(E-E_r)^2 + (\Gamma/2)^2}$$

$\Gamma = \Sigma_f \Gamma_f$ (total width), $\Gamma_0$(g.s. width)

$g \equiv (2J_f+1)/(2J_0+1)$

– Doppler broadening (thermal motion):

$$\sigma_D(E) \approx \frac{\sqrt{(\pi)}}{2}\sigma(E)\frac{\Gamma}{\Delta}\exp\left(-\frac{(E-E_r)^2}{\Delta^2}\right)$$

– isolated: narrow $\Gamma < \Delta < 10$eV and sparse $\rho < 10^4$MeV$^{-1}$
– narrow resonance → constant beam intensity:

$$I_{0\to J\to f} = \int \sigma_{J\to f}\, dE = \pi\left(\frac{\hbar c}{E_r}\right)^2 g\frac{\Gamma_0 \Gamma_f}{\Gamma}$$

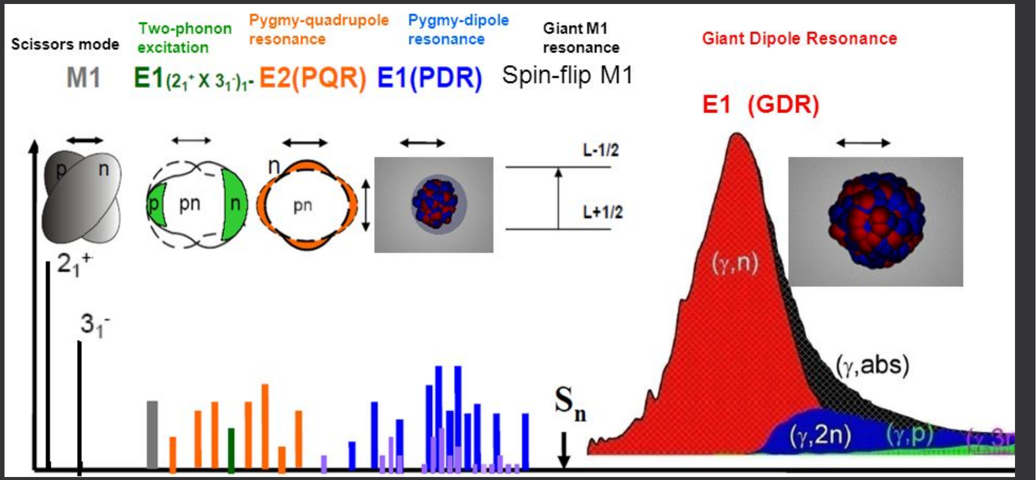


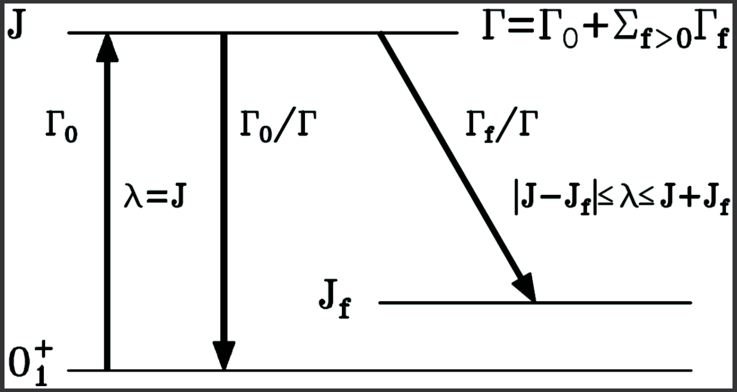

# Nuclear Resonance Fluorescence (I)

- $E_\gamma < S_n$: various collective resonances
- Breigt-Wigner cross-section:

$$\sigma(E) = g\frac{\pi}{2}\left(\frac{\hbar c}{E_r}\right)\frac{\Gamma_0\Gamma}{(E-E_r)^2+(\Gamma/2)^2}$$

$\Gamma = \Sigma_f \Gamma_f$ (total width), $\Gamma_0$(g.s. width)

$g \equiv (2J_f+1)/(2J_0+1)$

- Doppler broadening (thermal motion):

$$\sigma_D(E) \approx \frac{\sqrt{(\pi)}}{2}\sigma(E)\frac{\Gamma}{\Delta}\exp\left(-\frac{(E-E_r)^2}{\Delta^2}\right)$$

- isolated: narrow $\Gamma<\Delta<10$eV and sparse $\rho<10^4 MeV^{-1}$
- narrow resonance → constant beam intensity:

$$I_{0\to J\to f} = \int \sigma_{J\to f}\, dE = \pi\left(\frac{\hbar c}{E_r}\right)^2 g\frac{\Gamma_0\Gamma_f}{\Gamma}$$

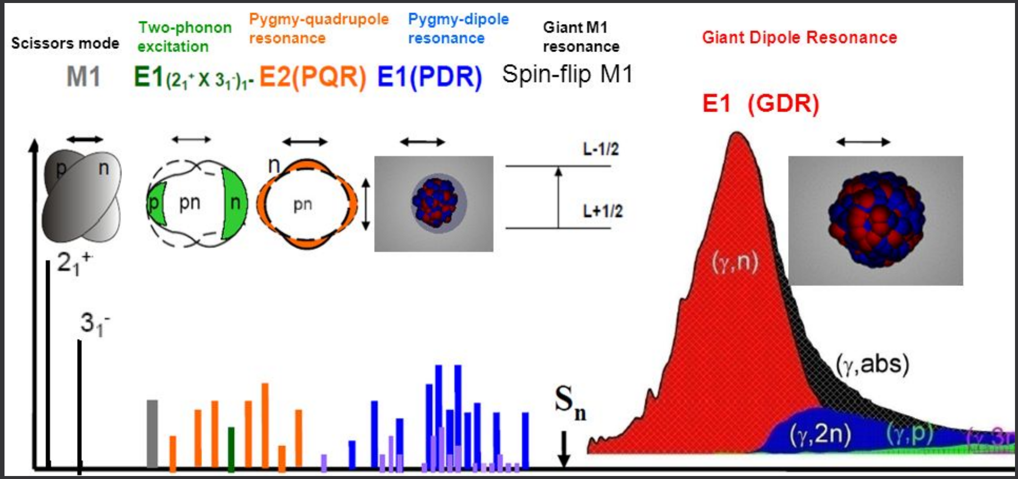


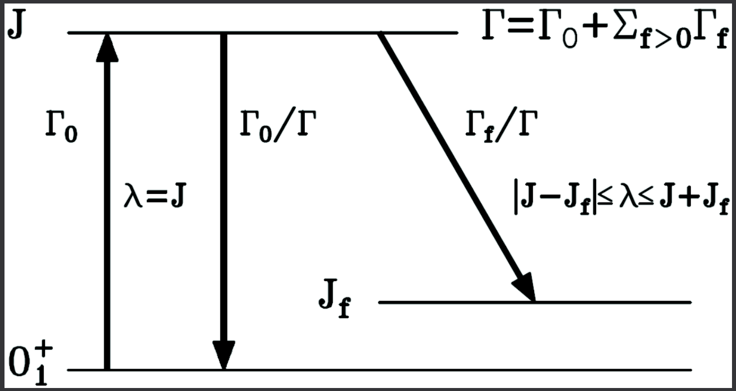


- NRF 0→J→0:

$$\frac{\Gamma_0^2}{\Gamma} = \frac{I_{0\to J\to 0}}{g(\pi\hbar c/E_r)^2}$$

- E1&M1 dipole transition strengths:

$$g\frac{\Gamma_0[meV]}{E_\gamma^3[MeV^3]} = \frac{B(E1)[e^2 fm^2]}{9.554\cdot 10^{-4}} = \frac{B(M1)[\mu_N^2]}{8.641\cdot 10^{-2}}$$

# Nuclear Resonance Fluorescence (II)

**ELIADE** array built at ELI-NP:
– 4 HPGe clover detectors at 90°
– 4 HPGe clover detectors at 135°:
intrinsic efficiency ~40%
energy resolution 2.3keV at 1.3MeV
time resolution <10ns
– 4 $LaBr_3$ detectors at 90°:
energy resolution 20-30keV at 1.3MeV
time resolution <1ns

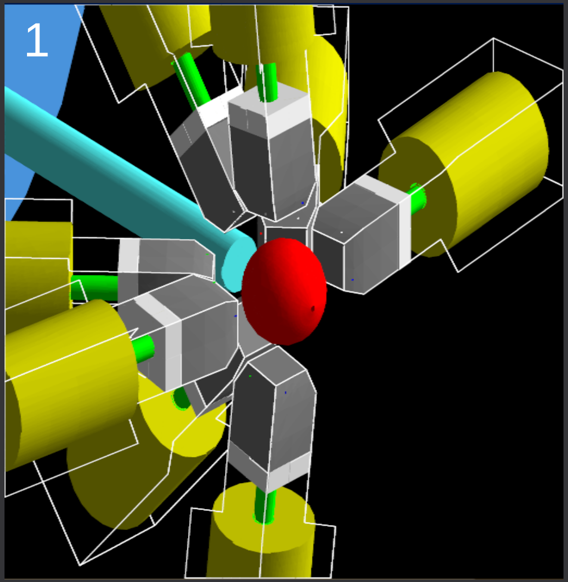


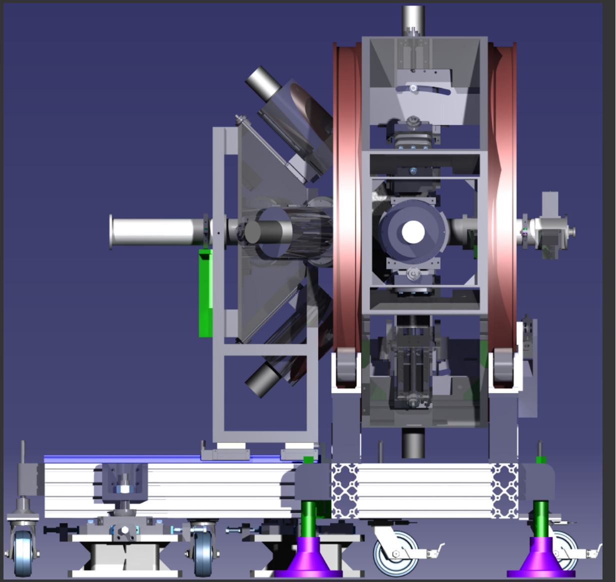

# Nuclear Resonance Fluorescence (II)

**ELIADE** array built at ELI-NP:
– 4 HPGe clover detectors at 90°
– 4 HPGe clover detectors at 135°:
intrinsic efficiency ~40%
energy resolution 2.3keV at 1.3MeV
time resolution <10ns
– 4 $LaBr_3$ detectors at 90°:
energy resolution 20-30keV at 1.3MeV
time resolution <1ns

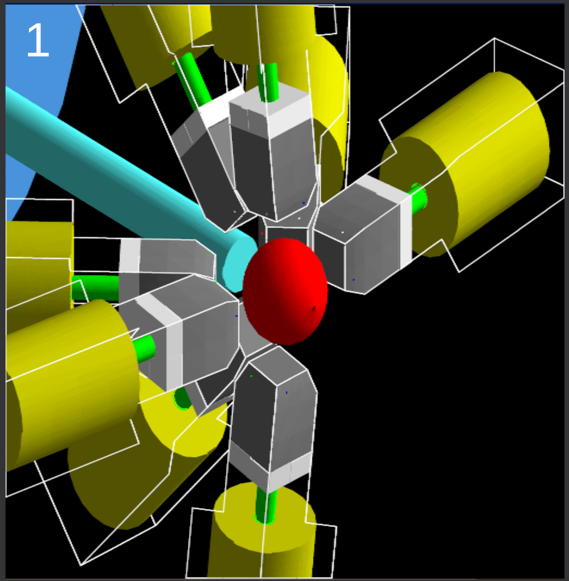


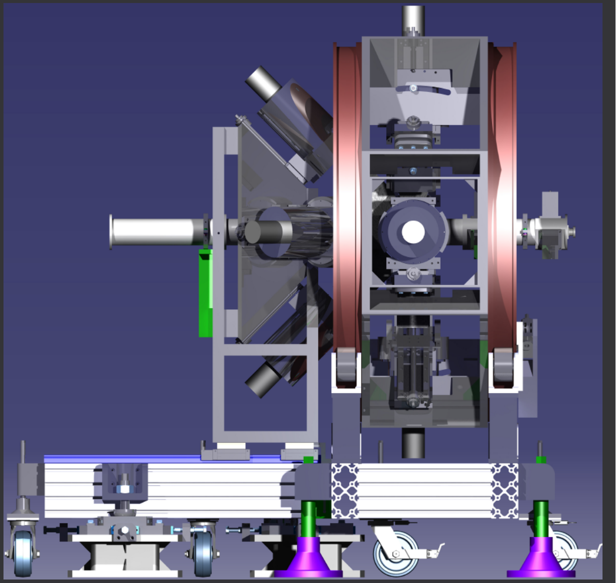

Dipole (E1&M1) states parity:
Outgoing γ polarization with Compton polarimeters: E<3MeV
Incoming γ polarization via off-axis bremsstrahlung: high flux but partial (10-20%) polarization
ICS facilities: high-flux, 99% polarized γ beams → measurements in 4-9 MeV range

# Nuclear Resonance Fluorescence (II)

**ELIADE** array built at ELI-NP:
– 4 HPGe clover detectors at 90°
– 4 HPGe clover detectors at 135°:
intrinsic efficiency ~40%
energy resolution 2.3keV at 1.3MeV
time resolution <10ns
– 4 $LaBr_3$ detectors at 90°:
energy resolution 20-30keV at 1.3MeV
time resolution <1ns

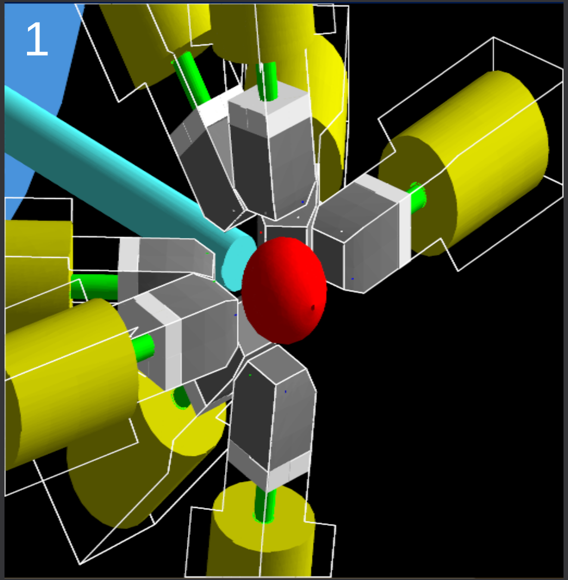


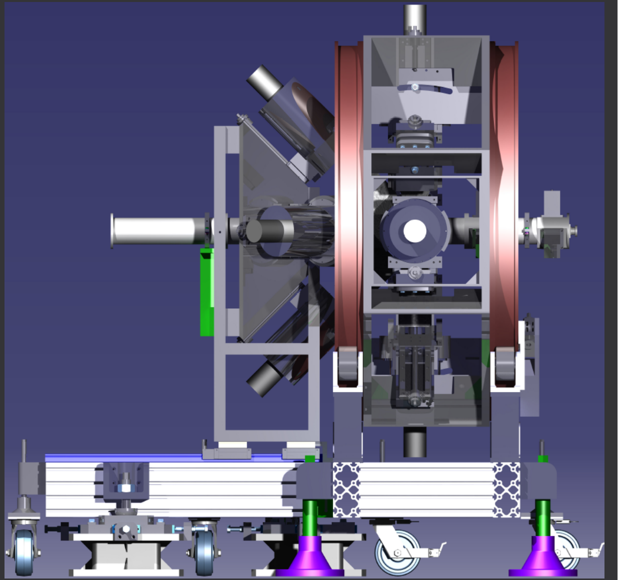

Dipole (E1&M1) states parity:
Outgoing γ polarization with Compton polarimeters: E<3MeV
Incoming γ polarization via off-axis bremsstrahlung: high flux but partial (10-20%) polarization
ICS facilities: high-flux, 99% polarized γ beams → measurements in 4-9 MeV range

*N. Pietralla et al., Phys. Rev. Lett. 88 (2002) 012502*

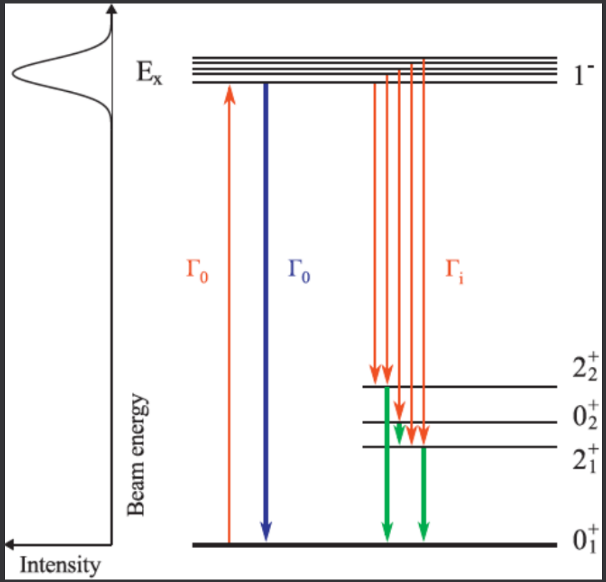


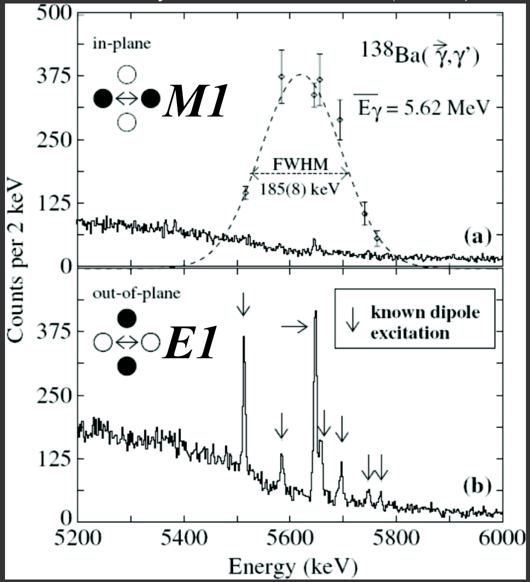

# Nuclear Resonance Fluorescence (II)

**ELIADE** array built at ELI-NP:
– 4 HPGe clover detectors at 90°
– 4 HPGe clover detectors at 135°:
intrinsic efficiency ~40%
energy resolution 2.3keV at 1.3MeV
time resolution <10ns
– 4 $LaBr_3$ detectors at 90°:
energy resolution 20-30keV at 1.3MeV
time resolution <1ns

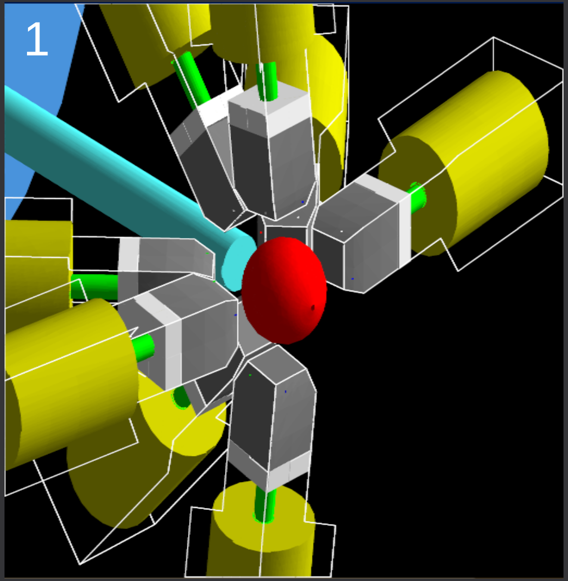


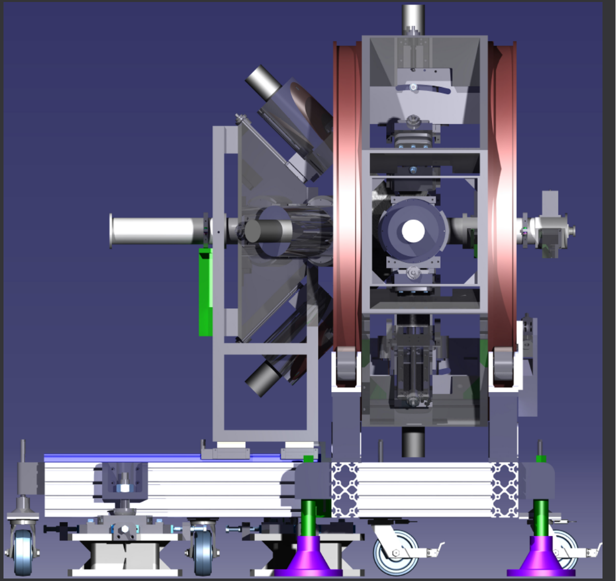

Dipole (E1&M1) states parity:
Outgoing γ polarization with Compton polarimeters: E<3MeV
Incoming γ polarization via off-axis bremsstrahlung: high flux but partial (10-20%) polarization
ICS facilities: high-flux, 99% polarized γ beams → measurements in 4-9 MeV range

HIγS:
– BW~3%
– SD~$10^2$ γ/s/eV

ELI–NP:
– BW~0.5%
– SD~$10^4$ γ/s/eV

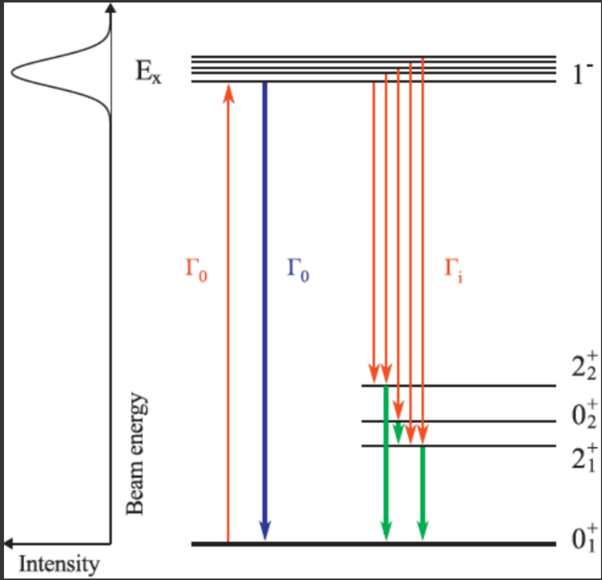


*N. Pietralla et al., Phys. Rev. Lett. 88 (2002) 012502*

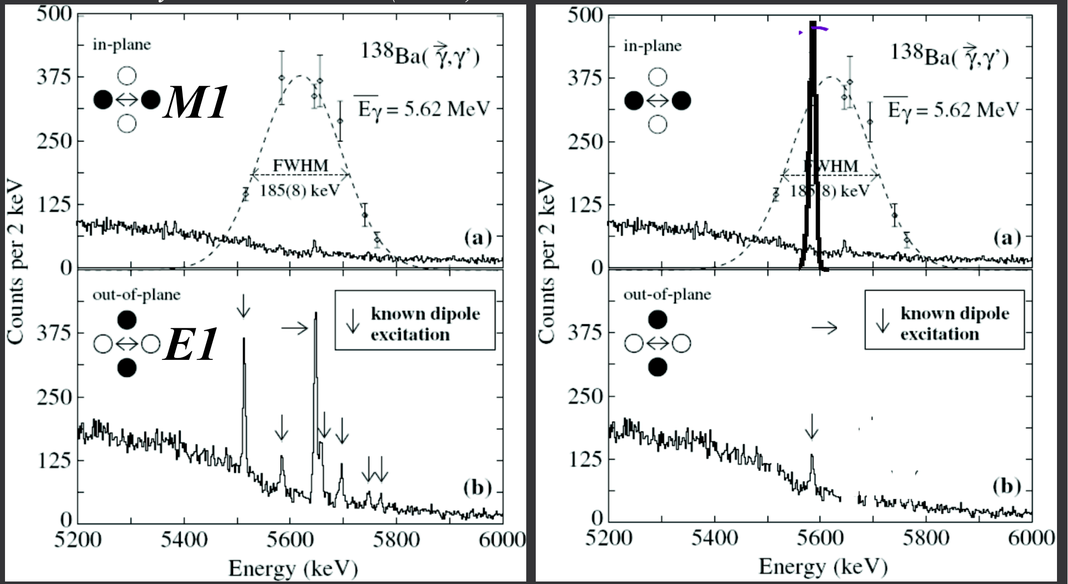

# Gamma and Neutron Above $S_n$

– $E_\gamma > S_n$: Giant Dipole Resonance

– absolute ($\gamma$,n) and ($\gamma$,2n) cross-sections
– p-process measurements:
$^{138}La(\gamma,n)^{137}La$
$^{181}Ta(\gamma,n)^{180}Ta$
$^{180m}Ta(\gamma,n)^{179}Ta$
– studies of GDR decays
– studies of M1 spin-flip resonances

# Gamma and Neutron Above $S_n$

– $E_\gamma > S_n$: Giant Dipole Resonance

– absolute ($\gamma$,n) and ($\gamma$,2n) cross-sections
– p-process measurements:
$^{138}La(\gamma,n)^{137}La$
$^{181}Ta(\gamma,n)^{180}Ta$
$^{180m}Ta(\gamma,n)^{179}Ta$
– studies of GDR decays
– studies of M1 spin-flip resonances

**ELIGANT** array built at ELI-NP:
– neutron detectors:
(1) thermal neutrons (~eV):
$^3$He tubes in polyethylene – counters based on $^3$He(n,p)t reaction
high-efficiency 4π array

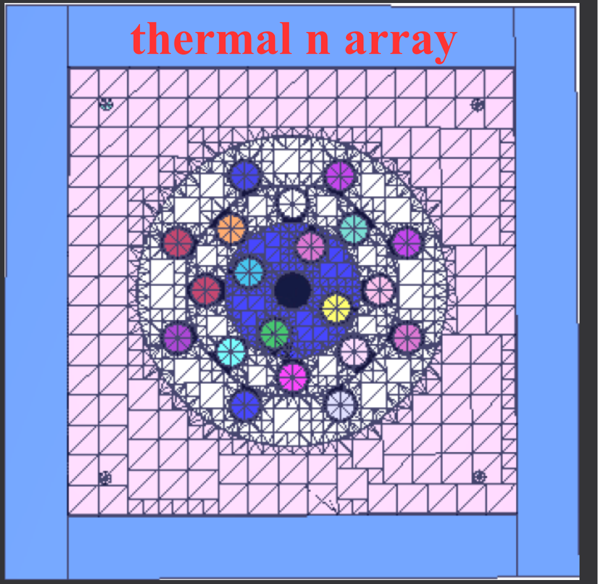

# Gamma and Neutron Above $S_n$

– $E_\gamma > S_n$: Giant Dipole Resonance

– absolute (γ,n) and (γ,2n) cross-sections
– p-process measurements:
$^{138}La(\gamma,n)^{137}La$
$^{181}Ta(\gamma,n)^{180}Ta$
$^{180m}Ta(\gamma,n)^{179}Ta$
– studies of GDR decays
– studies of M1 spin-flip resonances

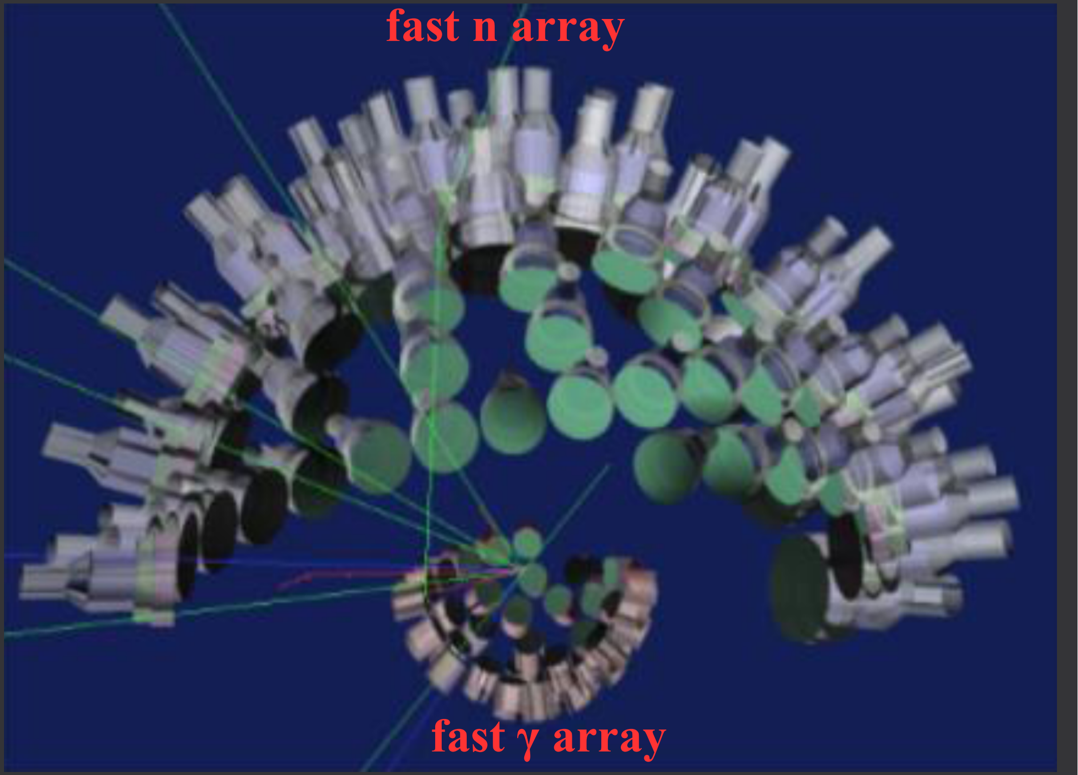


**ELIGANT** array built at ELI-NP:
– neutron detectors:
(1) thermal neutrons (~eV):
$^3He$ tubes in polyethylene – counters based on $^3He(n,p)t$ reaction
high-efficiency 4π array

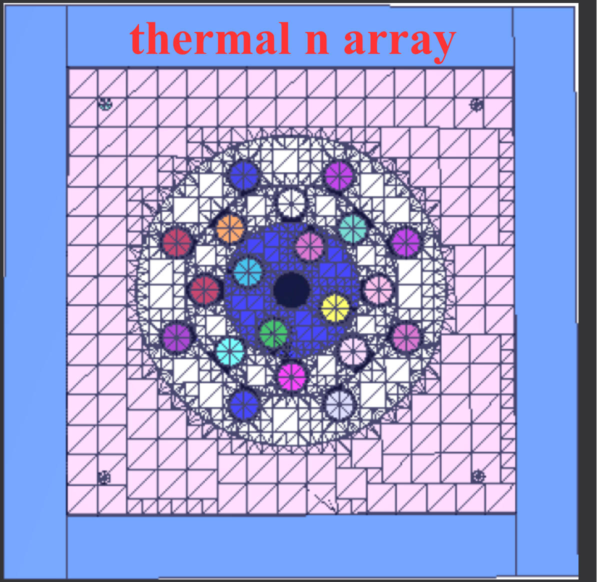


(2) fast neutrons: energy from TOF
$E_n$<1MeV: $^6Li$ glass scintillators – $^6Li(n,\alpha)^3H$ reaction
$E_n$>1MeV: liquid scintillators – (n,p) elastic scattering and p-fluorescence
– gamma detectors: $LaBr_3$+$CeBr_3$ array
energy resolution ~3% at 0.7MeV
time resolution ~0.5ns

# Summary

The newest EU physics research institute
is being built in the East: Prague, Bucharest, Szeged.

It will become operational in 1-2 years.

# Summary

The newest EU physics research institute
is being built in the East: Prague, Bucharest, Szeged.

It will become operational in 1-2 years.

Its nuclear physics pillar is in Magurele (near Bucharest) and offers two systems above state-of-the-art:

– HPLS (High Power Laser System): 2x10 PW lasers, the highest power worldwide
– GBS (Gamma Beam System): highest spectral density and resolution worldwide

# Summary

The newest European physics research institute
is being built in the East: Prague, Bucharest, Szeged.

It will become operational in 1-2 years.

Its nuclear physics pillar is in Magurele (near Bucharest) and offers two systems above state-of-the-art:

- HPLS (High Power Laser System): 2x10 PW lasers, the highest power worldwide
- GBS (Gamma Beam System): highest spectral density and resolution worldwide

Very rich research program: I have tentatively covered only ~1/3 here!!!

We are growing fast and looking for colleagues and collaborators interested in accessing these resources...


Extreme Light Infrastructure - Nuclear Physics
(ELI-NP) - Phase I
www.eli-np.ro
Project co-financed by the European Regional Development Fund
Thank you!

# Main Components of the ELI–NP GBS

**1) *Warm electron RF Linac*** (innovative techniques)

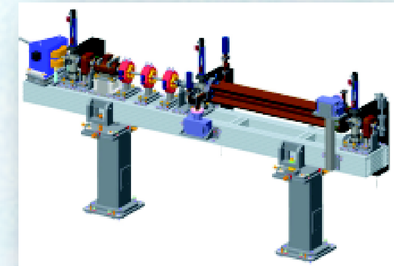

- multi–bunch photogun (32 $e^-$ microbunches of 250 pC @100 Hz RF)
- 2 x S–band (22 MV/m) and 12 x C–band (33 MV/m) acc. structures
- low emittance 0.2 – 0.6 mm · mrad
- two acceleration stages (300 MeV and 720 MeV)

**2) *High average power, high quality J–class 100 Hz ps Collision Laser***

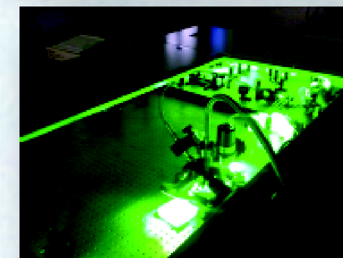

- state–of–the–art cryo–cooled Yb:YAG (200 mJ, 2.3 eV, 3.5 ps)
- two lasers (one for low–Eg and both for high–Eg)

**3) *Laser circulation with mm and mrad and sub–ps alignment/ synchronization***

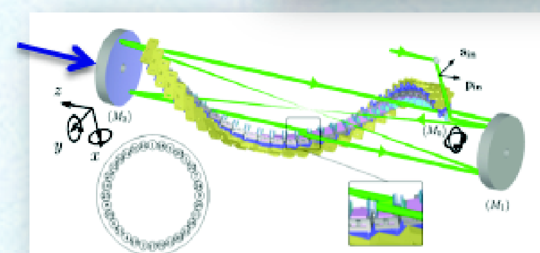

- complex opto/mechanical system
- two interaction points: Eg < 3.5 MeV & Eg < 19.5 MeV

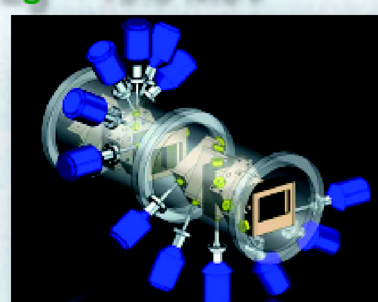

**4) *Gamma beam collimation system***

- complex array of dual slits
- relative bandwidths < 5 x $10^{-3}$

**5) *Gamma beam diagnostic system***

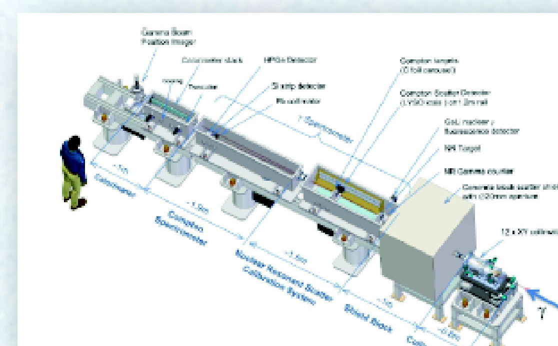

- beam optimization and characterization: energy, intensity, profile

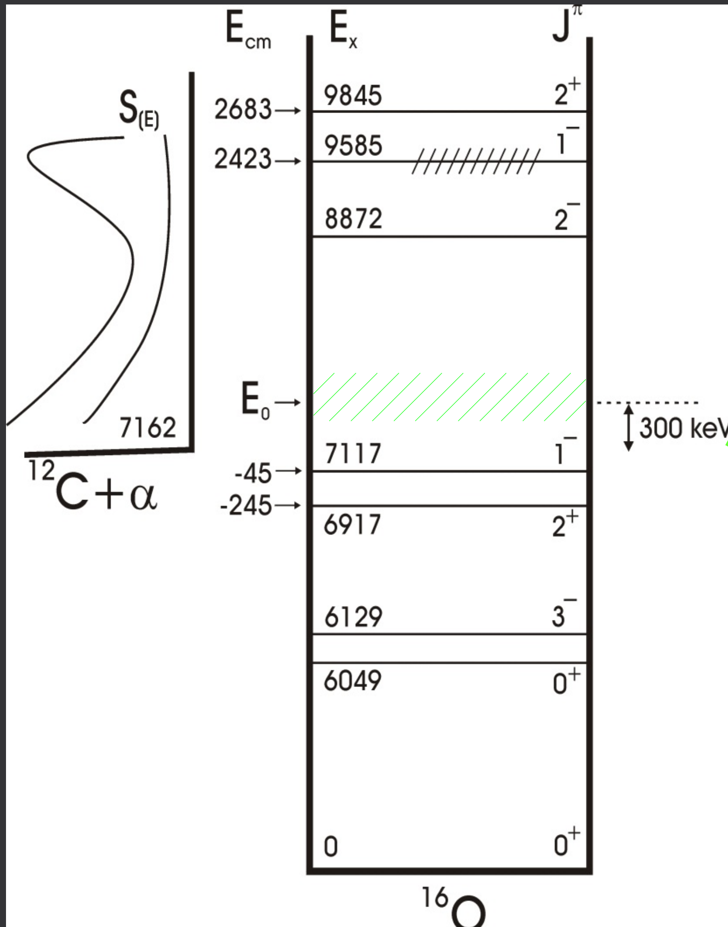


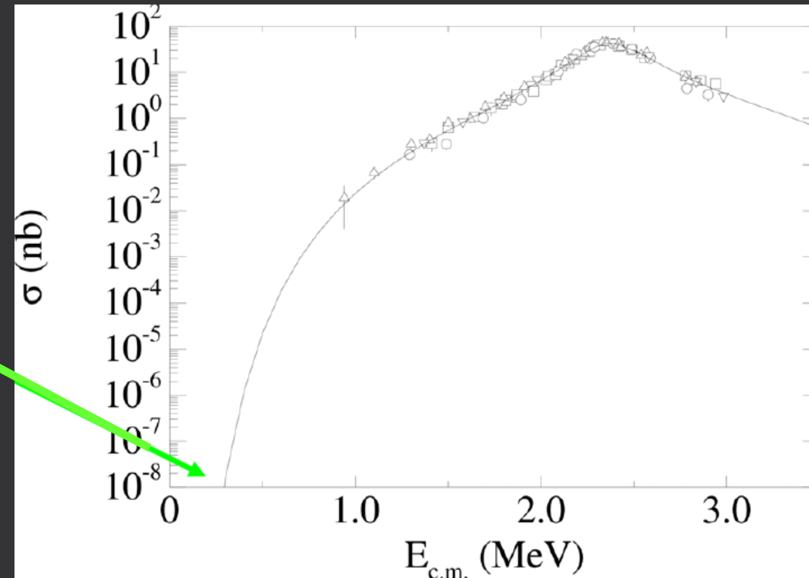


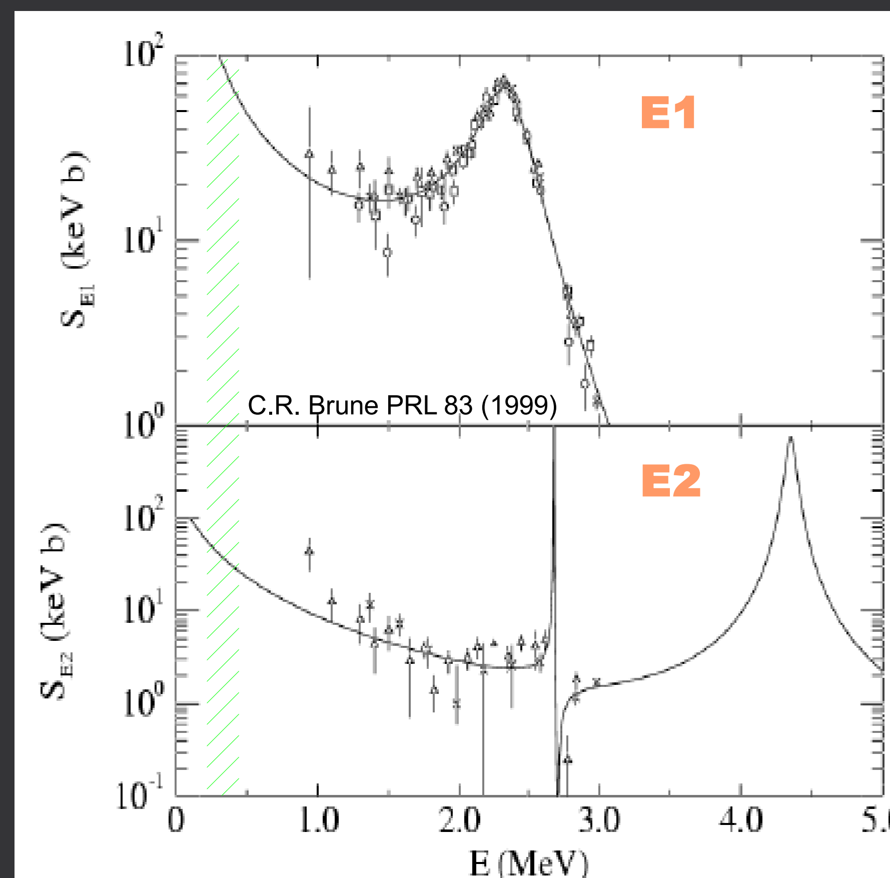


E1 ground state σ: resonant capture through $1^-$ states; σ at 300 keV dominated by the high-energy tail of 7.12-MeV state

$S_{E1}(300)=79\pm21$ keVb (Buchmann 94)

E2 ground state σ: resonant capture through $2^+$ states; direct capture (d→s); σ at 300 keV dominated by the high-energy tail of 6.92-MeV state;

$S_{E2}(300)=53\pm18$ keVb (Tischhauser 02)

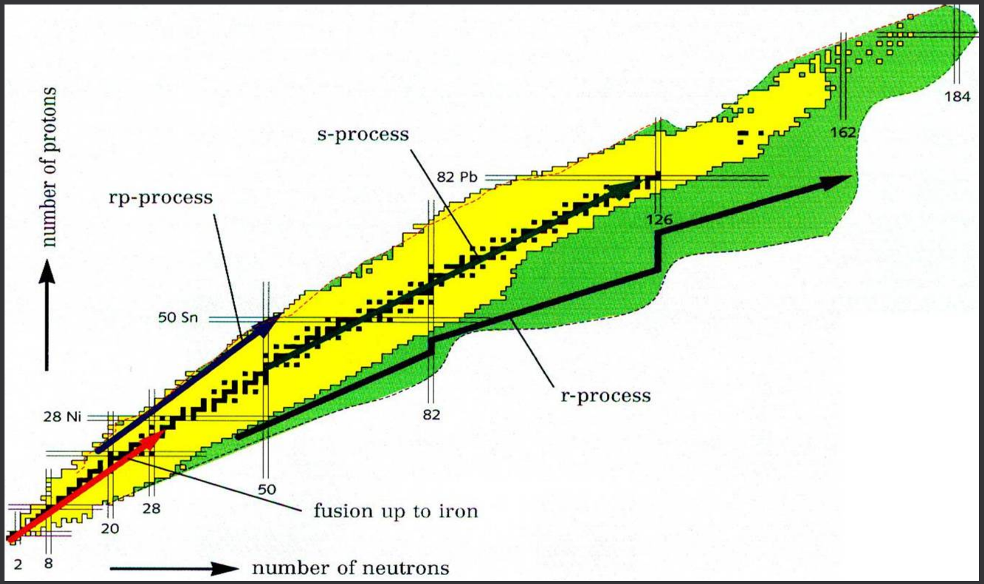


*W.R. Plass et al., NIM B 317 (2013) 457*

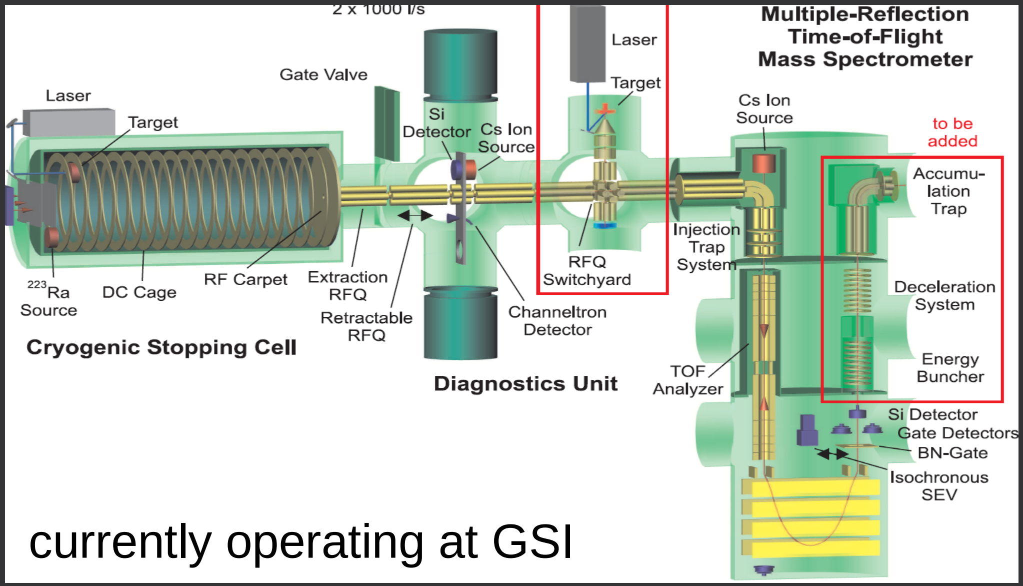


currently operating at GSI

# Fragment Stopping in Target (I)

Geant4 stopping power: J.F. Ziegler and J.M. Manoyan, NIM B 35 (1988) 215

$S_{ion} = (\gamma Z)^2 S_p$, $S_p$ = proton stopping (Bethe-Bloch)

$\gamma = q(1+s.c.)$ = ion effective charge, $q \equiv Q/Z$, s.c. = screening correction (Brant-Kitagawa)

$q \equiv Q/Z \sim 1 - \exp(-v/v_B \cdot Z^{-2/3})$ = ion charge state (Bohr approx)

$\gamma \approx q \approx 1$ for light ions (Z~1), high velocity ($v \gg v_B$=25 keV/u)

Significant for fission fragments: Z=30-60, KE~0.3-1.5 MeV/u

$q(v, Z, Z_{targ})$ measurement parameterizations:

1) Ziegler (1988): Geant4
2) Shima (1982): older, specific for slower heavy ions
3) Schiwietz (2001): newest (largest data set), differentiated for solid/gas targets

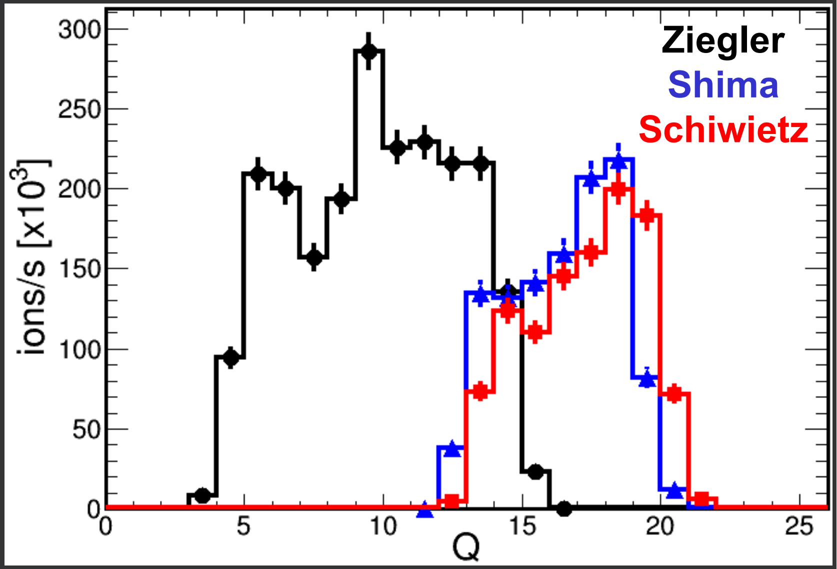


LOHENGRIN (ILL Grenoble): $(n_{th},f)$ of $^{235}$U, $^{239,241}$Pu

**$\langle Q \rangle$ = 20-22, $\sigma_Q$ = 2.0-2.4**

Ziegler: $\langle Q \rangle$ = 9.8, $\sigma_Q$ = 3.0

Shima: $\langle Q \rangle$ = 16.5, $\sigma_Q$ = 2.0

Schiwietz: $\langle Q \rangle$ = 17.3, $\sigma_Q$ = 2.1

Schiwietz&Shima:

- describe better data
- larger ionic charge
- stronger Z dependence
- smaller release efficiency